Out-of-equilibrium hydrodynamics with and without boost symmetry

Aruna Rajagopal

Faculty of Physical Sciences
University of Iceland
2021

Out-of-equilibrium hydrodynamics with and without boost symmetry

Aruna Rajagopal

Dissertation submitted in partial fulfillment of a
Philosophiae Doctor degree in Physics

Advisor
Prof. Lárus Thorlacius

PhD Committee
Prof. Lárus Thorlacius
Prof. Jelle Hartong
Prof. Valentina Giangreco M. Puletti
Prof. Þórður Jónsson

Opponents
Prof. Giuseppe Policastro
Ecole Normale Supérieure
Prof. Koenraad Eduard Schalm
Instituut-Lorentz, Universiteit Leiden
Faculty of Physical Sciences

School of Engineering and Natural Sciences
University of Iceland
Reykjavik, May 2021

Contents

Abstract

In this thesis, we explore the role of symmetries in hydrodynamics by studying certain properties of relativistic and non-relativistic fluids. In the first part of the thesis, we examine the theory of relativistic magnetohydrodynamics (Maxwell electromagnetism coupled to hydrodynamics) and its low temperature incarnation, force-free electrodynamics, reformulated in the language of higher-form symmetries and discuss the advantages of such a scheme. Using this framework, we analyse the regime of validity of force-free electrodynamics by evaluating the lifetime of the non-conserved electric field operator via a holographic model sharing the same global symmetries as that of a plasma. We are able to explicitly calculate the lifetime of the electric field, both parallel and perpendicular to the magnetic field, and find that there are indeed no long-lived modes that interfere with a hydrodynamic description of force-free electrodynamics. In the second part of the thesis, we study the thermodynamic properties of non-relativistic Lifshitz fluids with an arbitrary dynamic exponent z (encoding the anisotropy in the scaling of time and space coordinates). We study energy transport in such fluids far from equilibrium after performing a local quench between two semi-infinite fluid reservoirs. We find that the late time energy flow is universal and accommodated via a steady state occupying an expanding central region between outgoing shock and rarefaction waves (a *non-equilibrium steady state*), as seen previously for relativistic scale invariant fluids. Armed with an equation of state for a perfect Lifshitz fluid with an arbitrary z and moving with a velocity v, we proceed to study its holographic dual using the well-established Einstein-Maxwell-Dilaton model. We find that the fluid velocity appears as the chemical potential, conjugate to the dual momentum density and the solutions represent a physically distinct class of black branes possessing a linear momentum, different from *boosting* a static brane.

Útdráttur

Ritgerðin fjallar um bæði afstæðilega og sígilda vökvaaflfræði frá sjónarhóli samhverfu. Byrjað er á að kanna afstæðilega segulstraumfræði (e. magnetohydrodynamics), sem lýsir víxverkun rafhlaðins straumefnis við rafsegulsvið Maxwells, og skoðað tilfellið þegar efnisþéttleiki og hitastig eru nógu lág til að kerfið sé segulmiðað (e. force free electrodynamics). Þá er þrýstingur vegna segulsviðsins ráðandi miðað við þrýstinginn frá straumefninu. Í þessu markgildi má setja kenninguna fram á nýstárlegan hátt, þar sem svonefnd formsamhverfa (e. higher form symmetry) er í aðallhlutverki, og bera saman við eldri fræði. Með því að styðjast við þyngdarfræðilega heilmyndun (e. holographic duality) má reikna út dempun rafsviðs í straumefninu, bæði samsíða og þvert á segulsviðið, og staðfesta að engar langlífar örvanir séu til staðar í segulmiðuðu kerfi og því óhætt að treysta niðurstöðum vökvaaflfræðinnar. Síðari hluti ritgerðarinnar fjallar um varmafræði og vökvaaflfræði fyrir sterkt víxlverkandi skammtakerfi með Lifshitzskölun. Kannaður er orkuflutningur utan varmajafnvægis í slíkum kerfum í kjölfar þess að varmageymar við mismunandi hitastig eru leiddir saman. Kerfið leitar í ástand með stöðugu orkustreymi í gegnum rými sem umlykur samskeytin milli varmageymanna. Þetta rými vex með tímanum og er afmarkað af tveimur bylgjum á útleið, sín í hvora átt frá samskeytunum. Niðurstaðan er í góðu samræmi við eldri útreikninga fyrir afstæðilega vökvaaflfræði. Þyngdarfræðileg heilmyndun gefur einnig innsýn í ýmsa varmafræðilega eiginleika skammtakerfa með Lifshitzskölun og í ritgerðinni er stuðst við útreikninga í ákveðnu þyngdarfræðilíkani, sem gefist hefur vel í fyrri rannsóknum á þessu sviði

Acknowledgments

First and foremost, I would like to express my deep gratitude to my supervisor Lárus Thorlacius as well as Valentina Puletti for their guidance, help and patience throughout my years as a doctoral candidate.

I am also grateful for the opportunity to meet, interact with and often pester the post-docs Daniel Fernandez, Friðrik Freyr Gautason, Nick Poovuttikul and Watse Sybesma during the course of my PhD. A special thanks to my collaborators Daniel and Nick, working with whom I learnt a lot about research as well as life, and a shout-out to Watse for taking the pains of going through my unfinished thesis. I would like to thank my fellow PhD mates Lukas Schneiderbauer and Juan Angel-Ramelli, and my friends with whom I shared the office, for being with me for most of this journey and enriching it. I would like to thank my parents and sister, the people in my life who have made everything I have done so far possible, and believed in me even when I didn't believe in myself. Last but not the least, my partner Cyril who has always been with me, through thick and thin and made my sojourn in Iceland even more significent.

This work was supported in part by the Icelandic Research Fund under grant 195970-052, and by the University of Iceland Research Fund.

1 Introduction

Hydrodynamics [Landau and Lifshitz, 1987] is one of the oldest and well established theories describing the long wavelength, low frequency behaviour of interacting systems at finite temperature. Essentially, the hydrodynamic theory is a description of locally conserved currents and the manifestation of the corresponding symmetries in a system in thermal equilibrium. In both its relativistic and non-relativistic forms, we encounter hydrodynamics in a variety of real-world, observable phenomena where a fluid description is warranted. Even beyond this, it has been a source of ever increasing interest to theorists for several reasons. For instance, interpreting hydrodynamic fluctuations as the gravitational fluctuations of black holes opens up a wide world of possibilities [Policastro et al., 2002a,b] such as computation of transport coefficients in strongly coupled quantum systems from black hole physics, studies into various applications of relativistic hydrodynamics, charge transport in high temperature superconductors and graphene [Lucas et al., 2016a], manifestation of chiral anomalies in hydrodynamic equations [Son and Surówka, 2009], as well as a deeper understanding of thermalisation and hydrodynamisation of the quark-gluon plasma. In recent years, several strides have been made in the construction of an effective classical theory for hydrodynamics using the Schwinger-Keldysh formalism for thermal field theories [Haehl et al., 2016, Crossley et al., 2017, Jensen et al., 2018], that provides a systematic treatment of statistical and quantum hydrodynamical fluctuations at the nonlinear level via a path integral formulation for dissipative fluids. Theories with widely varying microscopics can have the same macroscopic hydrodynamic description. Such a universal description is possible because of the existence of various conserved currents.

It is clear that the significance of symmetries and symmetry principles in physics cannot be overstated. The goal of a physicist is to be able to explain various natural phenomena that occur around us. The simplest yet most powerful way of doing so is to reduce the physical system in question down to smaller constituents, analyse the patterns or connections between them, use these to eliminate redundant degrees of freedom and understand the original more complex system. While symmetries of course play an important role in the classification of various physical systems (whether they are crystals with specific lattice structures or quantum critical systems that scale a certain way), they also place constraints on physical theories by requiring them to be invariant under certain transformation groups (for instance diffeomorphism invariance of any theory of gravity). In this way, symmetries play a powerful part in unifying theories that follow a common set of transformation rules. One of the most ubiquitous capacities in which we come across symmetries, is their connection with conservation laws via Noether's theorem which states that for every continuous global symmetry, there exists an associated conserved current. It is this aspect and its manifestation in hydrodynamics that we explored in the work on which this thesis is based. While we studied the thermodynamics of out of equilibrium non-relativistic fluids with no boost symmetry (invariant under Lifshitz scaling) in [Fernández et al., 2019], the problem studied in [Poovuttikul and Rajagopal, 2021] pertained to that of relativistic fluids whose $U(1)$ symmetries can be formulated in the language of generalised global symmetries.

An appropriate hydrodynamic model for a system, incorporating the dissipative effects of thermal media (essential for a fluid to equilibriate after being perturbed away from equilibrium), consists of a gradient expansion of hydrodynamic fields up to any given order. At a given order, the conservation equations determine the expansion up to a finite number of undetermined coefficients. These coefficients may then be obtained either from physical measurements or from microscopic computations. For a strongly coupled quantum system, this becomes increasingly hard. Here is where the advantage of the *AdS/CFT* correspondence comes into play. The anti-de Sitter/conformal field theory (AdS/CFT) correspondence, as proposed in Maldacena's seminal paper [Maldacena, 1999] (further strengthening the belief that the universe follows a holographic principle as posited by 't Hooft ['t Hooft, 1993] and Susskind [Susskind, 1995]), has been one of the greatest achievements in string theory in the past century, providing as it does, a tool to investigate the behaviour of strongly coupled quantum field theories, otherwise notoriously hard to describe. It does so by means of a holographic reformulation of (strongly coupled) field theory dynamics in terms of (weakly coupled) classical gravity in one higher dimension by claiming that the former can be analysed by studying the corresponding AdS spacetime (maximally symmetric solution to Einstein's field equations with a constant negative curvature) on whose boundary it lives. In fact the isometry group of AdS_{d+1} which is $SO(d,2)$ coincides with that of the conformal group for a d-dimensional field theory. It has been shown that Einstein's field equations with a negative cosmological constant, supplemented with appropriate regularity restrictions and boundary conditions, reduce to the nonlinear equations of fluid dynamics in an appropriate parameter range, and a systematic framework to construct this universal nonlinear fluid dynamics, order by order in a boundary derivative expansion has been carried out in [Bhattacharyya et al., 2008, Baier et al., 2008]. While the pioneering work into the investigation of linearised fluid dynamics from the linearised Einstein field equations was carried out by [Policastro et al., 2001], there has been tremendous progress in this area over the years [Herzog and Son, 2003, Kovtun et al., 2003, 2005, Policastro et al., 2002a,b, Buchel, 2005]. Some comprehensive reviews on the fluid gravity correspondence and holographic methods used in condensed matter theory are [Hubeny et al., 2011, Hartnoll, 2009].

Since in standard AdS holography the dual field theories are relativistic, most of these developments have been focused on the dual gravitational formulation of relativistic hydrodynamics. However, most of the strongly correlated systems in nature are inherently non-relativistic. This seems to warrant a further investigation into bulk theories with asymptotic geometries that are not AdS [Kachru et al., 2008, Son, 2008, Balasubramanian and McGreevy, 2008]. The successes achieved by standard AdS/CFT correspondence have motivated a study into the application of holography to a wider setting, with the hopes of yielding a greater depth of understanding into real-world condensed matter systems, certain semi-conductors and heavy fermion compounds. While there has been an accelerating growth in research in this field [Taylor, 2008, Mann and McNees, 2011, Hoyos et al., 2013, Ross, 2011, Chemissany and Papadimitriou, 2015, Hartong et al., 2015b, Christensen et al., 2014b], there are still several aspects that have yet to be answered, and gaps in our knowledge that need to be filled. Keeping this in mind, we studied the holographic dual of non-relativistic Lifshitz fluids with an arbitrary scaling exponent z with no boost symmetry and analysed its equation of state in [Rajagopal and Thorlacius, 2021].

The outline of the rest of this thesis is as follows:

In 2, I will provide a brief introduction to the work carried out in [Poovuttikul and Rajagopal, 2021] and the results we obtained, along with an explanation of some of the concepts we used. This includes what higher-form symmetries are and how the usual equations of Maxwell electromagnetism may be reformulated in this language 2.1, the importance of operator lifetime in determining the regime of validity of hydrodynamics 2.2, the equations of ideal magnetohydrodynamics and force-free electrodynamics 2.3, and how we used holography to obtain our results 2.4.

In 3, I will discuss the importance of studying non-relativistic fluids, giving a brief introduction to the work carried out in [Fernández et al., 2019] and [Rajagopal and Thorlacius, 2021], and the results obtained therein. For reference, I will include the relativistic and non-relativistic symmetry algebras in 3.1, for the interested reader. In 3.2, I will describe the thermodynamic properties of the *ideal*, Lifshitz fluid that will be studying in the next few sections, and the form of the energy-momentum tensor. In sections 3.3, 3.4 and 3.5, I will describe briefly the meaning of a non-equilibrium steady state that develops following a thermal quench, the setup involving a pair of quantum critical heat baths brought into contact at time $t = 0$, and a quick review of the theory of shock and rarefaction waves (and associated stability conditions) respectively. In 3.6, I shall discuss the importance of studying non-relativistic holography while in 3.7, I will describe the gravitational model we use to study the thermodynamics of Lifshitz black brane with linear momentum in [Rajagopal and Thorlacius, 2021]. Finally, in 4 I will conclude the thesis with a discussion on the results obtained in the various problems studied above and some open questions.

2 Part I : Generalised global symmetries

The purpose of this section is to provide a broad understanding of the concepts used in [Poovuttikul and Rajagopal, 2021], where using the framework of higher-form global symmetries, we examined the regime of validity of force-free electrodynamics (FFE) by means of evaluation of the lifetime of the electric field operator which is non-conserved due to screening effect of the charges present in a plasma. We focused on the holographic model which has the same global symmetry as that of the plasma to calculate the life time of (non-conserved) electric flux in a strong magnetic field regime and finite temperature. To the best of our knowledge, there has not been a genuine computation of this quantity directly from quantum electrodynamics or first principles (in the sense of [Arnold et al., 2000]) when both temperature T and magnetic field $\mathbf{B}$ are turned on. Our quest for testing the feasibility of hydrodynamic description at low temperatures and strong magnetic field using the language of higher form symmetries led us to discover an inverse correlation between the strength of the magnetic field and the lifetime of electric flux operator. This implies that in a strong enough magnetic field, the electric field decays fast enough, so as to not interfere with the hydrodynamic modes, increasing the regime of validity of FFE, and laying the groundwork for further holographic studies into the model.

2.1 Higher-Form Symmetries

Inspired by the framework of generalised global symmetries introduced in [Gaiotto et al., 2015], the authors of [Grozdanov et al., 2017] developed a purely symmetry-based approach to study the hydrodynamic fluctuations of the conserved magnetic flux in the theory of $U(1)$ electromagnetism coupled to charged matter in four dimensions. In the conventional language of electromagnetism, Maxwell's equations are given by,

$$\frac{1}{g^2}\nabla_\mu F^{\mu\nu} = j^\nu_{el}, \tag{1}$$

$$\nabla_{[\mu} F_{\rho\sigma]} = 0, \tag{2}$$

where $F_{\mu\nu}$ is the usual 2−form electromagnetic field strength. Now, the symmetry associated with the $U(1)$ current j^μ_{el} is a gauge symmetry, which is simply a redundancy of the system. It does not give rise to new physics. If we now consider the object, $J^{\mu\nu} = \frac{1}{2}\varepsilon^{\mu\nu\sigma\rho}F_{\sigma\rho}$, the Bianchi identity gives us the following conservation equation,

$$\nabla_\mu J^{\mu\nu} = 0. \tag{3}$$

This statement encodes the conservation of magnetic flux through a two dimensional spatial surface, or in other words, the lack of magnetic monopoles.

In the language of [Gaiotto et al., 2015], a continuous generalised global p−form symmetry is associated with the conservation of a $p+1$ antisymmetric tensor current, $J^{\mu_1\mu_2\cdots\mu_{p+1}}$. Associated with these currents in d−dimensional systems, we have conserved "charges" which are obtained by integrating them over the spatial volume,

$$Q_{(p)} = \int_{\mathscr{M}_{d-p-1}} dS_{\mu_1\mu_2\ldots\mu_{p+1}} J^{\mu_1\mu_2\cdots\mu_{p+1}}, \tag{4}$$

where $S_{\mu_1\mu_2\ldots\mu_{p+1}}$ is $p+1-$ form and can be thought of as the analog of the normal vector to a spatial volume. The charge Q can be thought of as the quantity that counts the number of charged objects piercing the $\mathscr{M}_{d-p-1}$ surface. To understand this in more familiar terms, the ordinary charge $Q_{(0)}$, which is the integral of the Hodge dual of a one-form divergence-less current j^μ over a co-dimension 1 surface counts the number of point particles charged under it. $Q_{(1)}$ on the other hand, given by the integral of the Hodge dual of the two-form $J^{\mu\nu}$ over a co-dimension 2 surface, counts the number of magnetic field lines piercing the surface.

In order to study the hydrodynamics associated with these generalised global symmetries, it is useful to construct an effective action where the usual stress tensor $T^{\mu\nu}$, and the 2-form $J^{\mu\nu}$ are treated on equal footing, as slowly evolving conserved currents. The former is sourced by the background metric $g_{\mu\nu}$, while the latter is sourced by an external 2−form gauge field $b_{\mu\nu}$. This can be achieved by deforming the microscopic

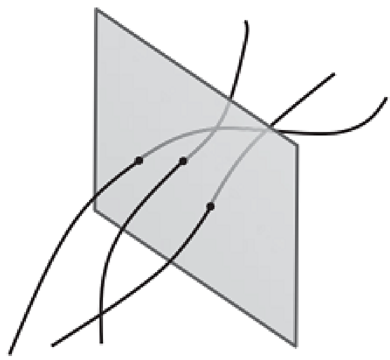

Figure 2.1. Conserved charge obtained by counting the number of strings that pierce a co-dimension 2 surface Figure from [Grozdanov et al., 2017].

on-shell action of the theory S_0, by a source term,

$$S = S_0 + S_b, \tag{5}$$

where $S_b \equiv \int d^4x\sqrt{-g}b_{\mu\nu}J^{\mu\nu}$. The currents are then defined as,

$$T^{\mu\nu} \equiv \frac{2}{\sqrt{-g}}\frac{\delta S}{\delta g_{\mu\nu}}, \quad J^{\mu\nu} \equiv \frac{1}{\sqrt{-g}}\frac{\delta S}{\delta b_{\mu\nu}}. \tag{6}$$

Invariance of the action under an infinitesimal diffeomorphism of the metric, gives the conservation equation of $T^{\mu\nu}$ in the presence of an external source, while invariance under an infinitesimal gauge transformation leads to the conservation equation of $J^{\mu\nu}$, that is,

$$\nabla_\mu T^{\mu\nu} = H^{\mu}_{\rho\sigma}J^{\rho\sigma}, \quad \nabla_\mu J^{\mu\nu} = 0. \tag{7}$$

Here $H = db$ is the 3−form field strength of the 2−form source, $b_{\mu\nu}$.

It is worth noting that while higher-form symmetries have been systematically categorised in [Gaiotto et al., 2015], they have previously made an appearance in other studies, for example, dislocation/disinclination in liquid crystals [Beekman et al., 2017] and systems consisting of extended objects such as superfluid vortices [Horn et al., 2015, Esposito et al., 2017, Nicolis and Penco, 2018].

With this formalism in place, I shall proceed to describe an example, where the usefulness of this reformulation is particularly clear.

2.2 Hydrodynamic equations and operator lifetime

In its standard form, hydrodynamics is formulated in the language of equations of motion rather than an action principle. This is mainly due to the presence of dissipative forces in thermal media for which the action principle is ill-equipped. Hydrodynamic equations of motion take the following schematic form,

$$\partial_t n_a + \partial_i J^i_a(n_a, \partial_j n_a \ldots) = 0, \tag{8}$$

where the n_a represent the conserved charge densities, and J^i_a are the corresponding currents. The constitutive relations express these currents in terms of the densities, or more conventionally, both n_a and J^i_a are expressed as $n_a(\phi)$ and $J^i_a(\phi)$, where ϕ are the thermodynamic quantities conjugate to n_a in the grand canonical ensemble, that is, temperature, fluid velocity and chemical potential. Under the assumption that derivative corrections to the conserved currents are small compared to the mean-free path, one can perform a gradient expansion of the various local hydrodynamic fields, evolving towards equilibrium.

All operators except conserved charges have parametrically short lifetimes compared to the scale of interest and, once the longest-lived non-conserved operator[1] has decayed away, the hydrodynamic description becomes viable (see Fig. 2.2).

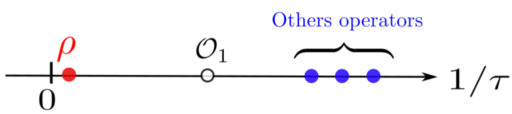

Figure 2.2. Illustration of the lifetime of operators of a theory that exhibit hydrodynamic behaviour at late time. Here, there is a parametrically large gap between conserved charges ρ and the rest. The life time τ_1 of the longest-lived operator, denoted by $\mathcal{O}_1$ set the time scale in which hydrodynamics becomes applicable.

For a system at finite temperature, the correlation function of a non-conserved operator $\mathcal{O}$ decays as $\langle \mathcal{O}(t)\mathcal{O}\rangle_\beta \sim e^{-t/\tau_1}$, where τ_1 is its relaxation time, that is the time it takes for $\mathcal{O}$ to decay away before the theory can be described by hydrodynamics alone. It is thus reasonable to make the statement that τ_1 sets the time scale for the hydrodynamic regime. Assuming all other (non-hydrodynamic) modes have parametrically shorter lifetimes, once we reach time scales of the order $\partial_t \sim 1/\tau_1$, there will be still

[1] While this operator language is more familiar in the context of quantum systems, it is also applicable to classical systems via e.g. memory matrix formalism [Zwanzig, 1961, Forster, 1995]. A more modern introduction may be found in [Hartnoll and Hofman, 2012].

a finite number of degrees of freedom, those of the actual hydrodynamic modes, and the mode representing $\mathscr{O}$. Thus, we can treat the conservation of $\mathscr{O}$ as a weakly broken symmetry, and include it in our effective theory.These concepts are used in [Poovuttikul and Rajagopal, 2021] to determine the regime of validity of Force-Free Electrodynamics from first principles.

If the boundary theory is perturbed by an operator $\mathscr{O}(t)$, the poles of the corresponding retarded two-point correlation function captures the dispersion relation of the low energy excitations. In hydrodynamics, the poles of the retarded two-point correlation function of the stress tensor leads to the dispersion relations of the the diffusive and sound modes

$$\omega = -i\mathscr{D}k^2 : \qquad \text{diffusive mode,} \tag{9}$$

$$\omega = \pm c_s k - i\tilde{\mathscr{D}}k^2 : \qquad \text{sound mode,} \tag{10}$$

where $\mathscr{D}$, $\tilde{\mathscr{D}}$ and c_s are the diffusion constant, sound attenuation constant and speed of sound respectively. The relaxation time of the operator is given by the inverse of the mode frequency. For details on the holographic computation of retarded Green's functions of conserved operators, and the calculation of the corresponding conductivities one may refer to [Davison and Goutéraux, 2015, Blake, 2015] or for a more comprehensive explanation (and references therein), [Hartnoll et al., 2016].

2.3 An Application : MHD-FFE

Magnetohydrodynamics or MHD is a theory that couples the equations of Maxwell electromagnetism with hydrodynamics to describe the large scale, slow dynamics of conducting fluids such as plasmas. Relativistic MHD [Dixon, 1982, Anile, 2005, Komissarov, 1999] has had great success in describing several astrophysical phenomena such as gravitational collapse and accretion disks, jet formation, gamma-ray bursts etc [Goedbloed and Poedts, 2004]. The equations of ideal MHD take the following familiar form:

$$\text{Continuity Equation} \qquad \frac{\partial \rho}{\partial t} + \vec{\nabla} \cdot (\rho \vec{v}) = 0, \tag{11}$$

$$\text{Momentum equation} \qquad \rho \left(\frac{\partial}{\partial t} + \vec{v} \cdot \vec{\nabla} \right) \vec{v} = -\vec{\nabla} p + \vec{J} \times \vec{B}, \tag{12}$$

$$\text{Ampere's Law} \qquad \vec{J} = \frac{1}{\mu_0} \vec{\nabla} \times \vec{B}, \tag{13}$$

$$\text{Faraday's Law} \qquad \frac{\partial B}{\partial t} = -\vec{\nabla} \times \vec{E}, \tag{14}$$

$$\text{Ideal Ohm's Law} \qquad \vec{E} + \vec{v} \times \vec{B} = 0, \tag{15}$$

$$\text{Divergence constraint} \qquad \vec{\nabla} \cdot \vec{B} = 0, \tag{16}$$

where $\vec{E}$ and $\vec{B}$ are the electric and magnetic fields respectively, $\vec{v}$ is the velocity, ρ is the mass density, p is the pressure, and μ_0 is the vacuum permeability. Equation (13) is Ampere's Law in the limit of low frequency $\partial_t \vec{E} \to 0$. Along with (15), $\vec{E}$ is completely fixed, and Gauss' Law plays no role.

With the recent surge of developments in hydrodynamics from its description as an effective theory, to the success of using holography and black hole physics as tools to compute transport coefficients, there has been renewed interest in developing a modern formulation of MHD. This includes the classification of dissipative corrections beyond the ideal limit and a concerted effort in reformulating hydrodynamic theories including MHD in the language of generalised global symmetries or higher-form symmetries [Schubring, 2015, Grozdanov et al., 2017, Hernandez and Kovtun, 2017, Armas and Jain, 2019, 2020], where the conservation of $T^{\mu\nu}$ and $J^{\mu\nu}$ (introduced in the previous section) form the basis of the theory.

There are several advantages to the reformulation of MHD in the language of higher forms. In its traditional form described above, ideal MHD only works under the assumptions of infinite conductivity and ideal Ohm's law. Moreover, the separation between fluid and charge carrying sectors (encoded in the equation of state $(\partial_t + \vec{v} \cdot \nabla)\left(\frac{p}{\rho^\gamma}\right) = 0$) assumes weakly coupled electromagnetism in a plasma, although there should a priori be no reason for this. The symmetry-based formulation on the other hand, doesn't make any of these assumptions. In addition, as this is a purely symmetry-based formulation, there is no need to introduce a microscopic gauge field, A_μ. It could also potentially make numerics easier. Finally, a nice feature of the reformulation is that the non-dynamical electric field doesn't explicitly enter the evolution equations.

Let us now proceed to study the force-free limit of MHD, where the effects of the

Lorentz force on the plasma can be ignored.

Force-Free Electrodynamics (FFE) constitutes a set of closed, hyperbolic equations that describe the evolution of a dissipation-less plasma. It has been studied extensively in the context of magnetospheres of compact spherical objects such as black holes, neutron stars, and relativistic jets [Blandford and Znajek, 1977, Goldreich and Julian, 1969, Gralla and Jacobson, 2014] and solar coronas [Wiegelmann and Sakurai, 2012]. [Komissarov, 2004] gives a concise explanation about the properties of black hole magnetospheres, and the various historical developments leading to it. The authors of [Grozdanov et al., 2017, Komissarov, 2002, Glorioso and Son, 2018] showed that the $T \to 0$ limit of MHD can lead to a consistent, hydrodynamic theory of a plasma without dissipation, and is identical to the equations of FFE. While the electromagnetic sector essentially decouples from the matter sector in this limit, the non-linear structure of MHD still persists.

These equations describe a magnetically dominated plasma wherein the population of charged particles is high enough to effectively shield them from the electric field. They can be expressed in the following covariant way:

$$F^{\mu\nu}F_{\mu\nu} > 0 \tag{17}$$

$$\varepsilon^{\mu\nu\rho\sigma}F_{\mu\nu}F_{\rho\sigma} = 0 \tag{18}$$

$$j^{\mu}_{el}F_{\mu\nu} = 0. \tag{19}$$

Equation (17) simply contains the information that the plasma is magnetically dominated ($E^2 < B^2$). The degeneracy condition (18), implies $\vec{E} \cdot \vec{B} = 0$, that is, the component of the electric field parallel to the magnetic field should vanish to ensure that the charges are freely available in FFE. It ensures the existence of a reference frame where an observer detects only the magnetic field. The last condition (19) from which (18) can be derived, is essentially the force-free condition, $\rho\vec{E} + \vec{j} \times \vec{B} = 0$ that ensures that the Lorentz force $j^{\mu}_{el}F_{\mu\nu}$ exerted on the plasma vanishes [Komissarov, 2002]. Combined with the usual Maxwell's equation, $\nabla_{\mu}F^{\mu\nu} = j^{\mu}_{el}$, we get,

$$F_{\sigma\nu}\nabla_{\mu}F^{\mu\nu} = 0. \tag{20}$$

These equations can be written in the form of conservation laws familiar from hydrodynamics. From the definition of the electromagnetic stress-energy tensor, $T^{\mu\nu} =$

$F^{\mu}_{\rho} F^{\nu\rho} - \frac{1}{4}(F_{\rho\sigma}F^{\rho\sigma})g^{\mu\nu}$, the force-free condition (20) gives us the equation,

$$\nabla_{\mu} T^{\mu\nu} = 0, \tag{21}$$

while the usual Bianchi identity gives us the equation,

$$\nabla_{\mu} J^{\mu\nu} = 0. \tag{22}$$

In this setup it is easy to see that while the energy, momentum and magnetic flux are conserved, the conservation of electric flux is explicitly broken (as $d \star F \neq 0$), as required by a plasma system. From a microscopic perspective, the electric flux lines can end on the locally excited charge particles and thus the total electric flux is not conserved. In operator language, this means that the electric flux operator acquires a finite lifetime, one that should be much smaller than the characteristic time scale of the system determined by the magnetic field and temperature (the only other parameters of the system). Thus, a reasonable test to determine the regime in which FFE is valid would be to measure the lifetime of these excitations when the electric field is an almost conserved quantity. As explained in [Grozdanov et al., 2019], the explicit presence of the relaxation time τ in the equations of almost conserved quantities gives an indication of the extent up to which hydrodynamics is valid.

Traditionally, FFE is meant to describe the dynamics of a plasma that has a high enough density of charges, such that there is an effective screening of the electric field, whilst simultaneously being dilute enough that there is negligible exchange of stress-energy between the fields. While this has been successful in describing a variety of astrophysical phenomena, it is not rigorous enough to account for certain observations such as particle acceleration in cosmic rays and jets, and radio emission from pulsars. It would be interesting to determine if standard FFE is valid even at low temperatures, and to what extent it can be trusted. Moreover, there has been recent progress in coming up with a systematic gradient expansion of conserved currents with higher-form global symmetries, allowing for the possibility of there being higher order derivative corrections to the usual FFE equations, as shown in [Grozdanov et al., 2017, Gralla and Iqbal, 2019]. A reasonable test to determine this would be to measure the lifetime of the non-conserved electric field operator, as explained in 1.

We expound on these ideas in [Poovuttikul and Rajagopal, 2021], using the ideas of operator lifetime, specifically that of the electric field, in order to determine the regime of validity of conventional FFE, following which, demonstrating the validity of FFE in a holographic model.

2.4 Holography as a tool

Holography has proven to be a highly useful method for probing the microscopic details of a strongly coupled quantum theory, that would have otherwise been intractable. Using standard holographic methods in hydrodynamics [Policastro et al., 2002a,b], the manifestation of higher-form symmetries in theories with holographic duals has been investigated in [Grozdanov and Poovuttikul, 2019, Hofman and Iqbal, 2018]. We propose to carry out our investigation into the applicability of FFE using this model, thereby simultaneously testing the strength of this method.

The simplest holographic dual to a strongly interacting field theory of matter charged under dynamical $U(1)$ electromagnetism, formulated in the language of higher-form symmetry (first constructed in [Grozdanov and Poovuttikul, 2019, Hofman and Iqbal, 2018]) is given by the five-dimensional bulk theory comprises of Einstein gravity coupled to a two-form bulk gauge field, $B_{\mu\nu}$, and a negative cosmological constant. $B_{\mu\nu}$ sources the two-form current associated with the $U(1)$ one-form global symmetry in the boundary theory. The model is described by the following action,

$$\begin{aligned} S = \int d^5X\sqrt{-G}\left(R - 2\Lambda - \frac{L^2}{3}H_{abc}H^{abc}\right) + \\ S_{bnd} - \frac{1}{\kappa(\Lambda)}\int_{r=\Lambda} d^4x\sqrt{-\gamma}(n^a H_{a\mu\nu})(n_b H^{b\mu\nu}), \end{aligned} \tag{23}$$

where $H = dB$ and B_{ab} is the bulk 2-form gauge field, Λ is the UV-cutoff, n^a is the unit normal to the boundary, and S_{bnd} denotes the Gibbons-Hawking and gravitational counter term.

The equations of motion are given by,

$$R_{ab} + 4G_{ab} = H_{acd}H_b^{cd} - \frac{2}{9}G_{ab}H_{cde}H^{cde}, \tag{24}$$

$$\frac{1}{\sqrt{-G}}\nabla_a(\sqrt{-G}H^{abc}) = 0. \tag{25}$$

The equilibrium solution of this holographic model is a domain wall interpolating between an asymptotic AdS_5 geometry in the UV ($r \to \infty$ in our convention), and a $BTZ \times \mathbb{R}^2$ in the near-horizon IR (as shown in [D'Hoker and Kraus, 2009], say). It is described by the following metric and gauge field

$$\begin{aligned} ds^2 = G_{ab}dX^a dX^b = -r^2 f(r)dt^2 + \frac{dr^2}{r^2 f(r)} + e^{2V(r)}(dx^2+dy^2) + e^{2W(r)}dz^2\,, \\ B = h(r)dt\wedge dz \qquad \text{with} \qquad \star_5 H = \mathscr{B} dx\wedge dy \end{aligned} \tag{26}$$

Roughly speaking, the two bulk fields G_{ab} and B_{ab}, asymptote to $g_{\mu\nu}$ and $b_{\mu\nu}$ respectively, which then source the currents, $T^{\mu\nu}$ and $J^{\mu\nu}$,

$$\langle T_{\mu\nu}\rangle \equiv \frac{2}{\sqrt{-g}}\frac{\delta S}{g_{\mu\nu}}\,, \qquad \langle J_{\mu\nu}\rangle \equiv \frac{1}{\sqrt{-g}}\frac{\delta S}{b_{\mu\nu}} \tag{27}$$

The indices a,b denote the bulk coordinates while μ,ν denote the boundary coordinates. The generating functional takes the form

$$Z[g_{\mu\nu},b_{\mu\nu}] = \left\langle \exp\left[i\int d^4x\sqrt{-g}\left(T^{\mu\nu}g_{\mu\nu} + J^{\mu\nu}b_{\mu\nu}\right)\right]\right\rangle, \tag{28}$$

and diffeomorphism invariance and gauge symmetry lead to the following equations,

$$\nabla_\mu\langle T^{\mu\nu}\rangle = \frac{1}{2}(db)^\nu_{\rho\sigma}\langle J^{\rho\sigma}\rangle\,, \qquad \nabla_\mu\langle J^{\mu\nu}\rangle = 0. \tag{29}$$

Here $H = db$ is the three-form field strength of the two-form external source, while the boundary two-form current $J_{\mu\nu}$ corresponds to the projection of the bulk three-form field strength, $n^a H_{a\mu\nu}$.

Performing a near-boundary expansion of the metric in the Fefferman-Graham coordinates [de Haro et al., 2001],

$$\begin{aligned} ds^2 = G_{ab}dX^a dX^b &= \frac{d\rho^2}{4\rho^2} + \gamma_{\mu\nu}(\rho,x)dx^\mu dx^\nu \\ &= \frac{d\rho^2}{4\rho^2} + \frac{1}{\rho}g_{\mu\nu}(\rho,x)dx^\mu dx^\nu, \end{aligned} \tag{30}$$

it was found in [Grozdanov et al., 2019] that the leading divergence of $B_{\mu\nu}$ is logarithmic, that is,

$$B_{\mu\nu}(\rho,x) = B^0_{\mu\nu}(x) + B^1_{\mu\nu}(x)\ln\rho + \mathscr{O}(\rho), \tag{31}$$

where $B^0_{\mu\nu}(x)$ and $B^1_{\mu\nu}(x)$ are just expansion coefficients at the moment. Although it appears at first glance that $B^0_{\mu\nu}(x)$ should be interpreted as the boundary source, we see that its value is actually ambiguous as it runs logarithmically near the boundary, which in turn implies that the physics depends upon the value of ρ at which the boundary conditions are applied. The definition of the source requires mixed boundary conditions, a common feature for the fields with this type of near-boundary behaviour where the counter term also plays the role of the double-trace deformation [Witten, 2001, Berkooz et al., 2002], see also [Hofman and Iqbal, 2018, Grozdanov and Poovuttikul, 2019] for discussion in the current context. The regularised source is thus defined as,

$$b_{\mu\nu} = B_{\mu\nu}(\Lambda) - \frac{1}{\kappa(\Lambda)}\langle J_{\mu\nu}\rangle , \qquad \text{with} \qquad \langle J^{\mu\nu}\rangle = -\sqrt{-G}n_\alpha H^{\alpha\mu\nu} . \tag{32}$$

Mapping $J^{\mu\nu}$ to the more familiar *dynamical* field strength via the Hodge dual, one can see that the double-trace deformation plays a role similar to the Maxwell term for the dynamical gauge field in the dual QFT with $1/\kappa(\Lambda)$ as a (logarithmically running) electromagnetic coupling. We can see that the boundary is now labelled by two parameters, Λ, and κ. Requiring the source $b_{\mu\nu}$ to be independent of the UV cutoff, that is, $\frac{\partial b_{\mu\nu}}{\partial \Lambda} = 0$, fixes the form of the 'coupling constant' $1/\kappa(\Lambda)$ which turns out to be logarithmically running.

$$\frac{1}{\kappa} = \frac{1}{\kappa'} + \ln\left(\frac{\Lambda'}{\Lambda}\right) , \tag{33}$$

where κ is the value of the coupling constant at a cut-off Λ, while κ' is the value it takes at another cut-off Λ'. The RG-invariant length scale on which physical variables should depend is then given by

$$r_\star = \Lambda e^{\frac{1}{\kappa}} . \tag{34}$$

A more detailed explanation of this idea is provided in 5.1.

In [Poovuttikul and Rajagopal, 2021], we use the above holographic model to explicitly evaluate the life time of (non-conserved) electric flux in a strong magnetic field regime in order to ascertain the regime of validity of Force-Free Electrodynamics.

3 Part II : Non-relativistic fluids

As mentioned in the introduction 1, hydrodynamics is formulated as a gradient expansion of conserved currents under the assumption that the derivative corrections to them are small compared to some intrinsic length scale of the microscopic system. The possible terms that appear in this expansion are restricted by the symmetries of this system. Thus, most standard formulations of hydrodynamics involve some kind of boost symmetry in order to simplify the system. However, it is not necessary to assume this, and many physical systems around us, be it the flocking mechanism of birds [Toner et al., 2005], various models of active matter [Hatwalne et al., 2004, Callan-Jones and Jülicher, 2011], or even condensed matter systems such as strange metals [Huang et al., 2015] and electron transport in graphene [Lucas and Fong, 2018], do not boast of this advantage. The lack of boost symmetry implies that the velocity of the fluid is a parameter of the theory and cannot be set to zero by simply changing the frame of reference.

There has been considerable recent interest in extending fluid theory to systems with unconventional symmetries, including Lifshitz scale symmetry, with potential applications to quantum critical systems [Hoyos et al., 2013, 2014, Kiritsis and Matsuo, 2015, Hartong et al., 2016]. Motivated by these developments, we considered the following two problems. We first studied out of equilibrium energy transport in Lifshitz fluids, that exhibit translational, rotational and *scaling* symmetry, but not boost invariance in [Fernández et al., 2019]. We showed that a non-equilibrium steady state (NESS), of the type seen previously in a relativistic scale invariant fluid, will also develop in non-relativistic quantum critical fluids when two reservoirs are brought into contact across a hypersurface. Using simple scaling arguments for a Lifshitz fluid with generic dynamical exponent z, we solved for the fluid variables in the central region between the reservoirs. We found that a NESS forms in this case as well, but the solution is genuinely non-thermal. Armed with a scale consistent equation of state for such a system, we were led to the interesting question of finding a dual gravitational description of non-equilibrium steady states of perfect Lifshitz fluids with generic z. This brings us to our second problem where we analysed the thermodynamics of a such a fluid in a holographic context by studying the hydrodynamics of a Lifshitz black brane characterised by generic z, moving with a velocity v in one of the transverse directions. We found a physically distinct class of moving Lifshitz black branes where the velocity of the boosted brane plays the role of chemical potential, dual to the momentum density.

The following sections are meant to provide a general background for the above. For a detailed breakup of the matter covered in each section, please refer to the end of 1.

3.1 Non-relativistic and relativistic symmetries and algebras

In this section, I will briefly review the relevant symmetry groups and their algebras which might be a useful reference for the rest of this thesis.

1. Relativistic spacetime symmetry groups

   Relativistic field theories are invariant under the Poincaré group consisting of spacetime translations, P^{μ} and Lorentz transformations, $M^{\mu\nu}$:

$$P^{\mu}: \quad x^{\mu} \to x'^{\mu} = x^{\mu} + a^{\mu}, \tag{35}$$

$$M^{\mu\nu}: \quad x^{\mu} \to x'^{\mu} = \Lambda^{\mu}_{\nu} x^{\nu}, \tag{36}$$

   where $\Lambda \in SO(d,1)$ and a^{μ} parametrises the translations. In addition, the theory can enjoy enhanced symmetry under scaling and conformal transformations, generated by the following operators:

$$\hat{\mathscr{D}}: \quad x^{\mu} \to x'^{\mu} = \lambda x^{\mu}, \tag{37}$$

$$K^{\mu}: \quad x^{\mu} \to x'^{\mu} = \frac{x^{\mu} + k^{\mu} x \cdot x}{1 + 2k \cdot x + k^2 x^2}. \tag{38}$$

   Here $\lambda \in \mathbb{R}$ parametrises the dilatations while the latter generates special conformal transformations parametrised by $k^{\mu} \in \mathbb{R}^d$ (an inversion of spacetime followed by a translation and another inversion). This theory is conformally invariant and the conformal group is $SO(d,2)$ in d spacetime dimensions. The commutation relations between the various generators are as follows:

$$
\begin{aligned}
&[P^{\mu}, P^{\nu}] = 0\,, \\
&[P_{\rho}, M_{\mu\nu}] = \eta_{\mu\rho} P_{\nu} - \eta_{\nu\rho} P_{\mu}\,, \\
&[M_{\mu\nu}, M_{\rho\sigma}] = \eta_{\nu\rho} M_{\mu\sigma} - \eta_{\mu\rho} M_{\nu\sigma} + \eta_{\sigma\nu} M_{\rho\mu} - \eta_{\sigma\mu} M_{\rho\nu}\,, \\
&[\hat{\mathscr{D}}, P_{\mu}] = P_{\mu}\,, \\
&[\hat{\mathscr{D}}, M_{\mu\nu}] = [K_{\mu}, K_{\nu}] = 0\,, \\
&[\hat{\mathscr{D}}, K_{\mu}] = -K_{\mu}\,, \\
&[P_{\mu}, K_{\nu}] = 2(\eta_{\mu\nu}\hat{\mathscr{D}} - M_{\mu\nu})\,, \\
&[M_{\mu\nu}, K_{\rho}] = \eta_{\mu\rho} K_{\nu} - \eta_{\nu\rho} K_{\mu}.
\end{aligned}
\tag{39}
$$

2. Non-relativistic spacetime symmetry group

   A spatially isotropic and homogeneous non-relativistic theory is invariant under the following *Euclidean* transformations:

$$\hat{H}: \quad t \to t' = t + a, \tag{40}$$

$$\hat{P}^i: \quad x^i \to x'^i = x^i + b^i, \tag{41}$$

$$\hat{\mathscr{J}}_{ij}: \quad x^i \to x'^i = \hat{\mathscr{J}}^i_j x^j, \tag{42}$$

   where $a \in \mathbb{R}$, $b^i \in \mathbb{R}^d$ and $\hat{\mathscr{J}} \in SO(d)$ parametrise time translations, space translations and rotations respectively. The generators spanning the Lie algebra have the following commutation relations:

$$
\begin{aligned}
&[\hat{P}^i, \hat{P}^j] = [\hat{P}_i, \hat{H}] = [\hat{\mathscr{J}}_{ij}, \hat{H}] = 0\,, \\
&[\hat{P}_k, \hat{\mathscr{J}}_{ij}] = \delta_{ik}\hat{P}_j - \delta_{jk}\hat{P}_i\,, \\
&[\hat{\mathscr{J}}_{ij}, \hat{\mathscr{J}}_{kl}] = \delta_{jk}\hat{\mathscr{J}}_{il} - \delta_{ik}\hat{\mathscr{J}}_{jl} + \delta_{jl}\hat{\mathscr{J}}_{ik} - \delta_{il}\hat{\mathscr{J}}_{jk}.
\end{aligned}
\tag{43}
$$

   - In addition to the Euclidean symmetries, if the theory also possesses the following scaling symmetry,

$$\vec{x}' = \Lambda\vec{x}, \qquad t' = \Lambda^z t\,, \tag{44}$$

     where the dynamic exponent $z \in \mathbb{R}$ determines the anisotropy of scaling, then various commutation relations are given by,

$$\begin{aligned} [\hat{\mathscr{D}}, \hat{H}] &= zH\,, \\ [\hat{\mathscr{D}}, \hat{P}_i] &= \hat{P}_i\,, \\ [\hat{\mathscr{D}}, \hat{\mathscr{J}}_{ij}] &= 0. \end{aligned} \tag{45}$$

- In addition to the Euclidean transformations, the system can also be invariant under Galilean transformations,

$$\hat{G}^i : \quad x^i \to x'^i = x^i - v^i t. \tag{46}$$

The generator has the following Lie algebra,

$$\begin{aligned} [\hat{G}_i, \hat{G}_j] &= 0\,, \\ [\hat{G}_i, \hat{P}_i] &= 0. \end{aligned} \tag{47}$$

Furthermore, the Galilei algebra allows for a central extension, known as the Bargmann algebra [Lax, 1972], by the inclusion of an additional symmetry generator $\hat{\mathscr{M}}$, such that the non-vanishing Galilean boost commutators are given by

$$\begin{aligned} [\hat{\mathscr{J}}_{ij}, \hat{G}_k] &= \hat{G}_j\,\delta_{ij} - \hat{G}_i\,\delta_{jk}\,, \\ [\hat{H}, \hat{G}_i] &= \hat{P}_i\,, \\ [\hat{P}_i, \hat{G}_j] &= \hat{\mathscr{M}}\,\delta_{ij}\,. \end{aligned} \tag{48}$$

- A non-relativistic, scale-invariant group that comprises of the generators of centrally extended Galilean group, a.k.a the Bargmann group $\{\hat{H}, \hat{P}_i, \hat{\mathscr{J}}_{ij}, \hat{G}_i, \hat{\mathscr{M}}\}$ along with the generator of the Lifshitz dilatations is the Schrödinger algebra involving the generators $\{\hat{H}, \hat{P}_i, \hat{\mathscr{J}}_{ij}, \hat{G}_i, \hat{\mathscr{M}}, \hat{\mathscr{D}}_z\}$. For the special case of $z = 2$, Bargmann algebra can be be further extended to Schrödinger algebra with a single special conformal transformation (see eg. [Taylor, 2016]) involving the set $\{\hat{H}, \hat{P}_i, \hat{\mathscr{J}}_{ij}, \hat{G}_i, \hat{\mathscr{M}}, \hat{\mathscr{D}}_{(z=2)}, K\}$ (38). In fact, the Schrödinger algebra derives its name from the fact that for $z = 2$ it is the symmetry group of a free particle described by the Schrödinger equation.

A key observation is that Lifshitz symmetry with generic $z > 1$ is in general *not* compatible with boost symmetry. Indeed, Lorentzian boost symmetry is only compatible with $z = 1$, which gives the scaling $\vec{x}' = \Lambda\vec{x}$, $t' = \Lambda t$ and the no-go result of [de Boer et al., 2018] implies that the Galilean boost symmetry (44) is only compatible with $z = 2$ Lifshitz scaling. As explained above, non-relativistic fluids with dynamical exponent $z = 2$ and $z \neq 2$ behave differently under group transformations. For this reason, when discussing the out of equilibrium dynamics of non-relativistic fluids, we will consider the two cases separately, leading to different conclusions about the nature of the emergent steady state.

3.2 Thermodynamics and stress-energy tensor

For simplicity, below I will focus on the special case of perfect fluids. These are idealised fluids, that are without shear, strain or bulk viscosity and do not conduct heat. Based on the considerations above, I will consider a fluid whose description is invariant under time and space translations as well as rotations. In addition, I will also assume a global $U(1)$ symmetry whose corresponding conserved charge is N. This is realized by the basic set of generators $\{\hat{H}, \hat{P}_i, \hat{\mathscr{J}}_{ij}, \hat{\mathscr{M}}\}$. Additional symmetries under boosts and rescaling will be considered below.

Global quantities in this fluid include the energy E, momentum $\vec{\mathbb{P}}$, entropy S and charge N. Locally, we have the energy density $\mathscr{E} = E/V$, momentum density $\mathscr{P}_i = \mathbb{P}_i/V$, entropy density $s = S/V$ and charge density $n = N/V$. Assuming a configuration where these can be uniformly defined, the fundamental thermodynamic relations relating the change of the internal energy to the changes in the rest of the thermodynamic state functions are

$$\mathrm{d}E = T\,\mathrm{d}S - P\,\mathrm{d}V + v^i\,\mathrm{d}\mathbb{P}_i + \mu\,\mathrm{d}N\,, \qquad E = T\,S - PV + v^i\,\mathbb{P}_i + \mu\,N\,, \tag{49}$$

or, in terms of the associated densities,

$$\mathrm{d}\mathscr{E} = T\,\mathrm{d}s + v^i\,\mathrm{d}\mathscr{P}_i + \mu\,\mathrm{d}n\,, \qquad \mathscr{E} = T\,s - P + v^i\,\mathscr{P}_i + \mu\,n\,. \tag{50}$$

The thermodynamic forces associated to these parameters are the temperature T, the pressure P, the fluid velocity $\vec{v}$ and the chemical potential μ.

As argued in [de Boer et al., 2018], assuming a fluid with uniform velocity $\vec{v}$ in the presence of rotational symmetry, the momentum density must be proportional to the only directed quantity in the fluid, *i.e.* the velocity,

$$\mathscr{P}_i = \rho\, v_i\,, \tag{51}$$

and the above thermodynamic relation becomes

$$\mathrm{d}\mathscr{E} = T\,\mathrm{d}s + v^i\,\mathrm{d}(\rho\, v_i) + \mu\,\mathrm{d}n\,. \tag{52}$$

The quantity ρ is referred to as the kinetic mass density. In a theory with Galilean boost symmetry it is proportional to the charge density n but in the absence of boost symmetry the relation between n and ρ is more complicated.

The dynamical variables enter into the stress-energy tensor of the fluid $T^\mu{}_\nu$ and the current J^μ, whose conservation equations read[2]

$$\partial_\mu T^\mu{}_\nu = 0, \qquad \partial_\mu J^\mu = 0\,. \tag{53}$$

Classically the symmetry generators are realised by

$$\begin{aligned} H &= -\int_V \mathrm{d}^d x\, T^0{}_0(x)\,,\\ P_i &= \int_V \mathrm{d}^d x\, T^0{}_i(x)\,,\\ \mathscr{J}_{ij} &= \int_V \mathrm{d}^d x\, \left(x^i T^0{}_j(x) - x^j T^0{}_i\right)\,,\\ N &= \int_V \mathrm{d}^d x\, J^0(x)\,, \end{aligned} \tag{54}$$

which provides direct interpretation for various components of the stress-energy tensor and current. In particular, the energy density is $\mathscr{E} = -T^0{}_0$, the momentum density is $\mathscr{P}_i = T^0{}_i$, and the charge density is $n = J^0$ in any frame.

For a *perfect fluid* there exists a reference frame, the rest frame, in which there is no momentum density. The charge current then reduces to just the charge density and the stress-energy tensor involves only two parameters, the energy density and pressure. Explicitly, in this frame we have

$$T^\mu{}_\nu = \begin{pmatrix} -\mathscr{E}_0 & 0 \\ 0 & P\,\delta^i_j \end{pmatrix}, \qquad J^\mu = (n, 0)\,. \tag{55}$$

[2]Despite the use of μ, ν indices, we are not assuming Lorentz symmetry and these indices are not to be raised or lowered using a spacetime metric.

In any other frame of reference the description will also depend on the velocity $\vec{v}$ and in the absence of boost symmetry the $\vec{v}$ dependence can be non-trivial.

If the perfect fluid has Lorentz boost symmetry, the stress-energy tensor and current in the moving frame are related to those in the rest frame by a Lorentz boost transformation (36). In case of a non-relativistic perfect fluid with Galilean boost symmetry under (46), the stress-energy tensor and current in the moving frame are obtained from the following transformation rules [de Saxcé and Vallée, 2012],

$$T'^{\mu}{}_{\nu} = \frac{\partial x'^{\mu}}{\partial x^{\rho}} \frac{\partial x^{\sigma}}{\partial x'^{\nu}} \left(T^{\rho}{}_{\sigma} + J^{\rho}\,\Gamma_{\sigma}\right), \qquad J'^{\mu} = \frac{\partial x'^{\mu}}{\partial x^{\rho}} J^{\rho}, \tag{56}$$

where we define $\Gamma_{\mu} = \left(\frac{1}{2}|v|^2, -\vec{v}\right)$. Note that the transformation of $T^{\mu}{}_{\nu}$ is a linear combination a general coordinate transformation and a local Galilean boost. It is possible to combine $T^{\mu}{}_{\nu}$ and J^{μ} into an $d \times (d+1)$ dimensional object $\tilde{T} = (T, J)$ which acts as a tensor.[3] The conservation equations (53) are merged into one, and spacetime is embedded into a higher-dimensional construction of Bargmannian coordinates where a tensorial description arises naturally. For an overview of this description in the context of Bargmann theory, see [de Saxcé and Vallée, 2012] and [de Saxcé, 2016]. The stress tensor defined in this manner is thus gauge invariant but not boost invariant.

Applying (56) to a perfect fluid which is flowing at constant velocity $\vec{v}$, and described in the rest frame by (55), we obtain the following stress-energy tensor and current components [Jensen, 2015]

$$\begin{aligned} T^{0}{}_{0} &= -\mathscr{E}, \\ T^{0}{}_{j} &= n\,v_{j}, \\ T^{i}{}_{0} &= -(\mathscr{E} + P)v^{i}, \\ T^{i}{}_{j} &= P\,\delta^{i}_{j} + n\,v^{i} v_{j}, \\ J^{0} &= n, \\ J^{i} &= n\,v^{i}, \end{aligned} \tag{57}$$

where $\mathscr{E} = \mathscr{E}_0 + \frac{1}{2} n v^2$ adds kinetic energy to the internal energy $\mathscr{E}_0$. From the off-diagonal components we read off the momentum density $\mathscr{P}_i = T^{0}{}_{i} = n\,v_i$, which fixes the coefficient in (51) to be $\rho = n$.

[3] Due to the last relation in (48), which relates the charge operator to a commutator of boosts and spatial translations, the conserved charges should ideally be arranged into a single object, not into two separate ones. For the Poincaré group, we have $[\hat{P}_i, \hat{L}_j] = \hat{P}_0\,\eta_{ij}$, so in the context of special relativity $\tilde{T}$ automatically decomposes into the tensors $T^{\mu}{}_{\nu}$ and J^{μ}.

This last observation can also be obtained from the Ward identity corresponding to Galilean boost symmetry. The boost generator can be written as $\hat{G}_i = t\,\partial_i = G^{\mu}{}_i\partial_{\mu}$. Due to the non-vanishing Poisson bracket $[\hat{P}_i, \hat{G}_j]$ in (48), the boost current is $b^{\mu}{}_i = t\,T^{\mu}{}_i - x_i\,J^{\mu}$ and the associated Ward identity gives $T^0{}_i = J_i$ [Festuccia et al., 2016b], from which $\rho = n$ follows. The physical interpretation is that the flow of matter gives rise to momentum density and the inhomogeneous term in the transformation of the stress-energy in (56) accounts for the addition of momentum density under Galilean boosts.

When we considered critical fluids with generic z in [Fernández et al., 2019], we did not assume any boost invariance, and the kinetic mass density ρ and the particle number density n are no longer identified with each other. Instead, we adopted a formalism where they appear separately in the stress-energy tensor and the current [de Boer et al., 2018],

$$T^{\mu}{}_{\nu} = \begin{pmatrix} -\mathscr{E} & \rho\, v^i \\ -(\mathscr{E}+P)\, v^i & P\,\delta^{ij} + \rho\, v^i v^j \end{pmatrix}, \qquad J^{\mu} = \left(n, n\, v^i\right), \tag{58}$$

and then studied out of equilibrium evolution.

The Lifshitz scaling relation (44) with $z \neq 1$ implies that space and time coordinates have different scaling behavior and this affects how scaling analysis is carried out. The energy is a conserved quantity associated to time translations, so it must scale as the inverse of time, and thus the energy density scales as $\mathscr{E}' = \Lambda^{-(d+z)}\mathscr{E}$. On the other hand, the individual terms in the thermodynamic relation (52) must all have the same scaling and from there one can infer the scaling behavior of the various thermodynamic variables of the Lifshitz fluid:

$$\begin{array}{llll} \mathscr{E}' = \Lambda^{-d-z}\mathscr{E}\,, & P' = \Lambda^{-d-z}P\,, & T' = \Lambda^{-z}T\,, & \mu' = \Lambda^{-z}\mu\,, \\ s' = \Lambda^{-d}\,s\,, & n' = \Lambda^{-d}\,n\,, & \rho' = \Lambda^{-d+z-2}\rho\,, & v' = \Lambda^{1-z}\,v\,. \end{array} \tag{59}$$

Note that it is only for $z = 2$ that the kinetic mass density scales in the same way as the charge density.

The symmetry under Lifshitz scaling (44) leads to the Ward Identity, $z\,T^0_0 + T^i_i = 0$, which in turn implies the equation of state

$$d\,P = z\mathscr{E} - \rho\, v^2\,, \tag{60}$$

where d is the number of spatial dimensions. For the particular case of $z = 2$, the equation of state reduces to $d\,P = 2\,\mathscr{E} - n\,v^2$ and it is easy to see that a Galilean boost of the form

(56) to the rest frame gives the equation of state for a fluid at rest $dP = 2\mathscr{E}$. However, as mentioned above, scale invariance with generic dynamical critical exponent z is incompatible with Galilean boost invariance which we showed explicitly in [Fernández et al., 2019]. In that case, the thermodynamic variables of a uniformly moving fluid are *not* equivalent to those of an equilibrium configuration viewed in a moving reference frame, and transforming to the LAB frame gives the equation of state $dP = 2\mathscr{E}_{ref}$.

3.3 Non-equilibrium steady states in quantum critical systems with Lifshitz scaling

While developing a general fluid dynamics formalism for systems that are far from thermal equilibrium remains an open problem, there has been interesting recent progress in this direction involving relativistic fluids. Investigating out of equilibrium energy transport between two relativistic quantum critical heat baths led to the discovery of the emergence of a universal Non-Equilibrium Steady State (NESS) between the two heat baths [Bernard and Doyon, 2012, Bhaseen et al., 2015, Lucas et al., 2016b, Spillane and Herzog, 2016, Pourhasan, 2016]. A Non-Equilibrium Steady State (NESS) is a state that might be attained by out of equilibrium systems that are subject to a constant external driving force. While the thermodynamic parameters themselves are time-independent, there is a net non-zero entropy production, and a flow of conserved currents across the region. In [Bhaseen et al., 2015], using a combination of gauge-gravity duality, relativistic hydrodynamics and field theory techniques, the authors showed that the results for non-equilibrium thermal transport in relativistic conformal field theories for $d \geq 1$ were universal, and could be described by a Lorentz boosted thermal distribution. They considered a setup where two semi-infinite halves of the system that are independently thermalised at left and right temperatures T_L and T_R, are brought into thermal contact at time $t = 0$. They showed that these semi-infinite subsystems play the role of heat baths that drive a non-vanishing energy current $J_E = T^{tx}$ through the system, where $T^{\mu\nu}$ is the energy-momentum tensor. We extended this analysis to non-relativistic fluids with Lifshitz scale symmetry in [Fernández et al., 2019], and found that a NESS emerges here as well. We found that for the special case of a Lifshitz fluid with dynamical critical exponent $z = 2$, the resulting NESS can be viewed as a Galilean boost of a thermal state. For Lifshitz fluids with $z \neq 2$, there is no underlying boost symmetry [de Boer et al., 2018]. It turns out there is still an emergent

NESS at generic z, but in this case it cannot be obtained as a boosted thermal state.

In Section 3.4, I will describe the setup that we used in [Fernández et al., 2019] in bringing together two quantum critical Lifshitz fluids into thermal contact at time $t = 0$, and the corresponding NESS that develops between the two. I will also briefly explain how this setup is in fact nothing but the well known Riemann problem in fluid dynamics. In Section 3.5, I will briefly review the theory of shock and rarefaction waves that appear at the discontinuity, and the stability conditions that favour the formation of one over the other.

3.4 Local quench between semi-infinite heat baths

The specific system we consider consists of two semi-infinite heat reservoirs in d spatial dimensions, which are brought into contact at time $t = 0$ across a flat interface orthogonal to the x-coordinate axis. An equilibrium state of a charged quantum critical fluid is characterized by two energy scales, often taken to be the temperature and the chemical potential (due to scale invariance it is only the ratio T/μ that is physically relevant). In the case at hand, we find it convenient to instead use the pressure $P_{L,R}$ and charge density $n_{L,R}$ of the two reservoirs to describe the initial state,

$$P(t=0,x) = P_L\,\theta(-x) + P_R\,\theta(x)\,, \qquad n(t=0,x) = n_L\,\theta(-x) + n_R\,\theta(x)\,. \tag{61}$$

Here $\theta(x)$ denotes the usual Heaviside step function. Our solution to the resulting fluid dynamical problem will be expressed in terms of the scale invariant ratios P_L/P_R and n_L/n_R. In what follows, we will consider $P_L/P_R > 1$ without loss of generality, and arbitrary charge ratio, $0 < n_L/n_R < \infty$.

A local quench of this type, with sharp jump functions $\theta(x)$, can serve as a first step towards studying out of equilibrium dynamics in a fluid. The pressure difference between the two reservoirs drives a fluid flow between them. One might intuitively expect the sharp initial gradient to be steadily smoothed out with the system approaching local equilibrium in the central region, but at the level of leading order hydrodynamics this is not the case. Instead, as time evolves, a non-equilibrium steady state (NESS) occupies a growing region between the two heat baths, characterised by the presence of a non-zero, constant energy flow, as was discussed in [Bernard and Doyon, 2012, Taroni, 2014]. The properties of the NESS are constrained by the equation of state of the heat baths and the conservation of the stress energy tensor and the charge current across the wavefronts, which emanate from the contact region (see Figure 3.3).

An initial value problem in hydrodynamics with piecewise constant initial data, where two fluids at equilibrium are joined across a discontinuity, is an example of a so-called Riemann problem [Riemann, 1860] in the theory of partial differential equations. A solution, which generically involves shock and rarefaction waves propagating outwards from the initial discontinuity, can be found via the techniques described in Section 3.5, allowing the fluid variables that characterise the resulting non-equilibrium steady state to be determined in terms of the relevant input data. A Riemann problem for a relativistic quantum critical fluid in general dimensions was studied in [Bhaseen et al., 2015]. Initially, both outgoing wavefronts were assumed to be shockwaves but it was later realized [Lucas et al., 2016b, Spillane and Herzog, 2016] that above two spacetime dimensions, a solution with one shockwave and one rarefaction wave is preferred, based on entropy arguments and backed by numerical analysis. The existence and universality of the steady state for higher dimensional CFTs was studied in [Chang et al., 2014].

3.4.1 Formulation of the Riemann problem

In the present Riemann problem, the heat reservoirs are brought into contact across a planar surface, that we can take to be orthogonal to the x-axis. Following [Bernard and Doyon, 2012, Taroni, 2014], we look for a solution with wave fronts, traveling in the x-direction, that separate space into regions.

1. A region on the left, with the fluid at rest and stress-energy tensor as in (55) with $\mathscr{E}_L$, P_L and n_L.

2. Steady state region (or regions) in the middle, with the fluid flowing at a *constant* flow velocity $\vec{v}$, and stress-energy tensor as in (57) with $\mathscr{E}_s$, P_s and n_s.

3. A region on the right, with the fluid at rest and stress-energy tensor as in (55) with $\mathscr{E}_R$, P_R and n_R.

Drawing from the expressions presented in (57), in each region the conservation equations (53) take the following form:

$$\begin{aligned} \partial_t \mathscr{E} + \partial_i \left((\mathscr{E} + P) v^i \right) &= 0, \\ \partial_t (\rho v^i) + \partial_j (P + \rho v_i v^j) &= 0, \\ \partial_t n + \partial_j (n v^j) &= 0. \end{aligned} \tag{62}$$

These equations are supplemented with the equation of state (60) that relates $\mathscr{E}$ and P in a way that reflects the scaling symmetry of the fluid system.
Thus, the dynamics is governed by a set of hyperbolic conservation laws of the form

$$\partial_t \phi + \partial_i f = 0, \tag{63}$$

where ϕ and f are functions of the same fluid variables and $f(t,x)$ represents the flux of the conserved quantity $\phi(t,x)$. In our non-relativistic quantum critical fluid, the conserved quantities are charge, momentum and energy densities, and the resulting conservation equations (62) may be written as

$$\partial_t \begin{pmatrix} \mathscr{E} \\ \rho v \\ n \end{pmatrix} = \partial_x \begin{pmatrix} (\mathscr{E}+P)v \\ P+\rho v^2 \\ nv \end{pmatrix}. \tag{64}$$

Let us now discuss briefly the possible wave solutions that will emerge in this system.

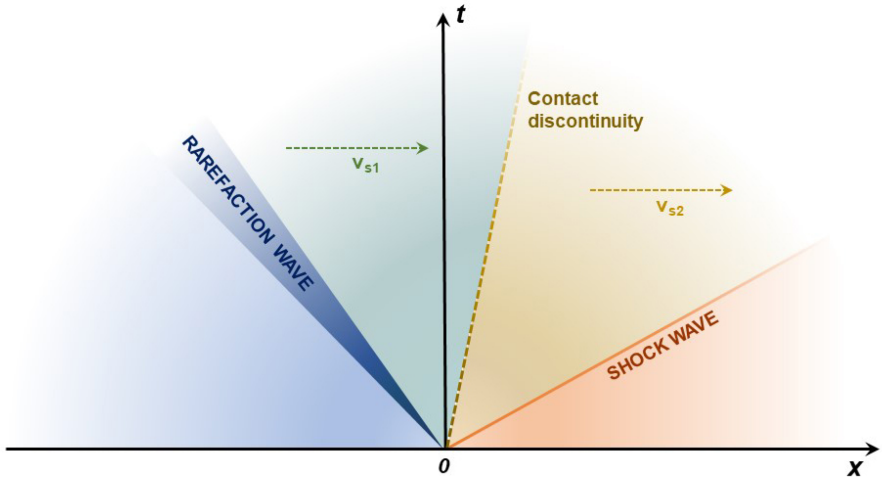

Figure 3.3. Propagation of shock, contact discontinuity and rarefaction waves for $P_L > P_R$. Here v_{s1} and v_{s2} denote the speed of the fluid flow between the rarefaction wave and contact discontinuity, and between the shock wave and contact discontinuity respectively.

3.5 Wave analysis

Generically, let us consider a conservation law of the form mentioned above,

$$\partial_t \phi + \partial_x f(\phi) = 0\,, \tag{65}$$

for a field $\phi(t,x)$, together with a piecewise constant initial condition:

$$\phi(0,x) = \begin{cases} \phi_L & \text{if } x < 0\,, \\ \phi_R & \text{if } x > 0\,. \end{cases} \tag{66}$$

This problem was first considered by Riemann in the 19th century [Riemann, 1860]. Note that for any given solution of this problem $\phi_{\text{sol}}(t,x)$, the rescaled function $\phi_\theta(t,x) = \phi_{\text{sol}}(\theta t, \theta x)$ is also a solution for any $\theta > 0$. In fact, the initial condition (66) selects, out of all possible solutions of the conservation equations, those which are invariant under such a scaling transformation. These solutions are constant along rays emanating from the origin $(t = 0, x = 0)$ due to the scaling, and they can generically be understood in terms of waves.

3.5.1 Linear problem

In the problem we will be considering, ϕ is a vector whose components are the energy density, pressure and fluid velocity, but, for the present discussion, we simply take it to be a generic vector of k components. A simple special case is obtained when $\partial_x f(\phi) \propto \partial_x \phi$, that is, for the strictly hyperbolic system

$$\partial_t \phi + A\, \partial_x \phi = 0\,, \tag{67}$$

where A is a matrix of constant coefficients. In this case, any solution can be written as a superposition of traveling waves. A generic initial condition $\phi(0,x) = \hat{\phi}(x)$ defines a wave profile that is shifted to the left and right as it evolves in time, in such a way that the height of the evolved profile at a given point is the sum (superposition) of heights at different points of the original profile.

The explicit solution takes the form

$$\vec{\phi}(t,x) = \sum_{i=1}^{k} \vec{r}_i\, \hat{\phi}_i(x - \lambda_i t)\,, \tag{68}$$

where λ_i are the eigenvalues of the matrix A, that determine the speed of propagation of each component of ϕ, while the coefficients of the superposition, $\vec{r}_i$, are the components of the corresponding eigenvectors of A, and they determine the direction of the rays along which the wave travels. By diagonalising the matrix, the problem is decomposed into k scalar Cauchy problems that can be solved separately.

3.5.2 Non-linear problem

More generally, the Jacobian in (65) is a function of ϕ itself,

$$A(\phi) = df(\phi) = \begin{pmatrix} \frac{\partial f_1}{\partial \phi_1} & \dots & \frac{\partial f_1}{\partial \phi_k} \\ \vdots & \dots & \vdots \\ \frac{\partial f_k}{\partial \phi_1} & \dots & \frac{\partial f_n}{\partial \phi_k} \end{pmatrix}. \tag{69}$$

This adds non-linearity to the problem. The solution can still be written in terms of waves, but the waves can interact with each other, producing additional waves. This is because the eigenvectors r_i are generalised into functions which depend on ϕ. The eigenvalues λ_i also depend on ϕ, and so the shape of the various components of the solution will vary in time, leading to wave dispersion and compression.

In [Lax, 1954], Lax provided a classification of the waves that can arise in non-linear wave problems with initial conditions of the form (66). To do so, he introduced a simplifying assumption: that each $\lambda_i(\phi)$, that is, the i^{th} eigenvalue of the Jacobian matrix (69), corresponds to either a *genuinely non-linear* wave, such that $\vec{\nabla}\lambda_i(\phi) \cdot \vec{r}_i(\phi) \neq 0$ for all ϕ, or to a *linearly degenerate* wave, such that $\vec{\nabla}\lambda_i(\phi) \cdot \vec{r}_i(\phi) = 0$ for all ϕ. The quantity $\vec{\nabla}\lambda_i \cdot \vec{r}_i$ can be understood as the directional derivative of $\lambda_i(\phi)$ in the direction of the vector $\vec{r}_i$.

As we will see below, this assumption holds in our Riemann problem for Lifshitz fluids and the resulting solutions have a simple structure consisting of different kinds of waves or discontinuities, which can be classified as follows:

• The linearly degenerate case $\vec{\nabla}\lambda_i \cdot \vec{r}_i = 0$, for which λ_i is constant along each integral curve of the corresponding field of eigenvectors r_i. In this case the profile of the solution does not change in time, generating a so-called contact discontinuity.

• The genuinely non-linear case with $\vec{\nabla}\lambda_i \cdot \vec{r}_i > 0$ such that the i^{th} eigenvalue λ_i is strictly increasing along the integral curve of the corresponding field of eigenvectors r_i. This leads to a rarefaction wave, displaying a smooth profile that widens and decays over time.

• The genuinely non-linear case with $\vec{\nabla}\lambda_i \cdot \vec{r}_i < 0$. This leads to a shock wave, displaying a compression which makes it become steeper over time.

When the simplifying assumption described above is valid, a set of stability conditions can be formulated which guarantee uniqueness and a continuous dependence on the initial data [Bianchini, 2003]. The one relevant for our analysis is Lax's shock wave admissibility condition [Lax, 1957], which can be easily visualised for the Riemann problem, where the initial configuration of $\phi(0,x)$ jumps from a left state ϕ_L to a right state ϕ_R at some value of x. The information contained in the piecewise initial condition propagates forward at speeds given by $\lambda_i(\phi_L)$ on the left and $\lambda_i(\phi_R)$ on the right. In order to prevent new characteristics spawning away from the shock interface, which would amount to non-uniqueness for our Cauchy problem, one must impose $\lambda_i(\phi_L) \geq \lambda_i(\phi_R)$. Furthermore, a shock wave connecting the states ϕ_L, ϕ_R moving at speed $\lambda = u_s$, must satisfy

$$\lambda_i(\phi_L) \geq u_s \geq \lambda_i(\phi_R) \,. \tag{70}$$

Lax's admissibility condition applies to shock waves but not to rarefaction waves. For a rarefaction wave, the solution's admissibility is determined by requiring $\lambda_i(\phi)$ to increase smoothly along the profile.

Given the conservation equations (64) and the equation of state (60), we are able to construct the Jacobian (69) for our system, and establish whether a given eigenvalue corresponded to a shock, rarefaction or contact discontinuity. We find that for the assumed initial condition $P_L > P_R$, the left-moving and right-moving waves correspond to rarefaction and shock waves respectively. Thereafter, we use the method of Riemann invariants (functions that remain constant along the integral curves of the eigenvector $\vec{r}_i$) for the smooth profile of the rarefaction wave to calculate the NESS variables to the left of the contact discontinuity in terms of the given initial data $\mathscr{E}_L$, P_L and n_L. For the sharp transitions that occur across the shock wave, we use Rankine-Hugoniot jump conditions [Lax, 1957, 1972] to establish the NESS variables to the right of the contact discontinuity in terms of $\mathscr{E}_R$, P_R and n_R. Finally, calculating the Riemann invariants for the contact discontinuity tell us that the pressure and speed must remain the same on either side of it. We then use this constraint to calculate all the NESS variables in terms of the initial conditions, thereby completing the construction of our non-equilibrium steady state. The details of these calculations can be found in sections 5 and 6 of [Fernández et al., 2019].

3.6 A moving Lifshitz black brane

The purpose of this section is to provide an introduction to the problem studied in [Rajagopal and Thorlacius, 2021], a description of the model and renormalisation scheme used therein, and a summary of the results obtained.

As mentioned in the Introduction 1, there is a need to widen the scope of holography to include bulk spacetimes that are not asymptotically AdS, in order to probe strongly coupled non-relativistic systems. These include spacetimes such as Lifshitz, Schrödinger and hyperscaling violating geometries (characterized by the dynamical exponent z, which expresses the anisotropy between space and time on the boundary). In [Fernández et al., 2019], we studied out-of-equilibrium energy transport in a quantum critical fluid with Lifshitz scaling symmetry following a local quench between two semi-infinite fluid reservoirs. Using scaling arguments, we hypothesised an equation of state for a perfect Lifshitz fluid with an arbitrary dynamic exponent z, and no boost symmetry. In this paper, we propose to justify this equation via a gravitational dual realization of the hydrodynamics of a perfect Lifshitz fluid, for generic z, and in 4 spacetime dimensions, moving with a velocity v in one of the transverse directions. The fact that these fluids are non-boost invariant is of particular relevance, as it is indeed the case with many systems in nature. We were further motivated by the existence of quantum critical condensed matter systems with a general dynamical critical exponent $z \neq 2$, such as the heavy fermion metals discussed in [Wölfle et al., 2017, Abrahams and Wölfle, 2012]. Moreover, it provides an application to a concrete physical setup of a recently developed general formalism for perfect fluids without boost symmetry [de Boer et al., 2018].

We find the following results:

- A physically distinct class of moving Lifshitz black branes where the the velocity of the boosted brane plays the role of chemical potential, dual to the momentum density.
- A boundary stress tensor the components of which may be expressed as the dual fluid variables, energy density $\mathscr{E}$, pressure P, fluid velocity v^i, and kinetic mass density ρ.
- We find that the conservation law for the stress tensor of the non-relativistic fluid has a similar form to that posited in the Newton-Cartan theory [Christensen et al., 2014b,a, Hartong et al., 2015a]. In fact, we find that the Ward identity associated to the Lifshitz scaling leads to $z\mathscr{E} - \rho v^2 = dP$, which is exactly the equation

of state we hypothesised for a perfect Lifshitz fluid with an arbitrary dynamic exponent z [de Boer et al., 2018].

3.7 The bulk gravitational theory

In [Rajagopal and Thorlacius, 2021] we consider a holographic theory with Lifshitz scaling defined in 4 bulk space-time dimensions but our results can easily be generalised to an arbitrary number of dimensions. The model we work with is a simple variant of Einstein-Maxwell-Dilaton (EMD) theory, which consists of Einstein gravity along with a massless $U(1)$ gauge field, A_μ and a scalar dilaton field, ϕ. Using a normalisation where $16\pi G_4 = 1$, the action is given by,

$$S_0 = \int d^4x\sqrt{-g}\left[R - 2\Lambda - \frac{1}{2}(\partial\phi)^2 - \frac{1}{4}e^{\lambda\phi}F^2\right] + 2\int d^3x\sqrt{-\gamma}K, \tag{71}$$

where the last term is the usual Gibbons-Hawking-York boundary term, which is needed in order to have a well-defined variational problem for the metric. The equations of motion for (71) are,

$$R_{\mu\nu} - \frac{1}{2}Rg_{\mu\nu} + \Lambda g_{\mu\nu} = T^{\phi}_{\mu\nu} + T^{(1)}_{\mu\nu} \tag{72}$$

$$\nabla^2\phi - \frac{\lambda}{4}e^{\lambda\phi}F_{\mu\nu}F^{\mu\nu} = 0 \tag{73}$$

$$\nabla_\mu e^{\lambda\phi}F^{\mu\nu} = 0, \tag{74}$$

with,

$$T^{\phi}_{\mu\nu} = \frac{1}{2}\partial_\mu\phi\partial_\nu\phi - \frac{1}{4}g_{\mu\nu}(\partial\phi)^2, \tag{75}$$

$$T^{F}_{\mu\nu} = \frac{1}{2}e^{\lambda\phi}\left(F_{\mu\sigma}F^{\sigma}_{\nu} - \frac{1}{4}g_{\mu\nu}F_{\sigma\rho}F^{\sigma\rho}\right). \tag{76}$$

Models of this kind were introduced in the context of non-relativistic holography in [Taylor, 2008]. While not the only model for Lifshitz holography available in literature, it has an important advantage in that there exists a full analytic solution to the field equations that describes a static black brane in asymptotically Lifshitz spacetime. The model can easily be generalized to include charged black brane solutions that are Lifshitz analogs of AdS-Reissner-Nordström black branes [Tarrio and Vandoren, 2011], which are key to a holographic dual description of non-relativistic quantum critical matter at finite temperature and chemical potential, see *e.g.* [Keranen and Thorlacius, 2012].

The model (71) admits the so-called Lifshitz spacetime as a solution,

$$ds^2 = l^2 \left(-r^{2z} dt^2 + \frac{dr^2}{r^2} + r^2 d\vec{x}^2 \right), \tag{77}$$

where l is a characteristic length scale of the geometry which we set to unity for notational simplicity. The metric exhibits the required Lifshitz scaling,

$$t \to \Lambda^z t\,, \qquad x \to \Lambda x\,, \qquad r \to \Lambda^{-1} r, \tag{78}$$

with $z \geq 1$. Spacetime geometries that are asymptotic to this metric provide a holographic dual description of a scale-invariant non-relativistic field theory formulated on a $\mathbb{R}^t \times \mathbb{R}^2$ boundary. The bulk theory can include matter fields of various types, which couple to the metric and possibly the dilaton field but, as we will see momentarily, do not couple directly to the background gauge field $F_{\mu\nu}$.

The metric (77) is a solution to the equations of motion provided the parameters of the model satisfy $\lambda = -\frac{2}{\sqrt{z-1}}$ and $\Lambda = -\frac{1}{2}(z+1)(z+2)$, and it is accompanied by a gauge field and dilaton background of the form,

$$A_t = \sqrt{\frac{2(z-1)}{z+2}} \left(\frac{r}{r_0} \right)^2 r^z, \qquad e^{\phi} = \left(\frac{r}{r_0} \right)^{2\sqrt{z-1}}, \tag{79}$$

where r_0 is an arbitrary constant. While this model has the advantage of analytic control, it has the disadvantage of a logarithmically running dilaton and diverging gauge field at the boundary. However, this is not a very serious disadvantage as long as the gauge field only serves to provide a background to support the Lifshitz geometry at the boundary and does not couple to any non-gravitational fields. Physical matter fields could be charged under additional gauge fields (not considered in the present case). In fact, A_μ should not be viewed as a gauge field but simply as a massless vector field that only interacts gravitationally (with a coupling that depends on the dilaton). With this in mind, we do not have to respect the $U(1)$ gauge symmetry of the bulk action in (71) when we construct boundary counterterms for holographic renormalisation of the model. Moreover, the model has a symmetry under a constant shift of the dilaton field while simultaneously absorbing a constant normalisation factor into the gauge field,

$$\phi \to \phi - \frac{2}{\lambda} \ln \alpha, \qquad A_\mu \to \alpha A_\mu\,. \tag{80}$$

This shift symmetry plays an important role when we construct boundary counter-terms for the holographic renormalisation of the model and it is also helpful in analysing the asymptotic behaviour of our bulk fields.

3.7.1 The moving brane

Along the lines of [Hartong et al., 2016], we would like to construct the gravitational dual of a perfect Lifshitz fluid moving at non-vanishing velocity. We are particularly interested in fluids at generic z, which do not have boost symmetry. In this case, it is not enough to perform a boost of the black brane along one of the transverse directions and study the associated thermodynamics as this does not give us a genuine dual of a moving Lifshitz fluid, but instead corresponds to studying a fluid at rest from a moving coordinate frame. The way around this is to construct from scratch, a bulk solution that describes a moving Lifshitz black brane at generic $z \neq 1$, with metric and gauge fields that encode the fluid momentum.

Consider a moving brane, such that one of the transverse directions, say, y direction is given a linear momentum. The metric becomes,

$$ds^2 = -F_1(r)r^{2z}dt^2 + \frac{dr^2}{r^2F_2(r)} + r^2F_3(r)dx^2 + F_4(r)(rdy + N(r)r^z dt)^2. \tag{81}$$

and the gauge field is now $A = r^z G_1(r)dt + G_2(r)(rdy + N(r)r^z dt)$. Note that this ansatz includes exact solution for a static black brane by simply setting $G_2 = N = 0$, $F_3 = F_4 = 1$, and letting $F_1 = F_2 = 1 - (r_h/r)^{z+2}$. The dilaton field of the black brane solution is unchanged from (79) provided we use the shift symmetry (80) to set r_0 equal to r_h, the radial location of the event horizon.

3.7.2 The reduced action and Noether charges

It is possible to reduce the action (71) to a one dimensional Lagrangian by performing a few integration by parts,

$$\begin{aligned} L_{1D} =& r^{z+1}\sqrt{F_1F_2F_3F_4}\Bigg(-2(z^2+2z+3)+\frac{1}{2}\frac{F_4N^2}{F_1}\Big(z-1+\frac{rN'}{N}\Big)^2-z\frac{rF_1'}{F_1} \\ & -(z+2)\frac{rF_2'}{F_2}-\frac{rF_3'}{F_3}-\frac{rF_4'}{F_4}+\frac{r^2}{2}\Big(\frac{F_1'}{F_1}\frac{F_3'}{F_3}+\frac{F_1'}{F_1}\frac{F_4'}{F_4}+\frac{F_3'}{F_3}\frac{F_4'}{F_4}\Big)-\frac{2\Lambda}{F_2}-\frac{1}{2}(r\phi')^2 \\ & +\frac{1}{2}e^{\lambda\phi}\Big(\frac{1}{F_1}(zG_1+rG_1'+G_2((z-1)N+rN'))^2-\frac{1}{F_4}(G_2+rG_2')^2\Big)\Bigg), \end{aligned} \tag{82}$$

where $' \equiv \frac{\partial}{\partial r}$. We found that there are two scaling symmetries that leave the above Lagrangian invariant. They are,

$$F_1 \to \alpha^2 F_1, \quad F_3 \to \alpha^{-1}F_3, \quad F_4 \to \alpha^{-1}F_4, \tag{83}$$

$$N \to \alpha^{\frac{3}{2}}N, \quad G_1 \to \alpha G_1, \quad G_2 \to \alpha^{-\frac{1}{2}}G_2 \tag{84}$$

And

$$F_3 \to \beta^2 F_3, \quad F_4 \to \beta^{-2}F_4, \tag{85}$$

$$N \to \beta N, \quad G_2 \to \beta^{-1}G_2. \tag{86}$$

They represent a diffeomorphism which preserves the volume element $dtdxdy$, and can thus be thought of as a Noether symmetry inherited by L_{1D}. They are also symmetries of the boosted metric ansatz (81), as long as the coordinates transform as $t \to \alpha^{-1}t$, $x \to \alpha^{\frac{1}{2}}x$, $y \to \alpha^{\frac{1}{2}}y$ and $x \to \beta^{-1}x$, $y \to \beta y$ respectively.

The two Noether charges associated with these symmetries are found to be,

$$\begin{aligned} Q_\alpha = & r^{z+2}\sqrt{F_1F_2F_3F_4}\Bigg(2(z-1)+\frac{r}{2}\Big(\frac{2F_1'}{F_1}-\frac{F_3'}{F_3}-\frac{F_4'}{F_4}\Big)-\frac{3}{2}\frac{F_4N^2}{F_1}\Big(z-1+\frac{rN'}{N}\Big) \\ & -\frac{1}{2}e^{\lambda\phi}\frac{G_2}{F_4}(G_2+rG_2')-e^{\lambda\phi}\Big(\frac{G_1}{F_1}+\frac{3}{2}\frac{G_2N}{F_1}\Big)\Big(zG_1+rG_1'+G_2N\Big(z-1+\frac{rN'}{N}\Big)\Big)\Bigg), \end{aligned} \tag{87}$$

$$Q_\beta = r^{z+2}\sqrt{F_1F_2F_3F_4}\Bigg(r\Big(\frac{F_3'}{F_3}-\frac{F_4'}{F_4}\Big)-\frac{F_4N^2}{F_1}\Big(z-1+\frac{rN'}{N}\Big)$$
$$-e^{\lambda\phi}\frac{G_2}{F_1}\Big(\frac{F_1}{F_4}(G_2+rG_2')+(zG_1+rG_1')N+G_2N^2\Big(z-1+\frac{rN'}{N}\Big)\Big)\Bigg) \tag{88}$$

The charges are combinations of bulk fields that do not depend on the radial bulk coordinate. This is particularly useful in relating horizon data to boundary data, and plays an important role in determining the thermodynamic equation of state when the exact interpolating solution is not known, as we will show below. In addition to the above symmetries, there is also a local gauge symmetry involving r diffeomorphisms, which we fix by setting $F_3(r) = 1$.

There is yet another conserved charge in our system associated with the shift symmetry of the dilaton (80). While it does not play a direct role in the thermodynamics, it will be useful later on when we consider solutions of the linearised field equations later on. It is given by,

$$Q_\phi = r^{z+2}\sqrt{F_1F_2F_3F_4}\Big(e^{\lambda\phi}\frac{G_2}{F_4}(G_2+rG_2')-e^{\lambda\phi}\frac{G_1}{F_1}\Big(zG_1+rG_1'+G_2N\Big(z-1+\frac{rN'}{N}\Big)$$
$$-\frac{2r\phi'}{\lambda}\Big) \tag{89}$$

3.8 Holographic Renormalisation

In this section, we work out the renormalised stress-energy tensor at the boundary from the renormalised EMD action, the conservation of which gives us the standard energy and momentum conservation equations. The generic form of a stress tensor for non-relativistic fluids has been discussed in 3.2. Along with the Gibbons-Hawking-York term required for a well-defined variational theory of gravity, the full action is given by

$$S = S_{bulk} + 2\int d^3x\sqrt{-\gamma}K, \tag{90}$$

where K is the extrinsic curvature and γ is the induced metric on the boundary. Its variation is then given by

$$\delta S = \int d^3x((K^{\alpha\beta} - K\gamma^{\alpha\beta})\delta\gamma_{\alpha\beta} - \pi_\alpha \delta A^\alpha - \mathscr{O}_\phi \delta\phi), \tag{91}$$

where,

$$\pi_\alpha = e^{\lambda\phi} n_\alpha F^{\alpha\beta}, \tag{92}$$

$$\mathscr{O}_\phi = n^\alpha \nabla_\alpha \phi \tag{93}$$

and n^α refers to the unit normal on the boundary as usual. In order for the action to be finite at the boundary, we need to add some local counter-terms to subtract the divergent pieces. Along the lines of [Ross and Saremi, 2009] (where the renormalisation was carried out for an Einstein-Maxwell-Proca model with a massive vector field), we propose to construct a non-relativistic stress tensor complex for our theory. The full renormalised action now has the following form,

$$S = S + S_{c.t}, \tag{94}$$

where the counter-term action is,

$$S_{c.t} = -\int d^3x \sqrt{-\gamma}(4 + \sqrt{2(z-1)(z+2)}\sqrt{-e^{\lambda\phi}A^2}) \tag{95}$$

The variation of the full action is then given by,

$$\delta S = \int d^3x (s_{\alpha\beta}\delta\gamma^{\alpha\beta} + s_\alpha \delta A^\alpha + s\delta\phi), \tag{96}$$

where,

$$s_{\alpha\beta} = \sqrt{-\gamma}\big(K_{\alpha\beta} - K\gamma_{\alpha\beta} + 2\gamma_{\alpha\beta} + \frac{\xi e^{\lambda\phi}}{2\sqrt{-e^{\lambda\phi}A^2}}(A_\alpha A_\beta - A^2\gamma_{\alpha\beta})\big), \tag{97}$$

$$s_\alpha = \sqrt{-\gamma}\big(\pi_\alpha + \frac{\xi e^{\lambda\phi}}{2\sqrt{-e^{\lambda\phi}A^2}} 2A_\alpha\big), \tag{98}$$

$$s = \sqrt{-\gamma}\big(-\mathscr{O}_\phi + \frac{\xi e^{\lambda\phi}}{2\sqrt{-e^{\lambda\phi}A^2}}\lambda A^2\big). \tag{99}$$

Here $\xi = \sqrt{2(z-1)(z+2)}$ has been introduced for simplifying the expressions. No further counterterms are needed to cancel the divergences for the problem at hand.

Requiring the action to be invariant under Lifshitz scaling leads to the following Lifshitz Ward identity,

$$zs^t_t + s^x_x + s^y_y + \frac{z-2}{2} s^t A_t - \sqrt{z-1}\, s = 0. \tag{100}$$

One can see from (78) that the space and time coordinates scale differently, disallowing the asymptotic boundary to be conformally invariant. One would thus like the different time scaling to be treated in a coordinate invariant way. It turns out that a convenient way to implement this is to work in an orthonormal frame rather than a coordinate frame. The boundary values of these frame fields then define the boundary data, which then serve as the sources for the stress tensor complex. The appropriate way to implement this variation (as shown in [Ross and Saremi, 2009] and in [Hollands et al., 2005] for the relativistic case) is to vary the boundary fields $\hat{e}^{(A)}_\alpha$ while keeping the tangent space indices of the other fields fixed. For the remainder of this section we shall follow the notation of [Ross and Saremi, 2009] as there are several points of similarity between the two cases. The capital letters $A, B, \dots$ used here denote tangent space indices. The bulk frame fields are related to their boundary counterparts via $e^{(0)}_\alpha = r^z \hat{e}^{(0)}_\alpha(r, x^\alpha)$, $e^{(I)}_\alpha = r\hat{e}^{(I)}_\alpha(r, x^\alpha)$ and $e^{(3)} = \frac{dr}{r}$, such that the boundary frame field components asymptote to finite values as $r \to \infty$. The variation of the bulk action (96) can then be written as,

$$\delta S = \int \sqrt{-h}((s^\alpha_\beta + s^\alpha A_\beta)e^\beta_{(B)}\delta\hat{e}^{(B)}_\alpha + s_B \delta A^B + \mathscr{O}_\phi \delta\phi), \tag{101}$$

where $\sqrt{-h}$ denotes the associated volume element on the boundary and $s^A = s^\alpha e^{(A)}_\alpha$. One can then relate the new stress tensor complex to the canonical momenta in the coordinate frame via a simple transformation,

$$T^\alpha_B = (2s^\alpha_B + s^\alpha A_\beta)e^\beta_{(B)}. \tag{102}$$

Varying the frame fields while keeping tangent space indices fixed is crucial, as that is what ensures that the off-diagonal pieces of the stress tensor complex are different, as required for a non-relativistic theory. As shown in [Ross and Saremi, 2009], the various components of the complex take the following form,

$$\mathscr{E} = 2s^t_t - s^t A_t, \qquad \mathscr{E}^i = 2s^i_t - s^i A_t, \tag{103}$$

$$\mathscr{P}_i = -2s^t_i + s^t A_i, \qquad \Pi^i_j = -2s^i_j + s^i A_j. \tag{104}$$

3.8.1 The asymptotic solution

Working in the orthonormal frame, it is useful to define the frame metric in the following way,

$$e^{(0)} = r^z \hat{e}^{(0)} = r^z H_1(r)dt + rv_1(r)dy, \tag{105}$$

$$e^{(1)} = r\hat{e}^{(1)} = rH_3(r)dx, \tag{106}$$

$$e^{(2)} = r\hat{e}^{(2)} = r^z v_2(r)dt + rH_4(r)dy, \tag{107}$$

$$e^{(r)} = \frac{dr}{rH_2(r)}. \tag{108}$$

We can choose the the frame field $e^{(0)}$ to be parallel to the projection of the gauge field along the boundary so it can have the following ansatz in the orthonormal frame,

$$A_0 = \sqrt{\frac{2(z-1)}{z+2}}\frac{r^2}{r_h^2}a_0(r), \qquad A_1 = A_2 = A_3 = 0. \tag{109}$$

This turns out to be quite useful as the boundary data in the spatial component of the gauge field is now absorbed by the frame fields, which then leads to independent $\mathscr{E}^i$ and $\mathscr{P}_i$ as required for a non-relativistic system [Ross, 2011, Ross and Saremi, 2009]. There is a straightforward mapping between the frame fields defined in (105)-(108) and coordinate fields (81), which we will use later to evaluate the Noether charges at the boundary. In order for the space-time to be asymptotically Lifshitz, we would require our small, constant perturbations to be such that $H_1(r), H_2(r), H_3(r), H_4(r)$ tend to unity as $r \to \infty$ while $v_1(r), v_2(r)$ and $a_0(r)$ vanish. Our ansatz for the black brane with linear momentum is such that all the fields depend only on the radial coordinate, r. We use a power law ansatz to solve for the linear fluctuations as all the terms turn out to have homogeneous powers in r. Working in the radial gauge and solving the linearised equations of motion near the Lifshitz fixed point, we find that that small fluctuations take the following form,

$$H_1 = 1 + \frac{c_1}{2} r^{-z-2} \tag{110}$$

$$H_2 = 1 + \frac{c_2}{2} r^{-z-2} \tag{111}$$

$$H_3 = 1 \tag{112}$$

$$H_4 = 1 + \frac{c_3}{2} r^{-z-2} \tag{113}$$

$$v_1 = c_{1y} r^{z-1} + \frac{c_{2y}}{r^3} + \frac{z+2}{3z} \frac{c_{3y}}{r^{2z+1}} \tag{114}$$

$$v_2 = \frac{c_{4y}}{r^{z-1}} + \frac{c_{2y}}{r^3} + \frac{c_{3y}}{r^{2z+1}} \tag{115}$$

$$a_0 = 1 + c_4 r^{-z-2} \tag{116}$$

$$\phi = 2\sqrt{z-1} \left(\ln \left(\frac{r}{r_h} \right) + \frac{c_5}{2} r^{-z-2} \right), \tag{117}$$

We find that the linearised field equations corresponding to the $-ty$ component of Einstein's tensor and the $-y$ component of Maxwell's equations decouple from the rest of the equations and can be solved separately. The general solution of the resulting 2×2 eigenvalue problem give the four eigenmodes listed in (114) and (115). The c_{1y} and c_{4y} modes are non-renormalisable source modes while c_{2y} and c_{3y} will appear in the momentum density and energy flux, respectively, in the renormalised stress energy complex.

The remaining linearised, coupled Einstein, Maxwell and dilaton equations can be solved for in a straightforward manner along the lines of [Keranen and Thorlacius, 2012]. The full linearised solution obtained by solving the 5×5 eigenvalue problem gives us eigenmodes that go as r^{-z-2} as well as $r^{\frac{1}{2}(-z-2\pm\sqrt{(z+2)(9z+10)})}$. A general holographic analysis of asymptotically Lifshitz space-times ([Ross and Saremi, 2009, Baggio et al., 2012, Zingg, 2011, Mann and McNees, 2011]) shows that a r^{-z-2} mode carries finite energy and is accordingly of primary interest in the analysis that follows. The remaining eigenmodes include a growing mode that would disrupt the asymptotic Lifshitz geometry and must therefore be absent in a physical solution and a mode that falls off at a faster rate than r^{-z-2} and can thus be ignored in our asymptotic analysis. Finally, we also leave out a constant mode which can be interpreted as a non-normalisable source mode.

Solving the eigenvalue problem for the mode corresponding to the relevant r^{-z-2}

mode gives us the following relations between the various constants,

$$c_2 = c_1 + c_3, \qquad c_5 = \frac{c_3}{2}. \tag{118}$$

Finally, conservation of the charge (89) that is associated with the shift symmetry of the dilaton field, gives an additional relation,

$$c_4 = \frac{c_1}{2} - \frac{z-2}{4} c_3. \tag{119}$$

This leaves us with two independent constants, c_1 and c_3, that determine the energy density and the pressure as we will see shortly.

3.9 Thermodynamics

We will now study the thermodynamics of the fluid that the above holographic dual is supposed to describe, that is, a perfect Lifshitz fluid whose description is invariant under time and space translations as well as rotations.

3.9.1 The near-horizon solution

We will use similar arguments to those made in [Hartong et al., 2016] to obtain a near-horizon expansion of the metric and gauge fields. As usual, the location of the horizon r_h is where g^{rr} vanishes. This means that F_2 will have a first order zero at r_h. Regularity of the metric in Eddington-Finklestein coordinates constrains F_1 to have a first order zero at r_h while requiring the gauge field to vanish at the horizon constrains G_1 similarly. The metric fields F_4 and N are free to have non-vanishing values at the horizon. Finally, apart from regularity, there are no constraints on the values of G_2 and ϕ here either. Thus an appropriate near-horizon Taylor series expansion of the various metric and gauge fields is given by (working in an $F_3 = 1$ gauge),

$$
\begin{aligned}
F_1 &= f_1 \frac{r-r_h}{r_h} + \dots \\
F_2 &= h_1 \frac{r-r_h}{r_h} + \dots \\
F_3 &= 1 \\
F_4 &= p_0 + p_1 \frac{r-r_h}{r_h} + \dots \\
N &= n_0 + n_1 \frac{r-r_h}{r_h} + \dots \\
G_1 &= g_1 \frac{r-r_h}{r_h} + \dots \\
G_2 &= m_0 + m_1 \frac{r-r_h}{r_h} + \dots \\
\phi &= l_0 + l_1 \frac{r-r_h}{r_h} + \dots .
\end{aligned}
$$

Then the near horizon metric is given by

$$ds^2 = -f_1 \rho r_h^{2z-1} dt^2 + \frac{d\rho^2}{r_h h_1 \rho} + r_h^2 dx^2 + p_0 r_h^2 (dy + N(r_h) r_h^{z-1} dt)^2, \tag{120}$$

where $\rho = r - r_h$. Making the following change of coordinates,

$$\tilde{\rho}^2 = \frac{4\rho}{r_h h_1}, \tilde{t} = (f_1 h_1)^{\frac{1}{2}} \frac{r_h^z t}{2}, \tag{121}$$

we get the following metric

$$ds^2 = -\tilde{\rho}^2 d\tilde{t}^2 + d\tilde{\rho}^2 + r_h^2 dx^2 + p_0 r_h^2 (dy + N(r_h) r_h^{z-1} dt)^2. \tag{122}$$

Thus, after going to Euclidean coordinates, the temperature is given by $T = \frac{r_h^z}{4\pi}(f_1 h_1)^{\frac{1}{2}}$. Using units where $16\pi G_N = 1$, the entropy is given by $s = \frac{A}{4G_N} = 4\pi p_0^{\frac{1}{2}} r_h^2$. So we have,

$$Ts = (p_0 f_1 h_1)^{\frac{1}{2}} r_h^{z+2}. \tag{123}$$

3.9.2 The static Lifshitz black brane

As a warm-up exercise, let us first study thermodynamics of a static Lifshitz brane with general z given by the static limit of (81) by evaluating the renormalised stress tensor at the boundary and using the method of Noether charges.

3.9.2.1

Plugging in the asymptotic solution (110)-(117) into the renormalised stress tensor complex (104) :

$$\mathscr{E}_0 = -2c_1, \tag{124}$$

$$\mathscr{E}_0^x = 0, \tag{125}$$

$$\mathscr{E}_0^y = 0, \tag{126}$$

$$\Pi^x_{x0} = zc_1, \tag{127}$$

$$\Pi^y_{y0} = zc_1, \tag{128}$$

$$\mathscr{P}_{y0} = 0. \tag{129}$$

The subscripts 0 denote the values that the various thermodynamic quantities take for the static fluid. One can easily verify that the scaling Lifshitz Ward identity (100) is satisfied. In fact, s_α and s vanish trivially for the static brane. Identifying c_1 and zc_1 as the internal energy and pressure P of the static brane, we obtain

$$z\mathscr{E}_0 = 2P, \tag{130}$$

which is the well-known equation of state for a perfect static Lifshitz fluid.

3.9.2.2

Plugging in the near horizon metric ansatz defined in (3.9.1) into our Noether charges obtained in (3.7.2), we find that while Q_β vanishes, Q_α can in fact be expressed in terms of the known horizon quantities, temperature T and entropy density s very simply,

$$Q_\alpha = Ts. \tag{131}$$

Plugging in the asymptotic metric ansatz (110)-(117) into the same Noether charge,

$$Q_\alpha = -(z+2)c_1. \tag{132}$$

Equating the right hand side of (131) and (132), and identifying $-c_1$ as $\frac{\mathscr{E}_0}{2}$, where $\mathscr{E}_0$ is the internal energy from (124), we get the exact Gibbs-Duhem relation expected for a Lifshitz fluid,

$$\mathscr{E}_0 = \frac{2}{z+2}Ts. \tag{133}$$

3.9.3 A moving Lifshitz brane

Let us now proceed to repeat the above exercise for the case of interest, that is, a Lifshitz black brane with a velocity along one of the transverse directions (which we choose to be the y direction without loss of generality).

3.9.3.1

Plugging in the asymptotic solution (110)-(117) into the renormalised stress tensor complex (104) and eliminating constants using (118) and (119):

$$\mathscr{E} = -2c_1 + zc_3, \tag{134}$$

$$\mathscr{E}^x = 0, \tag{135}$$

$$\mathscr{E}^y = -2(z-1)c_{3y}, \tag{136}$$

$$\Pi_x^x = zc_1 - \frac{1}{2}(z^2 - z - 2)c_3, \tag{137}$$

$$\Pi_y^y = zc_1 - \frac{1}{2}(z^2 + z + 2)c_3, \tag{138}$$

$$\mathscr{P}_y = -2(z-1)c_{2y}. \tag{139}$$

If we now identify $\mathscr{E}$ as the energy density and $\Pi_x^x = -P$ as the pressure of the system, $\Pi_y^y = -(P + \rho v^2)$ is the stress due to pressure and momentum flow along the $y-$ direction. Once again, plugging in the linearised modes into (100), one can verify that the Lifshitz Ward identity is satisfied, giving us the equation of state for a perfect Lifshitz fluid with an arbitrary scaling exponent,

$$z\mathscr{E} - \rho v^2 = 2P, \tag{140}$$

as hypothesised in [de Boer et al., 2018] and [Fernández et al., 2019]. The modes c_{2y} and c_{3y} appear only in the off-diagonal terms of the stress tensor complex and can be interpreted as the momentum density ρv and energy flux $(\mathscr{E} + P + \frac{1}{2}\rho v^2)v$ respectively. While they cannot be related with the other modes in the absence of an exact interpolating solution, it is safe to make this statement, as they show the exact scaling dimensions as required by (59).

3.9.3.2

Plugging in the near horizon metric ansatz defined in (3.9.1) into our Noether charges obtained in (3.7.2), we find that a simple linear combination of the two in fact gives us (123). Specifically,

$$Q_\alpha - \frac{3}{2}Q_\beta = Ts. \tag{141}$$

Plugging in the asymptotic metric ansatz (110)-(117) into the same Noether charges,

$$Q_\alpha = \frac{z+2}{2}(-2c_1 + zc_3), \tag{142}$$

$$Q_\beta = (z+2)c_3. \tag{143}$$

From (134) one can see that Q_α is equal to $\left(\frac{z+2}{2}\right)\mathscr{E}$ while from (137) and (138) it is clear that Q_β is equal to the difference of the pressure in the two transverse directions, that is, ρv^2. Let us rewrite (140) as,

$$\begin{aligned}\mathscr{E} + P &= \frac{z+2}{2}\mathscr{E} - \frac{1}{2}\rho v^2 \\ &= Q_\alpha - \frac{1}{2}\rho v^2.\end{aligned} \tag{144}$$

Then (141) simply gives us the well-known Gibbs-Duhem relation,

$$\mathscr{E} + P = Ts + \rho v^2. \tag{145}$$

Interpreting the various boundary data as field theory sources in this manner, we find that the velocity of the fluid v appears as the chemical potential conjugate to the momentum density ρv ([de Boer et al., 2018], [Hartong et al., 2016]).

4 Conclusion and Future Outlook

In this dissertation, we have tried to emphasise the role that symmetries play in physical systems, by moving away from the realm of standard relativistic hydrodynamics with a one-form $U(1)$ symmetry, and instead studying two very different problems. The first involves a reformulation of relativistic hydrodynamics in the language of higher form symmetries, and the other, involves a study of non-relativistic systems invariant under Lifshitz scaling (both with and without Galilean boost invariance). The motivation for studying the former comes from having the advantages of dealing with a purely symmetry-based formalism involving only macroscopic consistency, and not having to introduce additional microscopic gauge fields. The motivation for studying the latter comes from the existence of various quantum critical systems in nature that exhibit Lifshitz scaling, which deserves a much more thorough investigation.

I will now proceed to give a brief summary of the conclusions of the various problems considered in this thesis, the details of which are provided at the end of the respective articles.

In [Poovuttikul and Rajagopal, 2021], we studied the validity of the hydrodynamic description at low temperatures and strong magnetic field. Focusing on the holographic model that shares the same global symmetry as that of a plasma (that is, where energy, momentum and magnetic flux are the only conserved operators), we calculated the lifetime of the electric field operator in order to ascertain the regime in which Force-Free Electrodynamics is valid. We found that for electric flux $E_{\|}$ parallel to the magnetic field, the lifetime has a strong dependence on the double-trace coupling κ which plays a role similar to the renormalised electromagnetic coupling. In the extreme limit of $e_r^{-2} \gg |\mathbf{B}|/\mathbf{T^2}$, the lifetime can be large enough to be detectable by the analytic computation in both the 'usual' hydrodynamic regime $\omega/T \ll 1$ and even lower temperature regime where $\omega/\sqrt{\mathbf{B}} \ll 1$ while ω/T may remains finite. We found that the lifetime becomes shorter as one decreases the ratio of $T/\sqrt{|\mathbf{B}|}$. The latter indicates that the lifetime will become extremely short in the extremely strong magnetic field regime $T/\sqrt{|\mathbf{B}|} \ll 1$ and cannot interfere with the low energy regime of $\omega/\sqrt{|\mathbf{B}|} \ll 1$ where the FFE limit is thought to be applicable. For the component of electric flux $E_\perp$ perpendicular to the magnetic field, we find that there is no pole in the vicinity of $\omega/T \ll 1$ regime. The dependence of the lifetime on the renormalised electromagnetic coupling disappears as one enter the strong magnetic field limit. In the holographic context, it would be interesting to check if *all* the accessible non-conserved operator truly have parametrically short lifetime as well as confirming the low energy spectrum predicted by force-free electrodynamics (and its subsequent derivative corrections). One could also attempt to extract the FFE effective action from gravity along lines similar to [Nickel and Son, 2011, Glorioso et al., 2018, de Boer et al., 2019] or establish the full set of constitutive relations as in [Bhattacharyya et al., 2008, Banerjee et al., 2011, Erdmenger et al., 2009] as an even more definite proof of FFE description in the dynamically magnetised black brane geometry.

In [Fernández et al., 2019], we showed that a non-equilibrium steady state, as seen previously in a relativistic scale invariant fluid, will also develop in a charged non-relativistic Lifshitz quantum critical fluid when two reservoirs are brought into contact across a hypersurface. We showed that the non-relativistic NESS is bounded by an outgoing shock wave and on the other side by a rarefaction wave propagating in the opposite direction, consistent with Lax entropy conditions. In addition, we established that for the special case of $z = 2$ Lifshitz fluid, the theory can be obtained from a Galilean boost invariant theory and the NESS corresponds to that of a genuine boosted thermal state, while a Lifshitz fluid with generic $z \neq 1$ and $z > 2$, the theory does not enjoy boost symmetry and the corresponding NESS is not that of a boosted thermal state. While we have concentrated on perfect fluids without impurities or lattice effects which break translational invariance in this study, one could modify this to allow for diffusion and momentum relaxation in the hydrodynamics equations, to obtain the time scale up to which the non-relativistic NESS persists, along the lines of [Lucas et al., 2016b], say.

In [Rajagopal and Thorlacius, 2021], we studied the holographic dual of a perfect Lifshitz fluid with an arbitrary dynamical exponent, z, moving with a velocity, v, and found that the velocity appears as the chemical potential, conjugate to the dual momentum density. These represent a physically distinct class of black branes possessing a linear momentum, different from *boosting* a static brane. By solving the linearised perturbations of the Einstein and dilaton equations, we were able to find the asymptotic solutions of the metric and gauge fields, and used these to construct the boundary stress tensor of the fluid. By working in an orthonormal frame and using counter-terms similar to those proposed in Ross and Saremi [2009], we were able to construct the renormalised stress tensor complex and read the various thermodynamic variables off of it. We found that the the stress tensor thus constructed, satisfies the Ward identity associated to the Lifshitz scaling, $z\mathscr{E} - \rho v^2 = dP$, which is exactly the equation of state we hypothesised for a perfect Lifshitz fluid with an arbitrary dynamic exponent z, and no boost symmetry in [Fernández et al., 2019]. A straightforward extension of this problem would be to study the gravitational dual of charged perfect Lifshitz fluids with the addition of other $U(1)$ fields to the theory, for which the boundary theory that one might need to study would be that of non-relativistic electrodynamics coupled to torsionless Newton-Cartan theory, as recently explored in [Festuccia et al., 2016a]. Another extension would be to carry out the analysis performed in this paper to theories with a non-trivial coupling between the dilaton and cosmological constant, that is, boosted hyperscaling-violating Lifshitz geometries, and study the corresponding thermodynamics. Along holographic lines, one could follow the work done in [de Boer et al., 2020] where the complete first-order energy-momentum tensor in curved spacetime for a fluid without boost symmetry was computed, one can now consider trying to find the hydrodynamic modes of Lifshitz fluids from quasinormal modes and compare the results.

5 Appendix

5.1 Double-trace deformations and mixed boundary conditions

Along the lines of [Faulkner and Iqbal, 2013], we will first study the case of boundary deformation of a $2-D$ CFT leading to mixed boundary conditions for the bulk Maxwell electromagnetism in AdS_3, as an elucidatory example. We will then show how this connects with our story of a $2-$ form gauge field in a $5-D$ bulk Einstein-Maxwell theory.

Consider the bulk Maxwell action in Euclidean signature in $3-D$.

$$S_A = \frac{1}{4g_F^2} \int d^3x \sqrt{g} F^2. \tag{146}$$

In three bulk dimensions, one can always write field strength in terms of the Hodge dual of a scalar field via $dA \sim \star d\Theta$. One could replace the dynamical variable from A to F by introducing a Lagrange multiplier in the following manner,

$$Z_{bulk} = \int [DF][D\Theta] exp(-S_A + \frac{i}{2} \int d^3x \sqrt{g} \Theta(x) \varepsilon^{\mu\nu\rho} \partial_\mu F_{\nu\rho}(x)). \tag{147}$$

The addition of $\Theta(x)$ as a Lagrange multiplier was essential as in the absence of the gauge field as a dynamical variable, the Bianchi identity $dF = 0$ needs to be imposed by hand. The equations of motion yield $\frac{i}{g_F^2} F_{\nu\sigma} = \varepsilon^{\mu}_{\nu\sigma} \partial_\mu \Theta$, which when inserted into the partition function simply gives the theory of a free, massless scalar,

$$Z_{bulk} = \int [D\Theta] exp\big(-\frac{g_F^2}{2} \int d^3x \sqrt{g} (\nabla\Theta)^2 \big). \tag{148}$$

There are two subtle points one might take note of,

- The Bianchi identity $dF = 0$ now implies $d \star d\Theta = 0$, that is the dynamical scalar equation of motion.

- The original dynamical Maxwell equation $d\star F = 0$ now implies $d^2\Theta = 0$, which is simply an identity, and not dynamical.

From the AdS/CFT point of view, this can simply be interpreted as changing the source of the conserved current at the boundary from the boundary value of the gauge field $A_\mu(r\to\infty)$ to that of the field strength $F_{\mu\nu}(r\to\infty)$ which from the above analysis is,

$$\frac{i}{2}\varepsilon^{ab}F_{ab} = g_F^2\sqrt{g}g^{rr}\partial_r\Theta = -g_F^2\Pi. \tag{149}$$

Here Π is the canonical momentum conjugate to the bulk scalar field Θ. We can make these ideas more precise by working with a definite metric.

The Euclidean AdS_3 metric in $3-D$ is given by $ds^2 = r^2(d\tau^2+dx^2)+\frac{dr^2}{r^2}$. Let Θ be a massless scalar field who's Fourier space representation is,

$$\Theta(r,x,\tau) = \Theta(r)e^{i\omega\tau+ikx}. \tag{150}$$

The Klein-Gordon equation $\frac{1}{\sqrt{g}}\partial_M(\sqrt{g}g^{MN}\partial_N\Theta(r)) = 0$ in this metric becomes,

$$\partial_r(r^3\partial_r\Theta(r)) - \frac{p^2}{r} = 0, \tag{151}$$

where $p^2 \equiv \omega^2+k^2$.At the boundary ($r\to\infty$), the solution to (151) becomes,

$$\Theta(r\to\infty) \sim A + \frac{1}{r^2}\left(B - A\frac{p^2\ln r}{2}\right). \tag{152}$$

Now, there are two possible boundary conditions for $\Theta(r)$:

- Standard quantisation : Here the boundary value of $\Theta(r\to\infty)$ is taken to be the source. The logarithmic term in (152) is now sub-leading at large r. This corresponds to the dual field theory operator $\mathscr{O}$ having conformal dimension $\Delta_+ = d+\Delta = 2$. This does not correspond to a dynamical current at the boundary, as fixing the boundary value of Θ, automatically fixes the current it sources as can be seen from $\langle j^a\rangle = i\varepsilon^{ab}\partial_b\Theta(r)|_{r\to\infty}$. The dynamical field on the boundary, in this case, is the gauge field.

- The other option is to fix the canonical momentum conjugate to the scalar field, $\Pi = -\sqrt{g}g^{rr}\partial_r\Theta(r)$, as the source. This corresponds to fixing the boundary value of the field strength. The conformal dimension of $\mathscr{O}$ is $\Delta_- = d-\Delta = 0$. The current is now dynamical at the boundary. From (152), we can see that

$\Pi(r \to \infty) = 2B + \frac{Ap^2}{2} - p^2 \ln r$. The presence of the logarithmic term implies that it's value changes slowly at infinity with r, and never approaches a constant. From (151), near the boundary,

$$\frac{d}{d \ln r} \Pi(r) = -p^2 \Theta(r). \tag{153}$$

Let the boundary condition be imposed at some cut-off $r = \Lambda$. This implies that a linear combination of Π and Θ is being fixed at infinity,

$$\kappa \Pi(\lambda) = p^2 \Theta(\Lambda) \tag{154}$$

Such boundary conditions are known as mixed boundary conditions [Witten, 2001].

In short, switching from Dirichlet to Neumann boundary conditions is equivalent to changing the interpretation of the normalisable and non-normalisable mode of the field. In the dual theory, this corresponds to performing a Legendre transform of the boundary coupling.

We shall be working with the latter method. Suppose, that the boundary conditions had instead been imposed at a different cut-off $r = \Lambda'$, where $\Lambda' = \lambda \Lambda$. In that case,

$$\kappa' \Pi(\lambda \Lambda) = p^2 \Theta(\lambda \Lambda). \tag{155}$$

Now we know that at the boundary, $\Pi(r) = -p^2 \Theta \ln r$. This means that with the new cut-off,

$$\begin{aligned} \Pi(\Lambda') &= -p^2 \Theta \ln(\lambda r) \\ &= \Pi(\Lambda) - \Theta p^2 \ln \lambda. \end{aligned}$$

From (155),

$$\kappa' (\Pi(\Lambda) - \Theta p^2 \ln \lambda) = p^2 \Theta(\Lambda) \tag{156}$$

$$\implies \frac{\kappa' \Pi(\Lambda)}{1 + \kappa' \ln \lambda} = p^2 \Theta(\Lambda). \tag{157}$$

In order for the physics to be cut-off independent, (157) and (154) need to be equivalent, that is,

$$\frac{1}{\kappa} = \frac{1}{\kappa'} + \ln \lambda, \tag{158}$$

which shows the logarithmic running of coupling constant. The RG-invariant length scale is thus given by,

$$r_\star = \Lambda e^{\frac{1}{\kappa}}. \tag{159}$$

As shown in the Appendix of [Faulkner and Iqbal, 2013], the boundary action that is consistent with (154), is given by,

$$S_\partial = -\frac{g_F^2}{2\kappa}\int_{r=\Lambda} d^2x(\nabla\Theta)^2 = \frac{g_F^2}{2\kappa}\int_{r=\Lambda} d^2x j^a j_a. \tag{160}$$

In order to apply a field theory source, $b(x)$ to an operator corresponding to a conserved current, the following boundary condition is thus appropriate,

$$b(x) = \Pi(\Lambda,x) + \frac{1}{\kappa}\nabla^2\Theta(\Lambda,x), \tag{161}$$

where x denotes the field theory dimensions.

Now consider the case of a $2-$form gauge field in a $5-D$ bulk Einstein-Maxwell theory given by (23). The bulk equation of motion for the B_{ab} is $\partial_a(\sqrt{-g}H^{abc}) = 0$. If we parametrise the bulk field as $B_{ij} = \sigma_{ij}\beta(r)e^{i\omega\tau}$, where σ_{ij} is some polarisation vector, then in a pure Euclidean AdS_5 metric, the solution at infinity has the form,

$$\beta(r\to\infty) = \hat{b} - J\ln r, \tag{162}$$

analogous to (152). As it is logarithmically running at the boundary, the value of $\hat{b}$ (like $\Pi(r)$) is ambiguous, and it cannot be interpreted as the source in it's current form. As explained above, the solution to this is to deform the CFT by a double trace coupling of the form $\frac{J^2}{\kappa}$. Now applying the cut-off at $r = \Lambda$, the regularised source is given by,

$$b = \beta(\Lambda) - \frac{J}{\kappa}. \tag{163}$$

Thus, the boundary is now labelled by two parameters, Λ, and κ. As before, κ is logarithmically running.

Paper I

Operator lifetime and the force-free electrodynamic limit of magnetised holographic plasma

Napat Poovuttikul, Aruna Rajagopal

Prepared for submission to JHEP, 2021, 20

Operator lifetime and the force-free electrodynamic limit of magnetised holographic plasma

Napat Poovuttikul[1,2,*] and Aruna Rajagopal[2,†]

[1] *Department of Mathematical Sciences, Durham University, South Road, Durham DH1 3LE, UK*

[2] *University of Iceland, Science Institute, Dunhaga 3, IS-107, Reykjavik, Iceland*

Using the framework of higher-form global symmetries, we examine the regime of validity of force-free electrodynamics by evaluating the lifetime of the electric field operator, which is non-conserved due to screening effects. We focus on a holographic model which has the same global symmetry as that of low energy plasma and obtain the lifetime of (non-conserved) electric flux in a strong magnetic field regime. The lifetime is inversely correlated to the magnetic field strength and thus suppressed in the strong field regime.

* napat.poovuttikul@durham.ac.uk

† arr17@hi.is

CONTENTS

I. INTRODUCTION

Hydrodynamics [1] is a well-established theoretical framework which universally describes the long wavelength, low frequency behaviour of interacting systems at finite temperature. Essentially, hydrodynamic theory is a description of conserved quantities and the manifestation of the corresponding symmetries in a system in thermal equilibrium. Theories with widely varying microscopics can have the same macroscopic hydrodynamic description. One possible explanation why such a universal description is possible is that all operators except conserved charges have parametrically short lifetimes compared to the scale of interest and, once the longest-lived non-conserved operator[1] has decayed away, the hydrodynamic description becomes viable (see Fig. 1).

[1] While this operator language is more familiar in the context of quantum systems, it is also applicable to classical systems via e.g. memory matrix formalism [2, 3]. A more modern introduction may be found in [4].

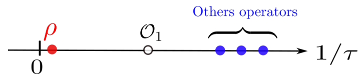

FIG. 1: A cartoon illustration of the lifetime of operators of a theory that exhibit hydrodynamic behaviour at late time. Here, there is a parametrically large gap between conserved charges ρ and the rest. The life time τ_1 of the longest-lived operator, denoted by $\mathcal{O}_1$ set the time scale in which hydrodynamics becomes applicable.

The hydrodynamic framework may be generalised to systems where the conserved charges are those of a higher-form symmetry [5] which counts the number density of extended objects. A recent exploration of this idea [6] (see also [7–10]) shows that the resulting hydrodynamics of a one-form $U(1)$ charge reproduces the theory of magnetohydrodynamics (MHD)[2]. This should not come as a big surprise. MHD is, after all, a low energy effective theory of plasma where the (dynamical) electric field is screened – the one-form U(1) symmetry associated to electric flux is explicitly broken. This implies that in, for example, a plasma at zero magnetic field (where the Ohm's law $\mathbf{j} = \sigma\mathbf{E}$ is a good approximation) the electric field has a finite lifetime,

$$\delta\mathbf{E} \propto \exp(-t/\tau_E) \qquad \Longleftrightarrow \qquad \langle E^i(-\omega)E^j(\omega)\rangle \sim \frac{\delta^{ij}}{\omega + i/\tau_E}\,, \tag{1.1}$$

with the lifetime of the electric field $\tau_E = 1/\sigma$. The conductivity σ can be computed from first principles. For instance, in quantum electrodynamics, it can be written as [14][3]

$$\sigma \propto \frac{T}{e^2 \log e^{-1}}\,, \tag{1.2}$$

where e is the electromagnetic coupling. The lifetime of electric field $\tau \sim 1/T$, is then much shorter than the scale $t \gg 1/T$ (or $\omega/T \ll 1$ in Fourier space) where hydrodynamic behaviour is expected. If, in this late-time limit, all other operators except energy density T^{tt} and the momentum T^{ti} have already decayed away, one can expect the hydrodynamic description of a plasma to be governed by

$$\partial_\mu T^{\mu\nu} = 0\,, \qquad \partial_\mu J^{\mu\nu} = 0\,. \tag{1.3}$$

The conserved currents $T^{\mu\nu}$ and $J^{\mu\nu}$ are expressed in terms of energy, momentum, magnetic flux $J^{ti} \equiv B^i$ and their conjugates, organised order by order in the gradient expansion. This formulation

[2] For the formulation of MHD that closely resembles higher-form symmetry formulation, see e.g. [11–13].

[3] The fact that this quantity has only been computed at the beginning of this century indicates the difficulty of the required computations.

of MHD only requires macroscopic consistency and does not require the introduction of the gauge field $\star J = F = dA$ which, due to screening effect, is not a long-lived degree of freedom.

This brings us to the central question of the present paper: Is a hydrodynamic description of the form (1.3) applicable in the limit low temperature compared to magnetic flux density $T^2/|\mathbf{B}| \ll 1$? This question is important if one wants to apply the MHD description to astrophysical plasmas where the magnetic field is many orders of magnitude larger than the scale set by the temperature. If one were to naively extrapolate (1.1)-(1.2), the lifetime of the electric field appears to become arbitrarily long as the temperature decreases. However, there exists a macroscopic description of plasma in this regime that has been successfully applied. This theory is called *force-free electrodynamics* or FFE, and has been used extensively in astrophysical setups such as in the magnetosphere of black holes [15, 16], neutron star [17] and solar corona [18] just to name a few. In its conventional form, this theory is applied to a system which is magnetically dominated (i.e. $|\mathbf{B}^2| > |\mathbf{E}^2|$ or, covariantly $F_{\mu\nu}F^{\mu\nu} > 0$) and whose dynamics is governed by

$$\epsilon^{\mu\nu\rho\sigma} F_{\mu\nu} F_{\rho\sigma} = 0\,, \tag{1.4a}$$

$$F^{\mu\nu} \nabla_\lambda F^\lambda{}_\nu = 0\,. \tag{1.4b}$$

Here, the first relation implies that $\mathbf{E} \cdot \mathbf{B} = 0$ while the second relation implies that the *force* $j^\mu_{el} F_{\mu\nu}$, with $j^\mu_{el} := \nabla_\nu F^{\nu\mu}$ via Maxwell's equations, acting on plasma vanishes (hence the name force-free electrodynamics). More details on the geometric and effective action view point of FFE can be found in e.g. [19, 20] and [21–24]. One should emphasise that the system of equations in Eq.(1.4) is independent of the microscopic details of the cold plasma, which then strongly resembles hydrodynamic descriptions. In fact, it turns out that (1.4) can arise in a special limit where $T \ll \sqrt{|\mathbf{B}|}$ of a hydrodynamics description with one-form $U(1)$ symmetry in (1.3), see [6, 23, 24][4].

The existence of FFE is usually justified by saying that the cold plasma is, on one hand, dense enough to screen the electric field (1.4a) but, on the other hand, dilute enough so that force-free condition (1.4b) is applicable. This statement can be made more precise in the light of relations between the equations of FFE and hydrodynamics. Thus, we propose a criterion for testing the validity of FFE using the lifetime of non-conserved operators – *FFE, or equivalently, hydrodynamic description of cold plasma in the $T \ll \sqrt{|\mathbf{B}|}$ limit, is valid when the lifetime of all non-conserved operators is parametrically shorter than the time scale of interest.* A key advantage of this approach

[4] Recasting of force-free electrodynamics in the hydrodynamic language also allows the systematic gradient expansions [23, 25]. This could serve to classify correction to FFE in order to account for phenomena such as pulsar radio emission where $\mathbf{E} \cdot \mathbf{B} \neq 0$.

is that the operator lifetime can be, in principle, computed explicitly from microscopic description and therefore allows one to find the 'cutoff' scale where FFE description should break down.

Computing the operator lifetime from microscopic description is, however, not always an easy task. In fact, we are not aware of a genuine computation directly from quantum electrodynamics (in the sense of [14]) when both T and $\mathbf{B}$ are turned on. To simplify the computations, we shall demonstrate the validity of FFE in the strongly interacting magnetised plasma with a holographic dual as proposed in [26, 27] where the one-form $U(1)$ global symmetry is taken into account via a two-form gauge field in the gravity dual. This provides two key advantages. First, the computation of correlation functions boils down to solving simple linearised differential equations (see e.g. [28]). Second, there is strong evidences that charge neutral operators, apart from energy and momentum, have a parametrically short lifetime in this class of theories [5]. Therefore, we shall focus on non-conserved operators in the electromagnetic sector of the theory: the electric flux operators, whose lifetime can be extracted via two-point correlation function as in (1.1). This will provide strong evidence for the validity of FFE limit in a strongly interacting holographic plasma.

On the technical side, the computations presented in this note show that there are no quasi-normal modes present in the vicinity of the hydrodynamic regime $\omega/T \ll 1$ (and $\omega/\sqrt{|\mathbf{B}|} \ll 1$). The pole in the electric flux correlation function in this regime then implies that the operator has a parametrically long lifetime which could interfere with the hydrodynamic modes. The presence of such long-lived mode can be determined analytically in the usual hydrodynamic regime of $\omega/T \ll 1$ for a large class of theories. It is usually difficult to go beyond this regime towards the limit $\omega/T \sim 1, \omega/\sqrt{|\mathbf{B}|} \ll 1$. Such computation can, however, be done analytically in the simple model of [26] thanks to the presence of the BTZ$\times\mathbb{R}^2$ bulk geometry in the deep IR [32]. We should also note that the treatment of a (long-lived) non-hydrodynamic modes has been extensively used to determine the breakdown of hydrodynamic descriptions in the context of QFTs with holographic duals, see e.g. [33–36] .

The remainder of this paper is organised as the follows. In section II, we summarise the procedure involved in the computation of the two-point correlation function in the holographic dual to one-form global symmetry. In section II A, we outline the method for exploring the existence of decaying modes in the vicinity of the usual hydrodynamic limit $\omega/T \ll 1$ at $T/\sqrt{|\mathbf{B}|} \ll 1$. Due to the simplicity of the bulk geometry, we are able to further extend the analysis to arbitrary value of

[5] To be more precise, it has been shown in $\mathcal{N}=4$ supersymmetric Yang-Mills theory, which constitutes the matter sector of the holographic model [26, 27], that there is no long-lived mode besides hydrodynamic modes at any $T \neq 0$ and $|\mathbf{B}| = 0$ [29]. A similar conclusion was reached for the same theory in the charge neutral sector at finite *non-dynamical* magnetic field [30, 31].

ω/T with $\omega/\sqrt{|\mathbf{B}|} \ll 1$ and $T/\sqrt{|\mathbf{B}|} \ll 1$. This is described in section II B. Further open questions and future directions are discussed in section III.

II. THE HOLOGRAPHIC MODEL

A simple holographic dual to a strongly interacting field theory of matter charged under dynamical $U(1)$ electromagnetism (that is, the dynamical plasma described by low energy MHD) and formulated in the language of higher-form symmetry was constructed in [26, 27]. We present a brief review here for completeness. The five-dimensional bulk theory is comprised of Einstein gravity coupled to a two-form bulk gauge field, $B_{\mu\nu}$, and a negative cosmological constant,

$$S = \int d^5X\sqrt{-G}\left(R - 2\Lambda - \frac{L^2}{3}H_{abc}H^{abc}\right) + S_{bnd} - \frac{1}{\kappa(\Lambda)}\int_{r=\Lambda} d^4x\sqrt{-\gamma}(n^a H_{a\mu\nu})(n_b H^{b\mu\nu}), \quad (2.1)$$

where $H = dB$ and B_{ab} is the bulk 2-form gauge field, Λ is the UV-cutoff, n^a is the unit normal to the boundary, and S_{bnd} denotes the Gibbons-Hawking and gravitational counter term. Roughly speaking, the two bulk fields G_{ab} and B_{ab}, asymptote to $g_{\mu\nu}$ and $b_{\mu\nu}$ respectively, which then source the currents, $T^{\mu\nu}$ and $J^{\mu\nu}$.

$$\langle T_{\mu\nu}\rangle \equiv \frac{2}{\sqrt{-g}}\frac{\delta S}{\delta g_{\mu\nu}}\,, \qquad \langle J_{\mu\nu}\rangle \equiv \frac{1}{\sqrt{-g}}\frac{\delta S}{\delta b_{\mu\nu}} \quad (2.2)$$

The generating functional takes the form,

$$Z[g_{\mu\nu}, b_{\mu\nu}] = \left\langle \exp\left[i\int d^4x\sqrt{-g}\left(\frac{1}{2}T^{\mu\nu}g_{\mu\nu} + J^{\mu\nu}b_{\mu\nu}\right)\right]\right\rangle \quad (2.3)$$

and diffeomorphism invariance and gauge symmetry lead to the following equations,

$$\nabla_\mu\langle T^{\mu\nu}\rangle = (db)^\nu_{\rho\sigma}\langle J^{\rho\sigma}\rangle\,, \qquad \nabla_\mu\langle J^{\mu\nu}\rangle = 0. \quad (2.4)$$

$H = db$ is the three-form field strength of the two-form external source. The equilibrium solution of this holographic model is a domain wall interpolating between an asymptotic AdS_5 geometry in the UV ($r \to \infty$ in our convention), and $BTZ \times \mathbb{R}^2$ in the near-horizon IR ($r = r_h$). It is described by the following metric and gauge field

$$\begin{aligned} ds^2 = G_{ab}dX^a dX^b &= -r^2 f(r)dt^2 + \frac{dr^2}{r^2 f(r)} + e^{2V(r)}(dx^2 + dy^2) + e^{2W(r)}dz^2\,, \\ B = h(r)dt\wedge dz \qquad &\text{with} \qquad \star_5 H = \mathcal{B}dx\wedge dy \end{aligned} \quad (2.5)$$

Modulo the subtleties due to the mixed boundary conditions, this is nothing but the hodge dual of the magnetised black brane solution of [32]. The radial coordinate is chosen such that $r \to \infty$ corresponds to the usual asymptotic AdS_5 with

$$f(r) = 1\,, \qquad e^{2V(r)} = e^{2W(r)} = r^2 \tag{2.6}$$

in the $r \to \infty$ limit. The $BTZ \times \mathbb{R}^2$ solution near the horizon can be written as

$$f(r) = 3\left(1 - \frac{r_h^2}{r^2}\right)\,, \qquad e^{2V} = \frac{\mathcal{B}}{\sqrt{3}}\,, \qquad e^{2W} = 3r^2\,. \tag{2.7}$$

The temperature is set by the horizon radius via $4\pi T = r_h^2|f'(r_h)| = 6r_h/L^2$. We set $L = 1$ for simplicity. Note also that $\mathcal{B}$ is related to the $z-$component of the 'physical' magnetic field $\mathbf{B}$ which differs by a prefactor L or the 2-form gauge field coupling in the bulk (e.g. if one were to define the action with $S \sim \int (1/g^2)H^2$). We will keep using $\mathcal{B}$ to emphasise its holographic origin but there is no harm in thinking of it as simply $\mathbf{B}$.

One interesting feature of this model is that the leading divergence of $B_{\mu\nu}$ in the Fefferman-Graham expansion is logarithmic. Thus, the definition of the source $b_{\mu\nu}$ requires mixed boundary condition

$$b_{\mu\nu} = B_{\mu\nu}(\Lambda) - \frac{1}{\kappa(\Lambda)}\langle J_{\mu\nu}\rangle\,, \qquad \text{with} \qquad \langle J^{\mu\nu}\rangle = -\sqrt{-G}n_\alpha H^{\alpha\mu\nu} \tag{2.8}$$

Requiring the source $b_{\mu\nu}$ to be independent of the UV cutoff fixes the form of the 'coupling constant' $1/\kappa(\Lambda)$ which turns out to be logarithmically running. This is a common feature for fields with this type of near-boundary behaviour where the counterterm also plays the role of the double-trace deformation [37, 38], see also [26, 27] for a discussion in the present context. Mapping $J^{\mu\nu}$ in to a more familiar *dynamical* field strength via $J^{\mu\nu} = \frac{1}{2}\epsilon^{\mu\nu\rho\sigma}F_{\rho\sigma}$, one can see that the double-trace deformation plays a role similar to the Maxwell term for the dynamical gauge field in the dual QFT with $1/\kappa(\Lambda)$ as a (logarithmically running) electromagnetic coupling.

The finite part of $1/\kappa(\Lambda)$ plays a crucial role in this setup. While the finite counterterm in the ordinary bulk Maxwell theory simply results in a contact term in the correlation function, the mixed boundary condition for B_{ab} implies the existence of the purely decaying mode $\omega = -i/\tau_E$ that can interfere with the gapless hydrodynamic excitation. This is nothing but the life-time of the electric flux operator $Q_E \sim \int dS_{ij}J^{ij}$ which appears in the following correlation function [27, 33]

$$\langle J^{ij}(t)J^{kl}(0)\rangle \sim \exp\left(-it/\tau_E\right)\,. \tag{2.9}$$

Note that, due to the anisotropy introduced by finite equilibrium magnetic field, the value of τ_E depends on which direction of the electric field in consideration. The limit where τ_E is small, but finite, compared to the length scale of interest (set by temperature or magnetic flux density) is of particular interest as it allows one to extract τ_E analytically, via a matching procedure that we outline below. As argued in the introduction, the lifetime of the electric flux determines the validity of MHD and FFE description.

A. Linearised solutions in $\omega/T \ll 1$ limit and matching procedure

In this section, we outline the computation required to obtain the relaxation time of the electric field. We focus on the hydrodynamic regime where $\omega/T \ll 1$, and the low temperature limit [6] $T/\sqrt{|\mathbf{B}|} \ll 1$. This allows us to solve the bulk equation of motion analytically via a matching method similar to that was employed in [29] (see also [33] for a recent review). We consider the decay rate of the electric field both along and perpendicular to the equilibrium magnetic field denoted by $E^{\parallel} = J^{xy}$ and $E^{\perp} = J^{xz}, J^{yz}$ respectively.

Before proceeding, let us summarise the matching procedure for the $\omega/T \ll 1$ expansion. It involves separating the bulk into three suitably defined pieces: inner region, intermediate region and outer region. The inner region is a suitably defined region close to the horizon while the outer region is defined to be the range of r such that $\omega/r \ll 1$ so that one can drop terms quadratic in $(\omega/r)^2$, which includes the near boundary region. The integration constants of the solution in the outer region are determined by matching the form of inner region solution for intermediate value of r that connect the two regions together. In our case, this is the region of r close to r_h but

$$\frac{\omega}{T} \log f(r) \ll 1 \tag{2.10}$$

This intermediate region defined above is also consistent with the outer region assumption where $\omega/r \ll 1$ and thus we are able to match the two solution together. Note that, while this procedure is applicable to any bulk solution with event horizon, the limit $\omega/T \ll 1$ is crucial.

We now present the key equations and resulting lifetime of the electric flux.

[6] Similar computation for the holographic theory dual to a system with ordinary(zero-form) $U(1)$ symmetry can be found in e.g. [39, 40].

1. Perturbation parallel to equilibrium magnetic field

As the magnetic field in equilibrium points along the $z-$direction, we are interested in $E^{\parallel} = \frac{1}{2}\varepsilon^{zxy}\langle J_{xy}\rangle$. The corresponding bulk perturbation is δB_{xy} which decouples from the metric perturbation in the zero wave vector limit. The bulk equation of motion can be written as

$$\left(r^2 f e^{W-2V}\delta B'_{xy}\right)' + \frac{\omega^2}{r^2 f} e^{W-2V}\delta B_{xy} = 0 \tag{2.11}$$

where $(...)'$ denotes a derivative w.r.t. the radial coordinate r. The inner region solution for δB_{xy}, where we substitute the $BTZ \times \mathbb{R}^2$ solution for f, V, W, with the ingoing boundary condition can be written as

$$\delta B^{inner}_{xy} = c^H \exp\left(-\frac{i\omega}{4\pi T}\log f(r)\right) \tag{2.12}$$

The outer region solution can be obtained by considering the solution at linear order in ω/r and one obtains,

$$\begin{aligned}\delta B^{outer}_{xy}(r) &= c_1 - c_2\left(\log\Lambda - \int_{\mathtt{r}=r}^{\Lambda} d\mathtt{r}\,\frac{e^{2V(\mathtt{r})-W(\mathtt{r})}}{\mathtt{r}^2 f(\mathtt{r})}\right) \\ &= c_1 - c_2\left(\log r - \phi(r) + \frac{e^{2V-W}}{r_h^2 f'}\Big|_{r=r_h}\log f\right),\end{aligned} \tag{2.13}$$

where $\phi(r)$ is a function regular everywhere in the bulk defined as

$$\phi(r) = \int_{\mathtt{r}=r}^{\Lambda} d\mathtt{r}\left[\frac{e^{2V(\mathtt{r})-W(\mathtt{r})}}{\mathtt{r}^2 f(\mathtt{r})} - \left(\frac{e^{2V(\mathtt{r})-W(\mathtt{r})}}{r_h^2 f'(\mathtt{r})}\right)_{\mathtt{r}=r_h}\frac{f'(\mathtt{r})}{f(\mathtt{r})} - \frac{1}{\mathtt{r}}\right].$$

This parametrisation allows us to single out leading contributions that dominate when considering the solution near $r = \Lambda$, where $\phi(r)$ and $\log(e^{-2V}r^2 f)$ vanish, as well as near $r \approx r_h$ where the $\log f$ term dominates. The integration constants c_1, c_2 in (2.13) are related to the source $b_{\mu\nu}$ and the 2-form current $\langle J^{xy}\rangle$. The precise relations can be obtained via Eq. (2.8) to be

$$\langle J^{xy}\rangle = c_2\,, \qquad b_{xy} = c_1 - \left(\log\,\Lambda + \frac{1}{\kappa(\Lambda)}\right)c_2 \tag{2.14}$$

Note that, for the source to be independent of the UV cutoff, one requires $\kappa(\Lambda)^{-1} =$ finite term $-$ $\log\Lambda$. This is the logarithmically running coupling usually found in a double-trace deformed theory and resembles the running of electromagnetic coupling as pointed out in [26, 27, 33].

For the outer and inner region solutions to match, we consider both solutions in the intermediate region where we can write the inner solution as

$$\exp\left(-\frac{i\omega}{4\pi T}\log f\right) \approx 1 - i\frac{\omega}{4\pi T}\log f + \mathcal{O}\left(\frac{\omega}{T}\right)^2 \tag{2.15}$$

The matching condition $\delta B^{inner}_{xy} = \delta B^{outer}_{xy}$ in this region prompts yield the following algebraic relations between the boundary quantities $b_{xy}, \langle J_{xy}\rangle$:

$$\begin{aligned} \frac{i\omega}{4\pi T} c^H &= \left(\frac{\mathcal{B}/r_h}{3r_h^2 f'(r_h)}\right) \langle J_{xy}\rangle \\ c^H &= b_{xy} + \left[\frac{1}{\kappa(\Lambda)} + \log\left(\frac{\Lambda}{r_h}\right) + \phi(r_h)\right] \langle J_{xy}\rangle \,. \end{aligned} \tag{2.16}$$

Solving these equations at vanishing source $b_{xy} = 0$ yields the spectrum of the form $\omega = -i/\tau_{E\parallel}$ where $\tau_{E\parallel}$ is the lifetime of the electric flux parallel to the equilibrium magnetic field. This is the first key result that we advertised earlier, namely

$$\tau_{E\parallel} = \frac{2\pi T}{\mathcal{B}} \left(e_r^{-2} + \phi(r_h)\right) , \tag{2.17}$$

where we write $e_r^{-2} = \log(\Lambda/r_h) + \kappa(\Lambda)^{-1}$ which plays the role of renormalised electromagnetic coupling. More details on the $T/\sqrt{\mathcal{B}}$ dependence of $\phi(r_h)$ can be found in Appendix A.

What does this result tell us about the lifetime of the electric flux operator? While the integral $\phi(r_h)$ can be a dimensionless function of T and $\mathcal{B}$, the renormalised electromagnetic coupling can be chosen in such a way that $e_r^{-2} \gg \phi(r_h)$ and $e_r^{-2}T^2/\mathcal{B} \ll 1$ so that $\omega\tau_{E\parallel} \sim \omega/T \ll 1$. The second limit is essential as the matching procedure assumes that $\omega/T \ll 1$ and the solution outside this regime has to be discarded. Taking these factors into account, one concludes that the temperature dependence of the electric flux is different from the high temperature $T/\sqrt{\mathcal{B}} \gg 1$ limit where $\tau_E \sim 1/T$ (see Fig 2). Naively taking the limit $T \to 0$ in (2.17) will result in the vanishing lifetime of the electric flux in contrast to the result in (1.2). However, one has to carefully remove the limit $\omega/T \ll 1$ in order to access the lower temperature limit $\omega/T \sim 1, \omega/\sqrt{\mathcal{B}} \ll 1$.

2. *Perturbation perpendicular to equilibrium magnetic field*

Unlike the previous case, the perturbation δB_{xz} that corresponds to $E^\perp = \frac{1}{2}\epsilon^{yzx}\langle J_{zx}\rangle$ is coupled to the metric perturbation. This is manifest in the equations of motion

$$\begin{aligned} \frac{d}{dr}\Big(r^2 f e^{-W}\delta B'_{xz} + \mathcal{B}(\delta G^x_t)\Big) + \frac{\omega^2 e^{-W}}{r^2 f}\delta B_{xz} = 0\,, \\ \frac{d}{dr}\left(e^{4V+W}(\delta G^x_t)' + 4\mathcal{B}\delta B_{xz}\right) = 0\,, \end{aligned} \tag{2.18}$$

where $\delta G_{\mu\nu}$ denotes the metric perturbations. Note that the coupled perturbations $\{\delta B_{xz}, \delta G_{tx}\}$ and $\{B_{yz}, \delta G_{yz}\}$ are equivalent due to $SO(2)$ symmetry in the plane perpendicular to the equilibrium magnetic field. Also, the second equation of motion in (2.18) can be written in a total derivative form $d\pi_{tx}/dr = 0$ with π_{tx} is related to the momentum $\langle T^{tx}\rangle$. Since we are working in

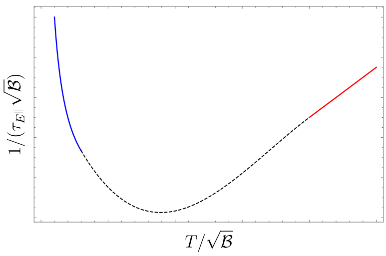

FIG. 2: A sketch of the decay rate (inverse of the lifetime) of the electric field as a function of $T/\sqrt{\mathcal{B}}$, measured in the unit of $\sqrt{\mathcal{B}}$. The high temperature regime (red) depict the result of decay rate at zero magnetic field found in [27, 33] which has the same temperature dependence as in (1.1)-(1.2). In the low temperature regime (blue), however, the operator lifetime becomes those found in (2.17).

the zero wavevector limit, the conservation of momentum implies that $\pi_{tx} = 0$ in Fourier space (which can be shown explicitly using the $rx-$component of the Einstein equation).

The solution for $\delta B_{xz}, \delta G_{tx}$ in the outer region can be found by using the property of the background geometry combined with the Wronskian method as in [33]. To be more precise, one first notes that the time-independent solution of the magnetised black brane can be written in a total derivative form, which implies the existence of two radially conserved currents.

$$Q_1 = r^2 f(V' - W')e^{2V+W} + 2\mathcal{B}h(r) = 0\,, \tag{2.19a}$$

$$Q_2 = e^{4V+W}\frac{d}{dr}\left(e^{-2V}r^2 f\right) - 4\mathcal{B}h(r) = sT\,, \tag{2.19b}$$

where we write the equilibrium ansatz for the gauge field as $B = h(r)\,dt \wedge dz$ with gauge choice $h(r_h) = 0$, which, together with the horizon regularity, sets $Q_1 = 0$. The relation between $h(r)$ and the 3-form field strength is

$$e^{2V-W}h' = \mathcal{B}\,. \tag{2.19c}$$

More details on obtaining these radially conserved quantities can be found in e.g. [41]. With this ansatz, we can compare (2.18) and (2.19) and find that one of the solutions of (2.18) when $\omega/r \to 0$ are

$$\delta B_{xz} = \Phi_1(r) = h(r) + \frac{sT}{4\mathcal{B}}\,, \qquad \delta G^x_t = \Psi_1(r) = -e^{-2V}r^2 f\,. \tag{2.20}$$

One can use the Wronskian method to find find a pair of solution of (2.18) that are linearly independent to $\{\Phi_1, \Psi_1\}$. These solutions are

$$\Phi_2(r) = \frac{1}{4\mathcal{B}} - \int_r^\infty d\mathtt{r} \left(\frac{\mathcal{B}e^{W(\mathtt{r})}\Psi_2(\mathtt{r})}{\mathtt{r}^2 f(\mathtt{r})}\right), \qquad \Psi_2(r) = \Psi_1(r)\int_r^\infty d\mathtt{r}\left(\frac{e^{-W(\mathtt{r})}}{\mathtt{r}^4 f(\mathtt{r})^2}\right) \tag{2.21}$$

As a result, the outer region solution can be written as

$$\begin{pmatrix} \delta B_{xz}^{outer} \\ (\delta G_t^x)^{outer} - \frac{1}{\mathcal{B}}\mathcal{J}_{xz} \end{pmatrix} = c_1 \begin{pmatrix} \Phi_1 \\ \Psi_1 \end{pmatrix} + c_2 \begin{pmatrix} \Phi_2 \\ \Psi_2 \end{pmatrix} \tag{2.22}$$

where $\mathcal{J}_{xz} := (r^2 f e^{-W}\delta B'_{xz} + \mathcal{B}\delta G_x^t)$ is an integration constant of (2.18) at $\omega = 0$. One can substitute the $BTZ \times \mathbb{R}^2$ ansatz into the solution in (2.22) to check that $\Phi_1, \Psi_{1,2}$ are finite at $r = r_h$ while Φ_2 is singular. It is convenient to separate out the singular part of Φ_2 in the following form

$$\Phi_2(r) = \phi_2(r) - \left(\frac{\mathcal{B}e^W\Psi_2}{r^2 f'}\right)_{r=r_h} \log f(r) \tag{2.23}$$

where $\phi_2(r)$ is the integral in (2.21) with the logarithmic divergence subtracted. The boundary condition where the source for both metric and 2-form gauge field fluctuation vanishes corresponds to the following values of c_1 and c_2

$$c_1 = \frac{\mathcal{J}_{xz}}{\mathcal{B}}, \qquad c_2 = -4\left(\frac{sT}{4\mathcal{B}} + h(\Lambda) + \frac{\mathcal{B}}{\hat{\kappa}(\Lambda)}\right)\mathcal{J}_{xz} \tag{2.24}$$

One can also check that $\mathcal{J}_{xz}$ is identical to the one-point function $\langle \delta J^{xz}\rangle$ via the definition (2.8). Note also that the ratio $c_2/\mathcal{J}_{xz}$ is finite due to the cancellation of the logarithmic divergence of $1/\kappa(\Lambda)$ and that of the near boundary solution of $h(r)$, obtained via (2.19c).

Let us also pointed out another way to organise the equations of motion for δB_{xz}. It turns out that (2.18) can be combined into a single equation of motion that reduces to a total derivative form at $\omega = 0$. Following the procedure in e.g. [42] and some manipulation, we find

$$\left([e^{4V+W}\left(e^{-2V}r^2 f\right)']^2 r^2 f e^{-W}\delta\tilde{B}'_{xz}\right)' + \frac{\omega^2}{r^2 f e^W}[e^{4V+W}(e^{-2V}r^2 f)']^2\delta\tilde{B}_{xz} = 0 \tag{2.25}$$

where $\delta\tilde{B}_{xz} = \delta B_{xz}/[e^{4V+W}(e^{-2V}r^2 f)']$. The outer region solution of (2.25) is easily obtained and can be shown to be identical to those of (2.22).

We can now proceed to the inner region solution. This can be found by solving Eq.(2.25) and one find

$$\delta B_{xz}^{inner} = c^H \exp\left(-\frac{i\omega}{4\pi T}\log f(r)\right). \tag{2.26}$$

In the intermediate region, we apply the expansion in (2.15). The coefficients c_1, c_2 are related to c^H via

$$\left(-\frac{i\omega}{4\pi T}\right) c^H = -\left(\frac{\mathcal{B}e^W \Psi_2}{r^2 f'}\right)_{r=r_h} c_2\,, \\ c^H = \left(\frac{sT}{4\mathcal{B}}\right) c_1 + \phi_2(r_h) c_2\,, \tag{2.27}$$

Substituting the form of c_1, c_2 in terms of $\langle \delta J_{xz} \rangle$, we can write the relations in a form similar to $\langle \delta J_{xy} \rangle$, namely

$$\left(-i\omega + \frac{1}{\tau_{E^\perp}}\right) \langle \delta J_{xz} \rangle = 0\,. \tag{2.28}$$

In the case of vanishing sources, we can write $\frac{c_2}{c_1} = -4\mathcal{B}\left(\frac{sT}{4\mathcal{B}} + h(\Lambda) + \frac{\mathcal{B}}{\kappa(\Lambda)}\right)$ and the relaxation time of the electric field perpendicular to the equilibrium magnetic field is

$$\tau_{E^\perp} = \frac{\sqrt{3}}{2\pi T \mathcal{B} \Psi_2(r_h)} \left[\frac{sT}{4\mathcal{B}} \frac{c_1}{c_2} + \phi_2(r_h)\right] \tag{2.29}$$

In contrast to the result at $e_r^{-2} \gg 1$ and zero equilibrium magnetic field in [27, 33], the lifetime at strong magnetic field $\mathcal{B}/T^2$ has a very different form. To see this, it is useful to examined that the combinations that enter the lifetime as follows

$$\Psi_2(r_h) \propto \frac{1}{\mathcal{B}T^2}\,, \qquad \phi_2(r_h) \propto \frac{1}{\mathcal{B}}\,, \qquad \frac{c_1}{c_2} \propto \frac{1}{\mathcal{B}^2} \quad \text{for large} 1/\kappa(\Lambda) \tag{2.30}$$

with proportionality constants given by some numbers of order $\mathcal{O}(1)$. In the limit of large electromagnetic coupling $1/\kappa(\Lambda) \gg 1$ and $\mathcal{B}/T^2 \gg 1$, we find that this gives a short lifetime of the form $\tau_{E^\perp} \propto T/\mathcal{B}$. However, the location of this decaying mode $\omega = -i/\tau_{E^\perp}$ lies outside the hydrodynamic regime $\omega/T \ll 1$. Thus, one conclude that there are no modes with long lifetime in this regime[7].

B. Checking $T \gtrsim 0$ limit in $\omega/\sqrt{|\mathbf{B}|} \ll 1$ regime

While the result in the previous section strongly indicated that the electric flux lifetime becomes very short at extremely low temperature, the simplicity of the holographic model also allows us to extend the analysis beyond the usual hydrodynamic $\omega/T \ll 1$ regime. We will first show that the zero temperature theory does not support the purely decaying mode of the form $\omega = -i/\tau$ in the

[7] Note also that, if one were to perform this analysis for a perturbation in the holographic dual to a theory with zero-form $U(1)$ at $T > 0, \mu = 0$ (as in [29], see also [33]), one would find a spectrum of the form $\omega \sim T$. This solution is spurious as it lies outside the hydrodynamic regime $\omega/T \ll 1$ and, in fact, is not present in the genuine spectrum obtained numerically at finite ω/T [43].

small $\omega/\sqrt{|\mathbf{B}|}$ regime. Next, we further extend the regime of validity to that of $\omega/\sqrt{|\mathbf{B}|} \ll 1$ but for arbitrary ω/T. The purpose of the latter is to show that $\tau_E \propto T/\sqrt{|\mathbf{B}|}$ without relying on the $\omega/T \ll 1$ limit.

1. Zero temperature

A simple argument for the non-existence of such a slowly decaying mode, is the presence of Lorentz symmetry at zero temperature on the AdS_3 submanifold in the deep infrared. On the other hand, one can also show this, using matching methods similar to those in [39, 44, 45].

To obtain this result, one first realises that the geometry of the magnetised black brane is that of an interpolation between IR $AdS_3 \times \mathbb{R}^2$ and UV AdS_5. Roughly speaking, the IR geometry starts to becomes a good approximation as one starts to probe the scale below the magnetic field i.e. $r \sim \sqrt{|\mathbf{B}|}$. The inner and outer regions are defined such that they start off from the IR and UV geometry respectively, and extend to cover the overlap region (see Figure 3). This is achievable when $\omega/\sqrt{|\mathbf{B}|} \ll 1$.

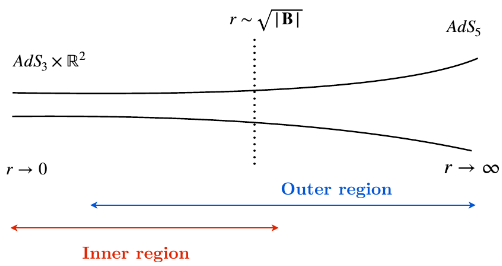

FIG. 3: A sketch of the bulk geometry at zero temperature. The inner region, whose solutions only depends on the ratio ω/r extended from the near horizon limit $r \to 0$ to the one where $\omega/r \sim \omega/\sqrt{|\mathbf{B}|} \to 0$ as we are working in the $\omega/\sqrt{|\mathbf{B}|} \ll 1$ limit. The outer region is defined to be the region where the ω^2/r^2 and higher power in ω/r is suppressed, which can be extended toward $r \gg \sqrt{|\mathbf{B}|}$ as long as the frequency is small.

For concreteness, let us demonstrate how this works in the $E^{\|}$ channel that involves the bulk field δB_{xy} governed by Eq.(2.11). The solution can be written in the same form as (2.13) evaluated at zero temperature (i.e. $r_h = 0$). It is worth noting that the singular behaviour near $r/\sqrt{\mathcal{B}} \to 0$ is different from that in earlier section. Instead, it can be written as

$$\delta B^{outer}_{xy}(r) = c_1 - c_2\left(\log\Lambda - \bar{\phi}(r) + \frac{\mathcal{B}/3}{6r^2}\right) + \mathcal{O}\left(\frac{\omega^2}{r^2}, \frac{\omega^2}{r^2}\log\left(\frac{\omega}{r}\right)\right) \tag{2.31}$$

where the integration constants can be related to source and response via (2.8). It is worth noting that the logarithmic divergence appears at order ω^2. This is can be confirmed via Frobenius analysis in AdS_5 region (see e.g. [46]) and $AdS_3 \times \mathbb{R}^2$ region (see appendix B). The prefactor of the r^{-2} divergence is obtained by evaluating $e^{2V(r)-W(r)}/f(r)$ at the horizon $r \to 0$. Here $\bar{\phi}(r)$ is the integral in (2.13) subtracted by the r^{-2} divergent and logarithmic divergent pieces. The resulting integral evalutated from $r = r_0 \sim \sqrt{\mathcal{B}}$ of the overlapping region to the UV cutoff $r = \Lambda$ is finite and its number is not extremely relevant for us as long as one keep e_r^{-2} large.

Next, we consider the inner region solution, which can be obtained by solving (2.11) in the $AdS_3 \times \mathbb{R}^2$ region. Upon imposing horizon regularity at $r \to 0$, we find that the inner region solution is

$$\delta B^{inner}_{xy} = c^H \zeta K_1(\zeta)\,, \qquad \zeta = \frac{3\omega}{r} \tag{2.32}$$

For these two branches of solutions to match, we extend the inner region solution to the regime where $\zeta = \omega/r \ll 1$. We find that the 'near boundary' expansion takes the form

$$\delta B^{inner}_{xy} = c^H\left(1 + \frac{1}{2}\gamma\zeta^2 + \frac{1}{2}\zeta^2\log\zeta + \ldots\right) \tag{2.33}$$

Matching this solution to the outer region, we find that $c_2 \propto \omega^2$ unlike what happened in the previous section. Carrying on the matching procedure, we find that the polynomial governing the spectrum only depends on ω^2 and thus rules out the purely imaginary mode $\omega = -i/\tau$. The same argument can also be made for the $E^{\perp}$ channel involving δB_{xz}. This is because, the part that is relevant to the matching procedure only depends on ζ^2. See appendix B for more details on the form of δB_{xz} in the $AdS_3 \times \mathbb{R}^2$ region.

2. $T \lesssim \omega \ll \sqrt{|\mathbf{B}|}$ limit

In this section, we show that the electric flux lifetime can also be obtained regime where $\omega/T \gtrsim 1$ and $\omega/\sqrt{|\mathbf{B}|} \ll 1$ while keeping $\sqrt{|\mathbf{B}|}/T \gg 1$. The calculations closely resembles that of the zero temperature case except that the deep IR geometry is now $BTZ \times \mathbb{R}^2$ instead of $AdS_3 \times \mathbb{R}^2$. Figure 4 illustrates this geometry where the AdS_5 joined with the $BTZ \times \mathbb{R}^2$ at the 'boundary' $AdS_3 \times \mathbb{R}^2$

of the IR geometry. We will only focus on the $E^{\parallel}$ fluctuations as it is the only channel that contains the decaying modes in the $\omega/T \ll 1$ regime. Similar computation for this type of geometry can also be found in [45].

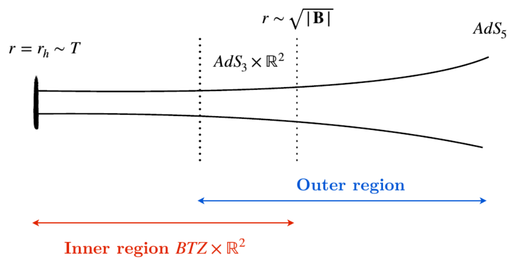

FIG. 4: A sketch of the bulk geometry at low temperature $T \ll \sqrt{|\mathbf{B}|}$. The inner region, whose solutions only depends on the ratio ω/r extends from the near horizon limit $r \to r_h \ll \sqrt{\mathbf{B}}$ to the one where $\omega/r \sim \omega/\sqrt{|\mathbf{B}|} \ll 1$, which corresponds to the near boundary region of $BTZ \times \mathbb{R}^2$ geometry, described by $AdS_3 \times \mathbb{R}^2$. The outer region is defined to be the region where ω^2/r^2 (and higher powers) is negligible and, therefore, can be extended toward $r \sim \sqrt{|\mathbf{B}|}$ in the $\omega/\sqrt{|\mathbf{B}|} \ll 1$ limit.

The outer region solution, which extends from the UV AdS_5 to the intermediate $AdS_3 \times \mathbb{R}^2$ region has the same form as in (2.31). This is possible only in the limit where $\sqrt{\mathcal{B}} \gg T$ so that $r/\sqrt{\mathcal{B}}$ is always much greater than $T/\sqrt{\mathcal{B}} \sim r_h/\sqrt{\mathcal{B}}$ in this region.

The inner region solution in the $BTZ \times \mathbb{R}^2$ region can be expressed in terms of a hypergeometric function (upon imposing ingoing boundary condition)

$$\delta B_{xy}^{inner} = c^H \left(1 - \frac{r_h^2}{r^2}\right)^{-i\mathfrak{w}/2} {}_2F_1\left(-\frac{i\mathfrak{w}}{2}, -\frac{i\mathfrak{w}}{2}, -\frac{i\mathfrak{w}}{2}; 1 - \mathfrak{w}; 1 - \frac{r_h^2}{r^2}\right) \tag{2.34}$$

where $\mathfrak{w} = \omega/(2\pi T) = \omega/3r_h$. Extending this solution in the $r \gg r_h$ limit (which is possible due to $r_h/r \to 0$ as we approach the limit $\omega/r \to 0$) yields the following expansion [47]

$$\delta B_{xy}^{inner} \propto c^H \left[1 + \frac{i\omega r_h}{6r^2} + \frac{1}{4}\left(\frac{\omega}{3r}\right)^2 \left(2 - 2\gamma - 2\psi(1 - i\mathfrak{w}/2) - \log\left(\frac{r_h^2}{r^2}\right)\right) + \mathcal{O}(\omega^3)\right] \tag{2.35}$$

where $\psi(x)$ is the digamma function and the constants of proportionality are combinations of gamma functions that can be absorbed in the definition of c^H. The first two terms in [...] are what important for us. By working to leading order in $\omega/r \ll 1$ as one approaches the intermediate $AdS_3 \times \mathbb{R}^2$ region, we find the following matching solution

$$c_1 - c_2 \log(\Lambda/\sqrt{\mathcal{B}}) + \bar{\phi} = c^H \,, \qquad \left(\frac{\mathcal{B}}{3}\right) c_2 = i\omega \left(\frac{2\pi T}{3}\right) c^H \tag{2.36}$$

We can convert c_1 to the source b_{xy} and c_2 as done in the previos sections. Upon taking $e_r^{-2} \gg \bar{\phi}$ (so that the solution lies in the regime of validity $\omega/\sqrt{\mathcal{B}} \ll 1$), we find the solution of the form $\omega = -i/\tau_{E\parallel}$ where $\tau_{E\parallel}$ is the same as in (2.17). This indicates that the lifetime indeed grows as $T/\sqrt{\mathcal{B}}$ increases regardless of the ratio ω/T.

III. CONCLUSION

The higher-form symmetry viewpoint of magnetohydrodynamics and its low temperature incarnation, the force-free electrodynamics, leads to new insights. The central focus of the present work was to established the absence of long-lived non-conserved operators. In turn, this indicates the validity of a hydrodynamic description at low temperature and strong magnetic field. The question of whether the only operators that govern the deep IR dynamics are the conserved charges is important and ought to be asked before any quantitative attempt is made to study hydrodynamic properties (such as shear viscosity etc). All non-conserved operators must decay much faster than the scale of interest if a hydrodynamic interpretation is to be meaningful.

We work with a holographic model which shares the same global symmetry as that of the plasma, namely only the energy, momentum and magnetic flux commute with the Hamiltonian. The model is simple enough for the lifetime of electric flux to be determined by classical bulk dynamics and the precise question is whether or not the electric flux is sufficiently long-lived to interfere with hydrodynamic modes. Due to the anisotropy of the system in the presence of a strong expectation value of magnetic field, the lifetime of the electric field depends on its orientation. Our results can be summarised as follows

- For electric flux $E_\parallel$ parallel to the magnetic field, the lifetime has a strong dependence on the double-trace coupling κ which plays a role similar to the renormalised electromagnetic coupling. In the extreme limit of $e_r^{-2} \gg |\mathbf{B}|/\mathbf{T^2}$, the lifetime can be large enough to be detectable by the analytic computation in both the 'usual' hydrodynamic regime $\omega/T \ll 1$ and on even lower temperature regime where $\omega/\sqrt{\mathbf{B}} \ll 1$ while ω/T may remains finite. We found that the lifetime becomes shorter as one decreases the ratio of $T/\sqrt{|\mathbf{B}|}$. The latter indicates that the lifetime will become extremely short in the extremely strong magnetic field regime $T/\sqrt{|\mathbf{B}|} \ll 1$ and cannot interfere with the low energy regime of $\omega/\sqrt{|\mathbf{B}|} \ll 1$ where the FFE limit is thought to be applicable.

- For the component of electric flux $E_\perp$ perpendicular to the magnetic field, we find that there is no pole in the vicinity of $\omega/T \ll 1$. The dependence of the lifetime on the renormalised electromagnetic coupling disappears as one approaches the strong magnetic field limit.

We also performed a consistency check at $T \to 0$ to ensure that there are no modes in the deep IR limit of $\omega/\sqrt{|\mathbf{B}|} \ll 1$. In this regime, the modes that indicate (potentially) long lifetime of $E_\parallel$ disappear from the low energy spectrum as anticipated.

These computations are basic checks on the validity of FFE description. In the holographic context, it would be interesting to check if *all* the accessible non-conserved operator truly have a parametrically short lifetime as well as confirming the low energy spectrum predicted by force-free electrodynamics (and its subsequent derivative corrections). Extraction of FFE effective action from gravity akin to [48–50] or the full constitutive relation as in [51–53] would be desirable as a definitive proof of FFE description in the dynamically magnetised black brane geometry. Last but not least, it would be very interesting to investigate operators lifetime in (weakly coupled) quantum electrodynamics at finite T and $\mathbf{B}$ to better understand FFE and its limitations in a system more directly connected to astrophysical plasma than the strongly coupled holographic model considered here.

ACKNOWLEDGEMENTS

We would like to thank Jay Armas, Sašo Grozdanov, Nabil Iqbal, Kieran Macfarlane, Watse Sybesma and Lárus Thorlacius for helpful discussions and comments. We are particularly grateful to S. Grozdanov, N. Iqbal and L. Thorlacius for commenting on the manuscript. The work of N. P. was supported by Icelandic Research Fund grant 163422-052 and STFC grant number ST/T000708/1. The work of A.R was supported in part by the Icelandic Research Fund under grant 195970-052 and by the University of Iceland Research Fund.

Appendix A: Numerical solution and evaluation of operators lifetime

In this section, remarks on the evaluation of the electric flux are elaborated. The numerical background solution for this geometry can be constructed in the same way as [32] using shooting method. The solution is a one-parameter family characterised by $\mathcal{B}/T^2$ which allows us the freedom to choose $r_h = 1, r_h^2 f'(r_h) = 1$ (or equivalently $T = 1/4\pi$). It is also convenient to set $V(r_h) = W(r_h) = 0$ which results in the UV boundary metric of the form

$$\lim_{r\to\infty} ds^2 = r^2\left(-dt^2 + v(dx^2+dy^2) + wdz^2\right) + \frac{dr^2}{r^2} \tag{A1}$$

Upon rescaling of spatial coordinates $\{dx, dy, dz\} \to \{dx/\sqrt{v}, dy/\sqrt{v}, dz/\sqrt{w}\}$, we recover the desired background solutions. Note also that the physical magnetic flux is related to the input parameter (that produced the metric in (A1)) by $\mathcal{B}_{\text{physical}} = \mathcal{B}_{\text{input}}/v$. A small caveat of this method is that one cannot find a smooth solution beyond $\mathcal{B}_{\text{input}} \gtrsim \sqrt{3}/2$ which corresponds to the temperature $T/\sqrt{\mathcal{B}} = (4\pi\sqrt{\mathcal{B}_{\text{input}}/v})^{-1} \approx 0.05$. This is most likely an artifact of the presented numerical method as there exists a smooth solution in the zero temperature limit corresponding to the $AdS_3 \times \mathbb{R}^2$ geometry in the deep IR. We should also note that this is a sufficiently low energy temperature as the entropy becomes sufficiently close to $s \propto T$ obtained from $BTZ \times \mathbb{R}^2$ geometry (c.f. [26, 32]). The background is generated for r from $[1+10^{-3}, 10^6]$ and varying the (numerical) cutoffs within this order of magnitude does not change the obtained numerical results.

Let us also remark on the the numerical value of the renormalised electromagnetic coupling $e_r^{-2} = \log(\Lambda/r_h) + \kappa(\Lambda)^{-1}$. This quantity strongly influences both the thermodynamics and low energy spectrum [26, 27, 33] of the model. In particular a small value of e_r^{-2} would result in the speed of sound becoming imaginary [26]. Another way to see that this quantity should be large is to write it in terms of a renormalisation group independent scale M_* that denotes the energy scale of a Landau pole [27] i.e. $e_r^{-2} \sim \log(M_\star/T)$ where $M_\star \gg T$. We take this to be the largest scale in the problem–much larger than the accessible value of $\sqrt{\mathcal{B}}/T$.

Numerical value of the integral for $\phi(r_h)$ in (2.17) is shown in Figure 5. For a larger temperature (when $\phi(r_h) \approx \mathcal{O}(1)$), the lifetime can be sensibly approximated to be $\tau_{E\parallel} \approx 2\pi(T/\mathcal{B})e_r^{-2}$. As $T/\sqrt{\mathcal{B}}$ decreases, the lifetime becomes shorter and, if we are to extrapolate the fitting function $\phi \sim \frac{\mathcal{B}}{T^2}\log\frac{\mathcal{B}}{T^2}$ to even lower temperature where $e_r^{-2} \gtrsim \phi$, it will escape the regime of the validity of small $\omega/T, \omega/\sqrt{\mathcal{B}}$ expansions. In this scenario, one shall conclude that there are no long-lived modes that can interfere with the low energy excitations.

Appendix B: Frobenius analysis in $AdS_3 \times \mathbb{R}^2$ region

Consider the equation of motion for δB_{xy} in the intermediate $AdS_3 \times \mathbb{R}^2$ region:

$$\delta B''_{xy}(r) + \frac{3}{r}\delta B'_{xy}(r) + \frac{\omega^2}{9r^2}\delta B_{xy}(r) = 0 \tag{B1}$$

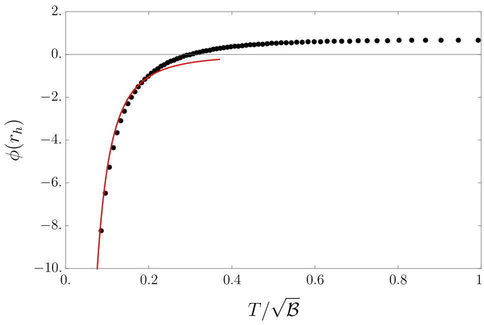

FIG. 5: Numerical evaluation of $\phi(r_h)$ in (2.17) as a function of $T/\sqrt{\mathcal{B}}$. The black dots denote the numerical evaluation while the red line denotes the fitting function for small $T/\sqrt{\mathcal{B}}$ as $\phi \approx -(0.008)\frac{\mathcal{B}}{T^2}\log(5.7\mathcal{B}/T^2)$. For high temperatures, the value of $\phi(r_h)$ is approximately constant around 0.69. The value of $\phi(r_h)$ at lowest achievable temperature is at $\phi(r_h) = -23.49$.

The solution in this region can be obtained via Frobenius method. More precisely, one can change the radial coordinate into $\zeta = 3\omega/r$ and redefine $\delta B_{xy} = \zeta c(\zeta)$. It follows that $c(\zeta)$ is the solution of the Bessel equation of order 1, which has a regular singular point at $\zeta = 0$. The near-boundary $r \to \infty$, or equivalently $\zeta \to 0$, akin to the Fefferman-Graham expansion in the usual holographic renormalisation, can be written as

$$\delta B_{xy}(\zeta) = c_1^M \mathcal{P}_1(\zeta) + \left(c_2^M + \mathfrak{h}\log\zeta\right)\mathcal{P}_2(\zeta) \tag{B2a}$$

where c_1^M, c_2^M are integration constants and $\mathcal{P}_i(\zeta)$ are regular polynomials of the following form

$$\mathcal{P}_1 = 1 + \sum_{n=1}^{\infty} p_1^{[n]}\zeta^n\,, \qquad \mathcal{P}_2 = \zeta^2\left(1 + \sum_{n=1}^{\infty} p_2^{[n]}\zeta^n\right) \tag{B2b}$$

Similar to the usual procedure in the holographic renormalisation [54], all the coefficients $p_1^{[n]}, p_2^{[n]}, \mathfrak{h}$ except $p_1^{[2]}$, which can be set to zero without loss of generality [46], can be obtained recursively. The important piece of information here is the coefficient $\mathfrak{h} = 1$ which can be obtained by recursively solving the equation (B1). Another easy way to see this is to recast (B1) as the Bessel equation of order 1 as pointed out earlier. Then, using the fact that the Bessel functions

$K_1(\zeta)$ and $I_1(\zeta)$ are two independent solutions of such equation and, for small ζ they admit the following asymptotic expansions (see e.g. §3.3 of [55])

$$I_1(\zeta) = \frac{\zeta}{2} + \frac{\zeta^2}{16} + \mathcal{O}(\zeta)^3\,, \qquad K_1(\zeta) = \left(\gamma + \log\frac{\zeta}{2}\right) I_1(\zeta) + \frac{1}{\zeta} \tag{B3}$$

will result in the series expansions of the solution in $AdS_3 \times \mathbb{R}^2$ region in (B2a).

A similar procedure can also be applied for $E^{\perp}$ using Eq.(2.25). Substituting $\delta\tilde{B}_{xz} = \zeta^2 c(\zeta)$, one finds that it obeys the Bessel equation of order 2 whose $\zeta \ll 1$ expansion only yields even power in ζ.

---

[1] L. D. Landau and E. M. Lifshitz, *Fluid Mechanics*. Butterworth-Heinemann, 2nd ed., 1987.

[2] R. W. Zwanzig, *Statistical mechanics of irreversibility*. Lectures on Theoretical Physics Volume 3, 139 (Interscience, 1961), 1961.

[3] D. Forster, *Hydrodynamic Fluctuations, Broken Symmetry, and Correlation Functions*. Perseus Books, 1995.

[4] S. A. Hartnoll and D. M. Hofman, "Locally Critical Resistivities from Umklapp Scattering," *Phys. Rev. Lett.* **108** (2012) 241601, `arXiv:1201.3917 [hep-th]`.

[5] D. Gaiotto, A. Kapustin, N. Seiberg, and B. Willett, "Generalized Global Symmetries," *JHEP* **02** (2015) 172, `arXiv:1412.5148 [hep-th]`.

[6] S. Grozdanov, D. M. Hofman, and N. Iqbal, "Generalized global symmetries and dissipative magnetohydrodynamics," *Phys. Rev. D* **95** no. 9, (2017) 096003, `arXiv:1610.07392 [hep-th]`.

[7] D. Schubring, "Dissipative String Fluids," *Phys. Rev. D* **91** no. 4, (2015) 043518, `arXiv:1412.3135 [hep-th]`.

[8] J. Hernandez and P. Kovtun, "Relativistic magnetohydrodynamics," *JHEP* **05** (2017) 001, `arXiv:1703.08757 [hep-th]`.

[9] J. Armas and A. Jain, "Magnetohydrodynamics as superfluidity," *Phys. Rev. Lett.* **122** no. 14, (2019) 141603, `arXiv:1808.01939 [hep-th]`.

[10] J. Armas and A. Jain, "One-form superfluids & magnetohydrodynamics," *JHEP* **01** (2020) 041, `arXiv:1811.04913 [hep-th]`.

[11] W. G. Dixon, *Special relativity: the foundation of macroscopic physics*. CUP Archive, 1982.

[12] A. M. Anile, *Relativistic fluids and magneto-fluids: With applications in astrophysics and plasma physics*. Cambridge University Press, 2005.

[13] S. S. Komissarov, "A Godunov-type scheme for relativistic magnetohydrodynamics," *Monthly Notices of the Royal Astronomical Society* **303** no. 2, (02, 1999) 343–366.

[14] P. B. Arnold, G. D. Moore, and L. G. Yaffe, "Transport coefficients in high temperature gauge theories. 1. Leading log results," *JHEP* **11** (2000) 001, `arXiv:hep-ph/0010177`.

[15] R. Blandford and R. Znajek, "Electromagnetic extractions of energy from Kerr black holes," *Mon. Not. Roy. Astron. Soc.* **179** (1977) 433–456.

[16] S. Komissarov, "Electrodynamics of black hole magnetospheres," *Mon. Not. Roy. Astron. Soc.* **350** (2004) 407, arXiv:astro-ph/0402403.

[17] P. Goldreich and W. H. Julian, "Pulsar Electrodynamics," *Astrophys. J.* **157** (Aug., 1969) 869.

[18] T. Wiegelmann and T. Sakurai, "Solar Force-free Magnetic Fields," *Living Rev. Sol. Phys.* **9** (2012) 5, arXiv:1208.4693 [astro-ph.SR].

[19] S. E. Gralla and T. Jacobson, "Spacetime approach to force-free magnetospheres," *Mon. Not. Roy. Astron. Soc.* **445** no. 3, (2014) 2500–2534, arXiv:1401.6159 [astro-ph.HE].

[20] G. Compère, S. E. Gralla, and A. Lupsasca, "Force-Free Foliations," *Phys. Rev. D* **94** no. 12, (2016) 124012, arXiv:1606.06727 [math-ph].

[21] T. Uchida, "Theory of force-free electromagnetic fields. i. general theory," *Phys. Rev. E* **56** (Aug, 1997) 2181–2197. https://link.aps.org/doi/10.1103/PhysRevE.56.2181.

[22] C. Thompson and O. Blaes, "Magnetohydrodynamics in the extreme relativistic limit," *Phys. Rev. D* **57** (1998) 3219–3234.

[23] S. E. Gralla and N. Iqbal, "Effective Field Theory of Force-Free Electrodynamics," *Phys. Rev. D* **99** no. 10, (2019) 105004, arXiv:1811.07438 [hep-th].

[24] P. Glorioso and D. T. Son, "Effective field theory of magnetohydrodynamics from generalized global symmetries," arXiv:1811.04879 [hep-th].

[25] B. Benenowski and N. Poovuttikul, "Classification of magnetohydrodynamic transport at strong magnetic field," arXiv:1911.05554 [hep-th].

[26] S. Grozdanov and N. Poovuttikul, "Generalised global symmetries in holography: magnetohydrodynamic waves in a strongly interacting plasma," *JHEP* **04** (2019) 141, arXiv:1707.04182 [hep-th].

[27] D. M. Hofman and N. Iqbal, "Generalized global symmetries and holography," *SciPost Phys.* **4** no. 1, (2018) 005, arXiv:1707.08577 [hep-th].

[28] D. T. Son and A. O. Starinets, "Minkowski space correlators in AdS / CFT correspondence: Recipe and applications," *JHEP* **09** (2002) 042, arXiv:hep-th/0205051.

[29] P. Kovtun, D. T. Son, and A. O. Starinets, "Holography and hydrodynamics: Diffusion on stretched horizons," *JHEP* **10** (2003) 064, arXiv:hep-th/0309213.

[30] J. F. Fuini and L. G. Yaffe, "Far-from-equilibrium dynamics of a strongly coupled non-Abelian plasma with non-zero charge density or external magnetic field," *JHEP* **07** (2015) 116, arXiv:1503.07148 [hep-th].

[31] S. Janiszewski and M. Kaminski, "Quasinormal modes of magnetic and electric black branes versus far from equilibrium anisotropic fluids," *Phys. Rev. D* **93** no. 2, (2016) 025006, arXiv:1508.06993 [hep-th].

[32] E. D'Hoker and P. Kraus, "Magnetic Brane Solutions in AdS," *JHEP* **10** (2009) 088, arXiv:0908.3875 [hep-th].

[33] S. Grozdanov, A. Lucas, and N. Poovuttikul, "Holography and hydrodynamics with weakly broken symmetries," *Phys. Rev. D* **99** no. 8, (2019) 086012, arXiv:1810.10016 [hep-th].

[34] R. A. Davison and B. Goutéraux, "Momentum dissipation and effective theories of coherent and incoherent transport," *JHEP* **01** (2015) 039, arXiv:1411.1062 [hep-th].

[35] C.-F. Chen and A. Lucas, "Origin of the Drude peak and of zero sound in probe brane holography," *Phys. Lett. B* **774** (2017) 569–574, arXiv:1709.01520 [hep-th].

[36] R. A. Davison, S. A. Gentle, and B. Goutéraux, "Impact of irrelevant deformations on thermodynamics and transport in holographic quantum critical states," *Phys. Rev. D* **100** no. 8, (2019) 086020, arXiv:1812.11060 [hep-th].

[37] E. Witten, "Multitrace operators, boundary conditions, and AdS / CFT correspondence," arXiv:hep-th/0112258.

[38] M. Berkooz, A. Sever, and A. Shomer, "'Double trace' deformations, boundary conditions and space-time singularities," *JHEP* **05** (2002) 034, arXiv:hep-th/0112264.

[39] R. A. Davison and A. Parnachev, "Hydrodynamics of cold holographic matter," *JHEP* **06** (2013) 100, arXiv:1303.6334 [hep-th].

[40] U. Moitra, S. K. Sake, and S. P. Trivedi, "Near-Extremal Fluid Mechanics," arXiv:2005.00016 [hep-th].

[41] S. S. Gubser and A. Nellore, "Ground states of holographic superconductors," *Phys. Rev. D* **80** (2009) 105007, arXiv:0908.1972 [hep-th].

[42] R. A. Davison, B. Goutéraux, and S. A. Hartnoll, "Incoherent transport in clean quantum critical metals," *JHEP* **10** (2015) 112, arXiv:1507.07137 [hep-th].

[43] P. K. Kovtun and A. O. Starinets, "Quasinormal modes and holography," *Phys. Rev. D* **72** (2005) 086009, arXiv:hep-th/0506184.

[44] E. D'Hoker, P. Kraus, and A. Shah, "RG Flow of Magnetic Brane Correlators," *JHEP* **04** (2011) 039, arXiv:1012.5072 [hep-th].

[45] E. D'Hoker and P. Kraus, "Magnetic Field Induced Quantum Criticality via new Asymptotically AdS_5 Solutions," *Class. Quant. Grav.* **27** (2010) 215022, arXiv:1006.2573 [hep-th].

[46] P. Kovtun and A. Starinets, "Thermal spectral functions of strongly coupled N=4 supersymmetric Yang-Mills theory," *Phys. Rev. Lett.* **96** (2006) 131601, arXiv:hep-th/0602059.

[47] M. Abramowitz and I. A. Stegun, *Handbook of Mathematical Functions with Formulas, Graphs, and Mathematical Tables*. Dover, New York, ninth dover printing, tenth gpo printing ed., 1964.

[48] D. Nickel and D. T. Son, "Deconstructing holographic liquids," *New J. Phys.* **13** (2011) 075010, arXiv:1009.3094 [hep-th].

[49] P. Glorioso, M. Crossley, and H. Liu, "A prescription for holographic Schwinger-Keldysh contour in non-equilibrium systems," arXiv:1812.08785 [hep-th].

[50] J. de Boer, M. P. Heller, and N. Pinzani-Fokeeva, "Holographic Schwinger-Keldysh effective field theories," *JHEP* **05** (2019) 188, arXiv:1812.06093 [hep-th].

[51] S. Bhattacharyya, V. E. Hubeny, S. Minwalla, and M. Rangamani, "Nonlinear Fluid Dynamics from Gravity," *JHEP* **02** (2008) 045, arXiv:0712.2456 [hep-th].

[52] N. Banerjee, J. Bhattacharya, S. Bhattacharyya, S. Dutta, R. Loganayagam, and P. Surowka, "Hydrodynamics from charged black branes," *JHEP* **01** (2011) 094, arXiv:0809.2596 [hep-th].

[53] J. Erdmenger, M. Haack, M. Kaminski, and A. Yarom, "Fluid dynamics of R-charged black holes," *JHEP* **01** (2009) 055, arXiv:0809.2488 [hep-th].

[54] S. de Haro, S. N. Solodukhin, and K. Skenderis, "Holographic reconstruction of space-time and renormalization in the AdS / CFT correspondence," *Commun. Math. Phys.* **217** (2001) 595–622, arXiv:hep-th/0002230.

[55] C. Bender and S. Orszag, *Advanced Mathematical Methods for Scientists and Engineers I: Asymptotic Methods and Perturbation Theory*. Springer New York, 2013.

Paper II

Non-equilibrium steady states in quantum critical systems with Lifshitz scaling

Daniel Fernández, Aruna Rajagopal, Lárus Thorlacius

JHEP, 12(2019), 29

Prepared for submission to JHEP

Non-equilibrium steady states in quantum critical systems with Lifshitz scaling

Daniel Fernández,[a] **Aruna Rajagopal,**[a] **Lárus Thorlacius**[a,b]

[a] *University of Iceland, Science Institute, Dunhaga 3, 107 Reykjavík, Iceland*
[b] *The Oskar Klein Centre for Cosmoparticle Physics & Department of Physics, Stockholm University, AlbaNova, 106 91 Stockholm, Sweden.*

E-mail: arr17@hi.is, fernandez@hi.is, lth@hi.is

Abstract: We study out-of-equilibrium energy transport in a quantum critical fluid with Lifshitz scaling symmetry following a local quench between two semi-infinite fluid reservoirs. The late time energy flow is universal and is accommodated via a steady state occupying an expanding central region between outgoing shock and rarefaction waves. We consider the admissibility and entropy conditions for the formation of such a non-equilibrium steady state for a general dynamical critical exponent z in arbitrary dimensions and solve the associated Riemann problem. The Lifshitz fluid with $z = 2$ can be obtained from a Galilean boost invariant field theory and the non-equilibrium steady state is identified as a boosted thermal state. A Lifshitz fluid with generic z is scale invariant but without boost symmetry and in this case the non-equilibrium steady state is genuinely non-thermal.

Contents

1 Introduction

Fluid theory is one of the oldest effective descriptions in physics.[1] It is based on general symmetry principles and applies in the limit of long wavelength and low frequency compared to characteristic microscopic length and time scales of the system in question. A fluid description can thus stand on its own and be useful even when no microscopic description, based on particles or quasiparticles, is available. There has been considerable recent interest in extending fluid theory to systems with unconventional symmetries, including Lifshitz scale symmetry, with potential applications to quantum critical systems [2–5]. Motivated by these developments, we will consider a problem involving out of equilibrium energy transport in fluids with Lifshitz symmetry.

It remains an open problem to develop a general fluid dynamics formalism for systems that are far from thermal equilibrium, but there has been interesting recent progress in

[1]For a classic textbook treatment see volume 6 of Landau and Lifshitz [1].

this direction involving relativistic fluids. Investigating out of equilibrium energy transport between two relativistic quantum critical heat baths led to the discovery of the emergence of a universal Non-Equilibrium Steady State (NESS) between the two heat baths, described by a Lorentz boosted thermal state [6–10]. In the present paper, we extend this analysis to more general quantum critical fluids, in particular to non-relativistic fluids with Lifshitz scale symmetry (referred to as Lifshitz fluids in the following), and find that a NESS emerges here as well. For the special case of a Lifshitz fluid with dynamical critical exponent $z = 2$, the resulting NESS can be viewed as a Galilean boost of a thermal state. For Lifshitz fluids with $z \neq 2$, there is no underlying boost symmetry [11]. It turns out there is still an emergent NESS at generic z, but in this case it cannot be obtained as a boosted thermal state.

In order to gain further insight into emergent hydrodynamic behaviour, we adapt the local quench construction of [6, 7] to the case of a non-relativistic fluid with Lifshitz scaling symmetry and study the subsequent time evolution for different values of the dynamical critical exponent. We begin in Section 2, where we introduce general properties of such fluids and continue in Section 3 by describing the setup involving a pair of quantum critical heat baths that are brought into contact at $t = 0$. In Section 4 we briefly review the theory of shock and rarefaction waves that can appear in this context and associated stability conditions. In Sections 5 and 6 we apply the general theory to our specific system, first for the case of a $z = 2$ scale invariant fluid with Galilean boost invariance and then for a general $z \neq 2$ fluid without boost symmetry. Finally, we discuss some open questions and possible future directions in Section 7.

2 Perfect fluids with Lifshitz symmetry

For simplicity, below we will focus on the special case of perfect fluids. These are idealised fluids, that are without shear, strain or bulk viscosity and do not conduct heat. We begin by introducing the symmetries we will be assuming and the definition of the dynamical critical exponent z.

2.1 Symmetries of relativistic and non-relativistic critical fluids

Symmetries play a central role in any fluid description. The most basic symmetries are time translations, spatial translations and spatial rotations, generated by the operators $\mathfrak{g} = \{\hat{H}, \hat{P}_i, \hat{\mathcal{J}}_{ij}\}$, respectively, whose commutators form the so-called Aristotelian algebra.

A relativistic fluid is not only invariant under these symmetries, but also under Lorentz boosts $\hat{L}_i$ relating observers moving with respect to each other with constant velocity,

$$\vec{x}' = \gamma\,(\vec{x} - \vec{v}t), \qquad t' = \gamma\left(t - \frac{\vec{v}\cdot\vec{x}}{c^2}\right), \tag{2.1}$$

where $\vec{v}$ describes the relative velocity between the two observers and $\gamma = 1/\sqrt{1 - v^2/c^2}$. At low velocities $v \ll c$, the Lorentz boost reduces to the Galilean boost $\hat{G}_i$,

$$\vec{x}' = \vec{x} - \vec{v}\,t, \qquad t' = t\,. \tag{2.2}$$

The Aristotelian algebra is extended to the Poincaré algebra or the Galilei algebra, depending on which of these boost generators is added to $\mathfrak{g}$. Furthermore, the Galilei algebra allows for a central extension, known as the Bargmann algebra [12], by the inclusion of an additional symmetry generator $\hat{\mathcal{M}}$, such that the non-vanishing Galilean boost commutators are given by

$$\begin{aligned} [\hat{\mathcal{J}}_{ij}, \hat{G}_k] &= \hat{G}_j \, \delta_{ij} - \hat{G}_i \, \delta_{jk} \, , \\ [\hat{H}, \hat{G}_i] &= \hat{P}_i \, , \\ [\hat{P}_i, \hat{G}_j] &= \hat{\mathcal{M}} \, \delta_{ij} \, . \end{aligned} \tag{2.3}$$

The charge $\hat{\mathcal{M}}$ corresponds to the non-relativistic kinetic mass [13] and needs to be included when describing a fluid with mass density. In a theory with Galilean boost symmetry, the kinetic mass is a measure of the amount of matter in the system and does not vary between inertial frames. It is a conserved quantity in an isolated system.

On top of this, in a relativistic *critical* fluid there is an additional symmetry under dilations of the form

$$\vec{x}' = \Lambda \vec{x}, \qquad t' = \Lambda t \, , \quad \text{with} \quad \Lambda > 0 \, . \tag{2.4}$$

Invariance under this symmetry implies that physical processes happen in the same way, at all distance scales or, alternatively, energy scales. For relativistic fluids, the scale symmetry is compatible with Lorentz symmetry and together they place powerful constraints on the allowed dynamics of the fluid.

A non-relativistic critical fluid can be scale invariant too, but in this case dilations $\hat{\mathcal{D}}$ take the more general form of a Lifshitz symmetry,

$$\vec{x}' = \Lambda \vec{x}, \qquad t' = \Lambda^z t \, , \tag{2.5}$$

where $z \geq 1$ is referred to as the dynamical critical exponent. In the absence of boost symmetries, a closed algebra exists for any z consisting of the generators $\mathfrak{g}_z = \{\hat{H}, \hat{P}_i, \hat{\mathcal{J}}_{ij}, \hat{\mathcal{D}}\}$.

A key observation, however, is that Lifshitz symmetry with generic $z > 1$ is in general *not* compatible with boost symmetry. Indeed, Lorentzian boost symmetry is only compatible with $z = 1$, which gives the scaling (2.4) and the no-go result of [11] implies that the Galilean boost symmetry (2.2) is only compatible with $z = 2$ Lifshitz scaling. In the special case of $z = 2$ the Bargmann algebra can be be further extended to the Schrödinger algebra [14] involving the set $\{\hat{H}, \hat{P}_i, \hat{\mathcal{J}}_{ij}, \hat{G}_i, \hat{\mathcal{D}}_{(z=2)}\}$. For this reason, when discussing the out of equilibrium dynamics of non-relativistic fluids, we will consider separately the cases $z = 2$ and $z \neq 2$, leading to different conclusions about the nature of the emergent steady state.

2.2 Thermodynamics and stress-energy tensor

Based on the considerations above, we will consider a fluid whose description is invariant under time and space translations as well as rotations. In addition, we will also assume a global $U(1)$ symmetry whose corresponding conserved charge is N. This is realized by the basic set of generators $\{\hat{H}, \hat{P}_i, \hat{\mathcal{J}}_{ij}, \hat{\mathcal{M}}\}$. Additional symmetries under boosts and rescaling will be considered below.

Global quantities in this fluid include the energy E, momentum $\vec{\mathbb{P}}$, entropy S and charge N. Locally, we have the energy density $\mathcal{E} = E/V$, momentum density $\mathcal{P}_i = \mathbb{P}_i/V$, entropy density $s = S/V$ and charge density $n = N/V$. Assuming a configuration where these can be uniformly defined, the fundamental thermodynamic relations relating the change of the internal energy to the changes in the rest of the thermodynamic state functions are

$$\mathrm{d}E = T\,\mathrm{d}S - P\,\mathrm{d}V + v^i\,\mathrm{d}\mathbb{P}_i + \mu\,\mathrm{d}N\,, \qquad E = T\,S - P\,V + v^i\,\mathbb{P}_i + \mu\,N\,, \tag{2.6}$$

or, in terms of the associated densities,

$$\mathrm{d}\mathcal{E} = T\,\mathrm{d}s + v^i\,\mathrm{d}\mathcal{P}_i + \mu\,\mathrm{d}n\,, \qquad \mathcal{E} = T\,s - P + v^i\,\mathcal{P}_i + \mu\,n\,. \tag{2.7}$$

The thermodynamic forces associated to these parameters are the temperature T, the pressure P, the fluid velocity $\vec{v}$ and the chemical potential μ.

As argued in [11], assuming a fluid with uniform velocity $\vec{v}$ in the presence of rotational symmetry, the momentum density must be proportional to the only directed quantity in the fluid, *i.e.* the velocity,

$$\mathcal{P}_i = \rho\,v_i\,, \tag{2.8}$$

and the above thermodynamic relation becomes

$$\mathrm{d}\mathcal{E} = T\,\mathrm{d}s + v^i\,\mathrm{d}(\rho\,v_i) + \mu\,\mathrm{d}n\,. \tag{2.9}$$

The quantity ρ is referred to as the kinetic mass density. In a theory with Galilean boost symmetry it is proportional to the charge density n but in the absence of boost symmetry the relation between n and ρ is more complicated.

The dynamical variables enter into the stress-energy tensor of the fluid $T^\mu{}_\nu$ and the current J^μ, whose conservation equations read[2]

$$\partial_\mu T^\mu{}_\nu = 0, \qquad \partial_\mu J^\mu = 0\,. \tag{2.10}$$

Classically the symmetry generators are realised by

$$\begin{aligned} H &= -\int_V \mathrm{d}^d x\, T^0{}_0(x)\,,\\ P_i &= \int_V \mathrm{d}^d x\, T^0{}_i(x)\,,\\ \mathcal{J}_{ij} &= \int_V \mathrm{d}^d x\, \left(x^i T^0{}_j(x) - x^j T^0{}_i\right)\,,\\ N &= \int_V \mathrm{d}^d x\, J^0(x)\,, \end{aligned} \tag{2.11}$$

which provides direct interpretation for various components of the stress-energy tensor and current. In particular, the energy density is $\mathcal{E} = -T^0{}_0$, the momentum density is $\mathcal{P}_i = T^0{}_i$, and the charge density is $n = J^0$ in any frame.

[2]Despite the use of μ, ν indices, we are not assuming Lorentz symmetry and these indices are not to be raised or lowered using a spacetime metric.

For a *perfect fluid* there exists a reference frame, the rest frame, in which there is no momentum density. The charge current then reduces to just the charge density and the stress-energy tensor involves only two parameters, the energy density and pressure. Explicitly, in this frame we have

$$T^{\mu}{}_{\nu} = \begin{pmatrix} -\mathcal{E}_0 & 0 \\ 0 & P\,\delta^i_j \end{pmatrix}, \qquad J^{\mu} = (n, 0)\,. \tag{2.12}$$

In any other frame of reference the description will also depend on the velocity $\vec{v}$ and in the absence of boost symmetry the $\vec{v}$ dependence can be non-trivial.

If the perfect fluid has Lorentz boost symmetry, the stress-energy tensor and current in the moving frame are related to those in the rest frame by a Lorentz boost transformation (2.1). In Section 5, we will be interested in describing a non-relativistic perfect fluid with Galilean boost symmetry under (2.2). In this case the stress-energy tensor and current in the moving frame are obtained from the following transformation rules [15],

$$T'^{\mu}{}_{\nu} = \frac{\partial x'^{\mu}}{\partial x^{\rho}} \frac{\partial x^{\sigma}}{\partial x'^{\nu}} \left(T^{\rho}{}_{\sigma} + J^{\rho}\,\Gamma_{\sigma}\right), \qquad J^{\mu} = \frac{\partial x'^{\mu}}{\partial x^{\rho}} J^{\rho}\,, \tag{2.13}$$

where we define $\Gamma_{\mu} = \left(\frac{1}{2}|v|^2, \vec{v}\right)$. Note that this version of $T^{\mu}{}_{\nu}$ does not follow the usual tensor transformation properties, because it does not have tensorial status in the context of Galilean relativity. However, it is possible to combine $T^{\mu}{}_{\nu}$ and J^{μ} into an $d \times (d+1)$ dimensional object $\tilde{T} = (T, J)$ which acts as a tensor.[3] The conservation equations (2.10) are merged into one, and spacetime is embedded into a higher-dimensional construction of Bargmannian coordinates where a tensorial description arises naturally. For an overview of this description in the context of Bargmann theory, see [15] and [16].

Applying (2.13) to a perfect fluid which is flowing at constant velocity $\vec{v}$, and described in the rest frame by (2.12), we obtain the following stress-energy tensor and current components [17],

$$\begin{aligned} T^{0}{}_{0} &= -\mathcal{E}, \\ T^{0}{}_{j} &= n\,v_j, \\ T^{i}{}_{0} &= -(\mathcal{E} + P)v^i, \\ T^{i}{}_{j} &= P\,\delta^i_j + n\,v^i v_j, \\ J^0 &= n, \\ J^i &= n\,v^i\,; \end{aligned} \tag{2.14}$$

where $\mathcal{E} = \mathcal{E}_0 + \frac{1}{2} n\,v^2$ adds kinetic energy to the energy density. From the off-diagonal components we read off the momentum density $\mathcal{P}_i = T^{0}{}_{i} = n\,v_i$, which fixes the coefficient in (2.8) to be $\rho = n$.

[3] Due to the last relation in (2.3), which relates the charge operator to a commutator of boosts and spatial translations, the conserved charges should ideally be arranged into a single object, not into two separate ones. For the Poincaré group, we have $[\hat{P}_i, \hat{L}_j] = \hat{P}_0\,\eta_{ij}$, so in the context of special relativity $\tilde{T}$ automatically decomposes into the tensors $T^{\mu}{}_{\nu}$ and J^{μ}.

This last observation can also be obtained from the Ward identity corresponding to Galilean boost symmetry. The boost generator can be written as $\hat{G}_i = t\,\partial_i = G^{\mu}{}_i\partial_\mu$. Due to the non-vanishing Poisson bracket $[\hat{P}_i, \hat{G}_j]$ in (2.3), the boost current is $b^{\mu}{}_i = t\,T^{\mu}{}_i - x_i\,J^{\mu}$ and the associated Ward identity gives $T^0{}_i = J_i$ [18], from which $\rho = n$ follows. The physical interpretation is that the flow of matter gives rise to momentum density and the inhomogeneous term in the transformation of the stress-energy in (2.13) accounts for the addition of momentum density under Galilean boosts.

In Section 6, where we consider critical fluids with generic z, we do not assume any boost invariance and the kinetic mass density ρ and the particle number density n are no longer identified with each other. Instead, we adopt an ansatz where they appear separately in the stress-energy tensor and the current [11],

$$T^{\mu\nu} = \begin{pmatrix} -\mathcal{E} & \rho\, v^i \\ -(\mathcal{E}+P)\, v^i & P\,\delta^{ij} + \rho\, v^i v^j \end{pmatrix}, \qquad J^{\mu} = \left(n, n\, v^i\right), \tag{2.15}$$

and then study out of equilibrium evolution.

The Lifshitz scaling relation (2.5) with $z \neq 1$ implies that space and time coordinates have different scaling behavior and this affects how dimensional analysis is carried out. The energy E is a conserved quantity associated to time translations, so it must scale as the inverse of time, and thus the energy density scales as $\mathcal{E}' = \Lambda^{-(d+z)}\mathcal{E}$. On the other hand, the individual terms in the thermodynamic relation (2.9) must all have the same scaling and from there one can infer the scaling behavior of the various thermodynamic variables of the Lifshitz fluid:

$$\begin{array}{llll} \mathcal{E}' = \Lambda^{-d-z}\mathcal{E}\,, & P' = \Lambda^{-d-z}P\,, & T' = \Lambda^{-z}\,T\,, & \mu' = \Lambda^{-z}\mu\,, \\ s' = \Lambda^{-d}\,s\,, & n' = \Lambda^{-d}\,n\,, & \rho' = \Lambda^{-d+z-2}\rho\,, & v' = \Lambda^{1-z}\,v\,. \end{array} \tag{2.16}$$

Note that it is only for $z = 2$ that the kinetic mass density scales in the same way as the charge density.

The symmetry under Lifshitz scaling (2.5) leads to the Ward Identity, $z\,T^0_0 + T^i_i = 0$, which in turn implies the equation of state

$$d\,P = z\,\mathcal{E} - \rho\,v^2\,, \tag{2.17}$$

where d is the number of spatial dimensions. For the particular case of $z = 2$, the equation of state reduces to $d\,P = 2\,\mathcal{E} - n\,v^2$ and it is easy to see that a Galilean boost of the form (2.13) to the rest frame gives the equation of state for a fluid at rest $d\,P = 2\,\mathcal{E}$. However, as mentioned above, scale invariance with generic dynamical critical exponent z is incompatible with Galilean boost invariance and we will see this explicitly in Section 6 when we study non-equilibrium steady states of a quantum critical fluid with $z \neq 2$. In this case, the state variables of a uniformly moving fluid are *not* equivalent to those of an equilibrium configuration viewed in a moving reference frame.

3 Local quench between semi-infinite heat baths

The specific system we consider consists of two semi-infinite heat reservoirs in d spatial dimensions, which are brought into contact at time $t = 0$ across a flat interface orthogonal to the x-coordinate axis. An equilibrium state of a charged quantum critical fluid is characterized by two energy scales, often taken to be the temperature and the chemical potential (due to scale invariance it is only the ratio T/μ that is physically relevant). In the case at hand, we find it convenient to instead use the pressure $P_{L,R}$ and charge density $n_{L,R}$ of the two reservoirs to describe the initial state,

$$P(t=0,x) = P_L\,\theta(-x) + P_R\,\theta(x)\,, \qquad n(t=0,x) = n_L\,\theta(-x) + n_R\,\theta(x)\,, \tag{3.1}$$

and our solution to the resulting fluid dynamical problem will be expressed in terms of the scale invariant ratios P_L/P_R and n_L/n_R. In what follows, we will consider $P_L/P_R > 1$ without loss of generality, and arbitrary charge ratio, $0 < n_L/n_R < \infty$.

A local quench of this type, with sharp jump functions $\theta(x)$, can serve as a first step towards studying out of equilibrium dynamics in a fluid. The pressure difference between the two reservoirs drives a fluid flow between them. One might intuitively expect the sharp initial gradient to be steadily smoothed out with the system approaching local equilibrium in the central region, but at the level of leading order hydrodynamics this is not the case. Instead, as time evolves, a non-equilibrium steady state (NESS) occupies a growing region between the two heat baths, characterised by the presence of a non-zero, constant energy flow, as was discussed in [6, 7]. The properties of the NESS are constrained by the equation of state of the heat baths and the conservation of the stress energy tensor and the charge current across the wavefronts, which emanate from the contact region (see Figure 1).

An initial value problem in hydrodynamics with piecewise constant initial data, where two fluids at equilibrium are joined across a discontinuity, is an example of a so-called Riemann problem [19] in the theory of partial differential equations. A solution, which generically involves shock and rarefaction waves propagating outwards from the initial discontinuity, can be found via the techniques described in Section 4, allowing the fluid variables that characterise the resulting non-equilibrium steady state to be determined in terms of the relevant input data. A Riemann problem for a relativistic quantum critical fluid in general dimensions was studied in [7]. Initially, both outgoing wavefronts were assumed to be shockwaves but it was later realized [8, 9] that above two spacetime dimensions, a solution with one shockwave and one rarefaction wave is preferred, based on entropy arguments and backed by numerical analysis. The existence and universality of the steady state for higher dimensional CFTs was studied in [20].

3.1 Formulation of the Riemann problem

In the present Riemann problem, the heat reservoirs are brought into contact across a planar surface, that we can take to be orthogonal to the x-axis. Following [6, 7], we look for a solution with wave fronts, traveling in the x-direction, that separate space into regions.

1. A region on the left, with the fluid at rest and stress-energy tensor as in (2.12) with $\mathcal{E}_L$, P_L and n_L.
2. Steady state region (or regions) in the middle, with the fluid flowing at a *constant* flow velocity $\vec{v}$, and stress-energy tensor as in (2.14) with $\mathcal{E}_s$, P_s and n_s.

3. A region on the right, with the fluid at rest and stress-energy tensor as in (2.12) with $\mathcal{E}_R$, P_R and n_R.

Drawing from the expressions presented in (2.14), in each region the conservation equations (2.10) take the following form:

$$\begin{aligned} \partial_t \mathcal{E} + \partial_i \left((\mathcal{E} + P) v^i \right) &= 0, \\ \partial_t (\rho v^i) + \partial_j (P + \rho v_i v^j) &= 0, \\ \partial_t n + \partial_j (n v^j) &= 0. \end{aligned} \tag{3.2}$$

These equations are supplemented with the equation of state (2.17) that relates $\mathcal{E}$ and P in a way that reflects the scaling symmetry of the fluid system.
Thus, the dynamics is governed by a set of hyperbolic conservation laws of the form

$$\partial_t \phi + \partial_i f = 0, \tag{3.3}$$

where ϕ and f are functions of the same fluid variables and $f(t, x)$ represents the flux of the conserved quantity $\phi(t, x)$. In our non-relativistic quantum critical fluid, the conserved quantities are charge, momentum and energy densities, and the resulting conservation equations (3.2) may be written as

$$\partial_t \begin{pmatrix} \mathcal{E} \\ \rho v \\ n \end{pmatrix} = \partial_x \begin{pmatrix} (\mathcal{E} + P) v \\ P + \rho v^2 \\ n v \end{pmatrix}. \tag{3.4}$$

Let us now discuss briefly the possible wave solutions that will emerge in this system.

4 Wave analysis

Generically, let us consider a conservation law of the form mentioned above,

$$\partial_t \phi + \partial_x f(\phi) = 0\,, \tag{4.1}$$

for a field $\phi(t, x)$, together with a piecewise constant initial condition:

$$\phi(0, x) = \begin{cases} \phi_L & \text{if } x < 0\,, \\ \phi_R & \text{if } x > 0\,. \end{cases} \tag{4.2}$$

This problem was first considered by Riemann in the 19th century [19]. Note that for any given solution of this problem $\phi_{\text{sol}}(t, x)$, the rescaled function $\phi_\theta(t, x) = \phi_{\text{sol}}(\theta t, \theta x)$ is also a solution for any $\theta > 0$. In fact, the initial condition (4.2) selects, out of all possible solutions of the conservation equations, those which are invariant under such a scaling transformation. These solutions are constant along rays emanating from the origin ($t = 0, x = 0$) due to the scaling, and they can generically be understood in terms of waves.

4.1 Linear problem

In the problem we will be considering, ϕ is a vector whose components are the energy density, pressure and fluid velocity, but, for the present discussion, we simply take it to be a generic vector of k components. A simple special case is obtained when $\partial_x f(\phi) \propto \partial_x \phi$, that is, for the strictly hyperbolic system

$$\partial_t \phi + A\, \partial_x \phi = 0\,, \tag{4.3}$$

where A is a matrix of constant coefficients. In this case, any solution can be written as a superposition of traveling waves. A generic initial condition $\phi(0,x) = \hat{\phi}(x)$ defines a wave profile that is shifted to the left and right as it evolves in time, in such a way that the height of the evolved profile at a given point is the sum (superposition) of heights at different points of the original profile.

The explicit solution takes the form

$$\vec{\phi}(t,x) = \sum_{i=1}^{k} \vec{r}_i\, \hat{\phi}_i(x - \lambda_i t), \tag{4.4}$$

where λ_i are the eigenvalues of the matrix A, that determine the speed of propagation of each component of $\vec{\phi}$, while the coefficients of the superposition, $\vec{r}_i$, are the components of the corresponding eigenvectors of A, and they determine the direction of the rays along which the wave travels. By diagonalising the matrix, the problem is decomposed into k scalar Cauchy problems that can be solved separately.

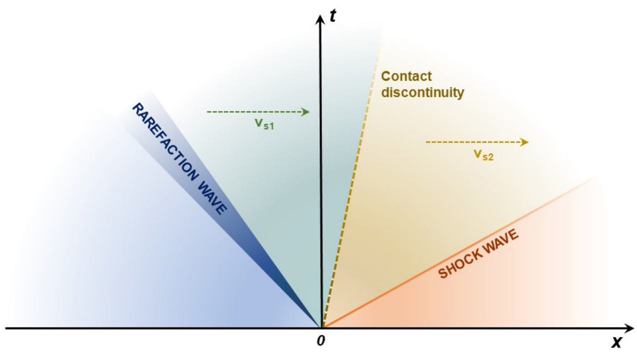

Figure 1: Propagation of shock, contact discontinuity and rarefaction waves for $P_L > P_R$.

4.2 Non-linear problem

More generally, the Jacobian in (4.1) is a function of ϕ itself,

$$A(\phi) = df(\phi) = \begin{pmatrix} \frac{\partial f_1}{\partial \phi_1} & \cdots & \frac{\partial f_1}{\partial \phi_k} \\ \vdots & \dots & \vdots \\ \frac{\partial f_k}{\partial \phi_1} & \cdots & \frac{\partial f_n}{\partial \phi_k} \end{pmatrix} . \tag{4.5}$$

This adds non-linearity to the problem. The solution can still be written in terms of waves, but the waves can interact with each other, producing additional waves. This is because the eigenvectors r_i are generalised into functions which depend on ϕ. The eigenvalues λ_i also depend on ϕ, and so the shape of the various components of the solution will vary in time, leading to wave dispersion and compression.

In [21], Lax provided a classification of the waves that can arise in non-linear wave problems with initial conditions of the form (4.2). To do so, he introduced a simplifying assumption: that each $\lambda_i(\phi)$, that is, the i^{th} eigenvalue of the Jacobian matrix (4.5), corresponds to either a *genuinely non-linear* wave, such that $\vec{\nabla}\lambda_i(\phi) \cdot \vec{r}_i(\phi) \neq 0$ for all ϕ, or to a *linearly degenerate* wave, such that $\vec{\nabla}\lambda_i(\phi) \cdot \vec{r}_i(\phi) = 0$ for all ϕ. The quantity $\vec{\nabla}\lambda_i \cdot \vec{r}_i$ can be understood as the directional derivative of $\lambda_i(\phi)$ in the direction of the vector $\vec{r}_i$.

As we will see below, this assumption holds in our Riemann problem for Lifshitz fluids and the resulting solutions have a simple structure consisting of different kinds of waves or discontinuities, which can be classified as follows:

• The linearly degenerate case $\vec{\nabla}\lambda_i \cdot \vec{r}_i = 0$, for which λ_i is constant along each integral curve of the corresponding field of eigenvectors r_i. In this case the profile of the solution does not change in time, generating a so-called contact discontinuity.

• The genuinely non-linear case with $\vec{\nabla}\lambda_i \cdot \vec{r}_i > 0$ such that the i^{th} eigenvalue λ_i is strictly increasing along the integral curve of the corresponding field of eigenvectors r_i. This leads to a rarefaction wave, displaying a smooth profile that widens and decays over time.

• The genuinely non-linear case with $\vec{\nabla}\lambda_i \cdot \vec{r}_i < 0$. This leads to a shock wave, displaying a compression which makes it become steeper over time.

When the simplifying assumption described above is valid, a set of stability conditions can be formulated which guarantee uniqueness and a continuous dependence on the initial data [22]. The one relevant for our analysis is Lax's shock wave admissibility condition [23], which can be easily visualised for the Riemann problem, where the initial configuration of $\phi(0, x)$ jumps from a left state ϕ_L to a right state ϕ_R at some value of x. The information contained in the piecewise initial condition propagates forward at speeds given by $\lambda_i(\phi_L)$ on the left and $\lambda_i(\phi_R)$ on the right. In order to prevent new characteristics spawning away from the shock interface, which would amount to non-uniqueness for our Cauchy problem, one must impose $\lambda_i(\phi_L) \geq \lambda_i(\phi_R)$. Furthermore, a shock wave connecting the states ϕ_L, ϕ_R moving at speed $\lambda = u_s$, must satisfy

$$\lambda_i(\phi_L) \geq u_s \geq \lambda_i(\phi_R) \, . \tag{4.6}$$

Lax's admissibility condition applies to shock waves but not to rarefaction waves. For a rarefaction wave, the solution's admissibility is determined by requiring $\lambda_i(\phi)$ to increase smoothly along the profile.

5 Rarefaction and shock waves for a $z = 2$ Lifshitz fluid

As already mentioned in Section 2, a non-relativistic Lifshitz fluid with scaling exponent $z = 2$ is special. This is due to a number of reasons. First of all, a Galilean boost invariant field theory describing such a fluid has been explicitly constructed [3, 24]. In addition, for $z = 2$, the Schrödinger group (consisting of the Bargmann group, enhanced by the addition of the dilation operator $\hat{\mathcal{D}}$), can have an additional generator, $\hat{C}$, corresponding to special conformal transformations. Finally, as shown in [11] and [25], it is only for this particular value of z that one can have a Galilean boost invariant fluid with Lifshitz scaling symmetry with a discrete Hamiltonian and number operator spectrum.

In view of this, we first consider a $z = 2$ Lifshitz fluid in d spatial dimensions taken to be invariant under Galilean boosts in addition to the scaling symmetry. In this case, we have the relation $\rho = n$ by virtue of a Ward identity, so the momentum density (2.8) is

$$\mathcal{P}_i = n\, v_i\,, \tag{5.1}$$

and the equation of state (2.17) reduces to

$$d\, P = 2\,\mathcal{E} - n\, v^2\,. \tag{5.2}$$

Then, the conservation equations (3.4) become

$$\partial_t \begin{pmatrix} \mathcal{E} \\ q \\ n \end{pmatrix} = \partial_x \begin{pmatrix} \frac{(d+2)}{d}\frac{q\,\mathcal{E}}{n} - \frac{1}{d}\frac{q^3}{n^2} \\ \frac{2}{d}\,\mathcal{E} + \frac{(d-1)}{d}\frac{q^2}{n} \\ q \end{pmatrix}, \tag{5.3}$$

where the combination

$$q = n\, v \tag{5.4}$$

has been introduced and the right hand side has been expressed solely as a function of the conserved variables. This has the form of a Riemann problem (4.1) with $\phi = (\mathcal{E}, q, n)$. The flux vector $f(\phi)$ can be read off from the right hand side and the Jacobian matrix is easily evaluated,

$$df(\phi) = \begin{pmatrix} \frac{(d+2)}{d}\frac{q}{n} & \frac{(d+2)}{d}\frac{\mathcal{E}}{n} - \frac{3}{d}\frac{q^2}{n^2} & -\frac{(d+2)}{d}\frac{q\mathcal{E}}{n^2} + \frac{2}{d}\frac{q^3}{n^3} \\ \frac{2}{d} & \frac{2(d-1)}{d}\frac{q}{n} & -\frac{(d-1)}{d}\frac{q^2}{n^2} \\ 0 & 1 & 0 \end{pmatrix}. \tag{5.5}$$

One of the eigenvalues of the Jacobian, along with the corresponding eigenvector, is

$$\lambda_1 = \frac{q}{n}, \quad r_1 = \begin{pmatrix} \frac{q^2}{2n} \\ q \\ n \end{pmatrix}. \tag{5.6}$$

This is linearly degenerate, $\vec{\nabla}\lambda_1(\phi) \cdot \vec{r}_1(\phi) = 0$, and corresponds to a contact discontinuity.

The remaining eigenvalues and eigenvectors are

$$\lambda_2 = \frac{q}{n}\left(1 - \frac{\sqrt{d+2}}{d}\sqrt{\frac{2\mathcal{E}n}{q^2} - 1}\right), \qquad r_2 = \begin{pmatrix} \frac{(d+2)}{d}\,\mathcal{E}n - \frac{1}{d}\,q^2 - \frac{\sqrt{d+2}}{d}\,q^2\,\sqrt{\frac{2\mathcal{E}n}{q^2} - 1} \\ q\left(1 - \frac{\sqrt{d+2}}{d}\sqrt{\frac{2\mathcal{E}n}{q^2} - 1}\right) \\ n \end{pmatrix}; \tag{5.7}$$

and

$$\lambda_3 = \frac{q}{n}\left(1 + \frac{\sqrt{d+2}}{d}\sqrt{\frac{2\mathcal{E}n}{q^2} - 1}\right), \qquad r_3 = \begin{pmatrix} \frac{(d+2)}{d}\,\mathcal{E}n - \frac{1}{d}\,q^2 + \frac{\sqrt{d+2}}{d}\,q^2\,\sqrt{\frac{2\mathcal{E}n}{q^2} - 1} \\ q\left(1 + \frac{\sqrt{d+2}}{d}\sqrt{\frac{2\mathcal{E}n}{q^2} - 1}\right) \\ n \end{pmatrix}; \tag{5.8}$$

which are genuinely non-linear, *i.e.* $\vec{\nabla}\lambda_i(\phi) \cdot \vec{r}_i(\phi) \neq 0$. These two families of solutions correspond to rarefaction and shock waves. Notice that from (5.2) and (5.4) it follows that their eigenvalues can be written as $\lambda_2 = v - c$ and $\lambda_3 = v + c$, where c is the local speed of sound in the fluid,

$$c = \sqrt{\frac{(d+2)}{d}\frac{P}{n}}. \tag{5.9}$$

It follows that the λ_2 (λ_3) eigenvalue corresponds to a left-moving (right-moving) wave.

Lax's admissibility condition for a shock wave turns out to be satisfied if and only if the pressure in the region behind the wave front exceeds the pressure in the region ahead of it. In our problem, where we assume that $P_L > P_R$, this is the $i = 3$ right-moving wave. The left-moving $i = 2$ wave, on the other hand, advances into a region of higher pressure and is therefore a rarefaction wave, whose profile widens over time.[4] Figure 2 shows a snapshot of the wave profile for a particular choice of initial data in (3.1), with a rarefaction wave on the left, a shock wave on the right, and a contact discontinuity in between. The shape is similar to the solution of the corresponding Riemann problem for a relativistic critical

[4]Under the reverse assumption, $P_L < P_R$, the only change is that the rarefaction and shock wave profiles are switched between the left- and right-moving waves.

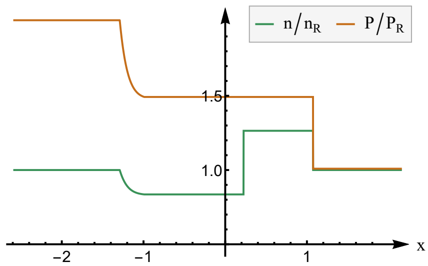

Figure 2: Snapshot of wave profiles for the pressure and charge density at $t = t_0 > 0$ for $P_L > P_R$ and $n_L = n_R$. The NESS region, bordered by the left-moving rarefaction wave and the right-moving shock wave, contains a contact discontinuity in the charge density.

fluid considered in [8, 9]. In particular, as we'll see below, the pressure remains constant across the contact discontinuity in the NESS region while the charge density jumps. In the relativistic case, the charge density decouples from the equations that determine the pressure but this is not the case here. For a non-relativistic Lifshitz fluid, the pressure still remains constant across the contact discontinuity but its value in the NESS region is nevertheless influenced by the initial values for the charge density of the two reservoirs (see *e.g.* (5.33) below).

5.1 Rarefaction wave profile

Let us start by analysing the $i = 2$ rarefaction wave. For this it is convenient to introduce the concept of *Riemann invariants*. A function $R^{(i)}(\phi)$ that is constant along the integral curves of the eigenvector r_i,

$$\vec{\nabla} R^{(i)}(\phi) \cdot \vec{r}_i = 0, \tag{5.10}$$

is called an i-Riemann invariant. A system with k eigenvalues has $k-1$ linearly independent i-Riemann invariants and they provide a convenient way to construct elementary wave solutions that are the building blocks of a full solution to the Riemann problem [19]. In the case at hand, we have two independent Riemann invariants per family of solutions, satisfying

$$\left(\frac{\partial R_A^{(i)}}{\partial \mathcal{E}}, \frac{\partial R_A^{(i)}}{\partial q}, \frac{\partial R_A^{(i)}}{\partial n} \right) \cdot \vec{r}_i = 0 \,, \quad \text{for} \quad A = 1, 2 \,. \tag{5.11}$$

For the first family, $\lambda_1 = \frac{q}{n} = v$ is itself a Riemann invariant, which means that the speed of the fluid is the same on both sides of the contact discontinuity, and additionally that the discontinuity itself moves at the same constant speed. In fact, this wave is called a contact discontinuity precisely because it moves at the fluid flow speed. A second Riemann invariant for the first family is given by the pressure, $P = \frac{2\mathcal{E}}{d} - \frac{q^2}{d\,n}$, so this quantity remains constant across the discontinuity as well.

For the two genuinely non-linear families, we find the following pairs of Riemann invariants:

$$
\begin{aligned}
R_1^{(2)} &= n^{-\gamma}\Big(2\mathcal{E} - \frac{q^2}{n}\Big), \qquad & R_2^{(2)} &= \frac{q}{n} + \sqrt{d+2}\sqrt{\frac{2\mathcal{E}}{n} - \frac{q^2}{n^2}}\,, \\
R_1^{(3)} &= n^{-\gamma}\Big(2\mathcal{E} - \frac{q^2}{n}\Big), \qquad & R_2^{(3)} &= \frac{q}{n} - \sqrt{d+2}\sqrt{\frac{2\mathcal{E}}{n} - \frac{q^2}{n^2}}\,,
\end{aligned}
\tag{5.12}
$$

where $\gamma \equiv \frac{d+2}{d}$. In order to facilitate their interpretation, these expressions can be rewritten using the equation of state,

$$
\begin{aligned}
R_1^{(2)} &= n^{-\gamma} P\,, \qquad & R_2^{(2)} &= v + d\,c\,, \\
R_1^{(3)} &= n^{-\gamma} P\,, \qquad & R_2^{(3)} &= v - d\,c\,,
\end{aligned}
\tag{5.13}
$$

where c was defined in (5.9) and we have dropped a multiplicative constant from $R_1^{(2)}$ and $R_1^{(3)}$. We note that c and γ are, respectively, the speed of sound and the ratio of specific heats at fixed pressure and volume in an ideal gas of $z = 2$ Lifshitz particles in d spatial dimensions [11].

The first Riemann invariant is the same for both the second and third families and involves a combination of pressure and particle density, $P\,n^{-\gamma}$, which remains constant during an isentropic process in an ideal gas. In other words, the conservation of $R_1^{(i)}$ amounts to the conservation of specific entropy, *i.e.* the entropy per particle, along integral curves of r_i. To see this, write the first law of thermodynamics in the form

$$
T\,\mathrm{d}s = \mathrm{d}e - \frac{P}{n^2}\mathrm{d}n, \tag{5.14}
$$

where s and e are, respectively, the specific entropy and specific internal energy. When expressed in terms of the specific internal energy, the equation of state (2.17) becomes

$$
d\,P = zne + \frac{z-2}{2}nv^2, \tag{5.15}
$$

which reduces to $d\,P = 2ne$ for $z = 2$. This implies

$$
\mathrm{d}e = \frac{1}{\gamma - 1}\left(\frac{1}{n}\mathrm{d}P - \frac{P}{n^2}\mathrm{d}n\right). \tag{5.16}
$$

Inserting (5.16) into (5.14) and applying the ideal gas law, one obtains

$$
\mathrm{d}s = \frac{1}{\gamma - 1}\,\mathrm{d}\log\left(n^{-\gamma}P\right). \tag{5.17}
$$

Thus, the first Riemann invariant in (5.12) may be interpreted in terms of entropy and we note that the second one has the expected form of a Riemann invariant obtained for a compressible Eulerian fluid [26].

For the $i = 2$ rarefaction wave, the conservation equations (3.4) are solved implicitly by the requirement that both Riemann invariants remain constant along the wave profile,

$$R_1^{(2)}(\mathcal{E}, q, n) = R_1^{(2)}(\mathcal{E}_L, q_L, n_L), \qquad R_2^{(2)}(\mathcal{E}, q, n) = R_2^{(2)}(\mathcal{E}_L, q_L, n_L)\,. \tag{5.18}$$

The left reservoir values $\mathcal{E}_L, q_L, n_L$ are realised at the leading edge of the rarefaction wave profile and can therefore be taken as a reference. The above requirement translates into the following two relations:

$$\frac{P_{s1}}{P_L} = \left(\frac{n_{s1}}{n_L}\right)^{\frac{d+2}{d}}, \qquad v_{s1} = v_L + d\, c_L \left(1 - \left(\frac{n_{s1}}{n_L}\right)^{\frac{1}{d}}\right), \tag{5.19}$$

where v_{s1} denotes the fluid flow velocity to the right of the rarefaction wave (see Figure 1) and v_L is the fluid flow velocity in the heat bath on the left ($v_L = 0$ in a heat bath at rest). Equivalently, the first relation in (5.19) can be used to express the flow velocity in terms of pressure rather than charge density,

$$v_{s1} = v_L + d\, c_L \left(1 - \left(\frac{P_{s1}}{P_L}\right)^{\frac{1}{d+2}}\right). \tag{5.20}$$

The phase velocity of the wave is given by the eigenvalue λ_2, as seen in (4.4), which in the present case is given by $\lambda_2 = v - c$ (with $c > 0$). Taking the wave profile to be parametrised by n, the condition for a valid rarefaction wave solution is

$$\lambda_2(\phi(n_L)) \leq \lambda_2(\phi(n))\,. \tag{5.21}$$

On the curve we have

$$\lambda_2(n) = v(n) - c(n) = v_L + c_L \left(d - (d+1)\left(\frac{n}{n_L}\right)^{\frac{1}{d}}\right), \tag{5.22}$$

and the rarefaction condition holds provided the charge density is higher in the region ahead of the wave front than behind the wave. This is indeed the case when $P_L > P_R$.

Note that since the wave has a smooth profile with spatial dependence $n(x,t)$, the phase velocity of the rarefaction wave also acquires a profile, $\lambda_2(x,t)$. On the leading left wavefront, where $n = n_L$, it evaluates to $\lambda_2 = -c_L$, that is, to the speed of sound in the heat bath on the left.

Similar considerations apply when $P_L < P_R$, except in this case the rarefaction wave belongs to the $i = 3$ family and moves to the right.

5.2 Jump conditions and shock wave

Riemann invariants are useful when the wave profile is smooth but other methods are needed for dealing with the sharp transitions that occur across a shock wave. A solution can be found by imposing so-called Rankine-Hugoniot jump conditions [23, 27], which express the conservation laws across the wavefront and relate variables in adjacent regions. For the problem (3.3), the jump conditions can be stated as

$$u_s[\phi] = [f], \tag{5.23}$$

where u_s is the speed at which the wave front propagates. The symbol $[q]$ indicates a jump in the variable q across a front, that is, $[q] = q_R - q_L$.

For our conservation equations (3.4), we get

$$\begin{aligned} u_s[n] &= [nv], \\ u_s[nv] &= [P + nv^2], \\ u_s[\mathcal{E}] &= [(\mathcal{E} + P)v], \end{aligned} \tag{5.24}$$

where u_s is the speed of the wave front in question and $[x]$ denotes the change in the variable x across the wave front, as described above. Writing $w = v - u_s$ and $\nu = n\,w$, these conditions can be expressed as

$$[\nu] = 0, \tag{5.25}$$

$$[P + \nu\, w] = 0, \tag{5.26}$$

$$[d\,\nu c^2 + \nu\, w^2] = 0, \tag{5.27}$$

where we have used the equation of state (5.2) and the definition $c^2 = \gamma \frac{P}{n}$.

A trivial and immediate solution is $\nu = [P] = 0$, which is the contact discontinuity described by the linearly degenerate $i = 1$ family of the previous subsection. As discussed below (5.11), the pressure and fluid speed are the same on both sides of the contact discontinuity, $P_{s1} = P_{s2} \equiv P_s$ and $v_{s1} = v_{s2} \equiv v_s$, but in general the energy and particle densities will be discontinuous across the wave front.

A right-moving $i = 3$ wave presents a non-trivial solution to the jump conditions. Assuming that $\nu \neq 0$, we introduce dimensionless variables:

$$\Pi_s \equiv \frac{P_s}{P_R}, \quad y \equiv \frac{n_{s2}}{n_R} = \frac{w_R}{w_s}\,, \tag{5.28}$$

where the right-most equality follows from the first jump condition (5.25). The remaining jump conditions (5.26) and (5.27) can be re-expressed as

$$\left(\frac{w_R}{c_R}\right)^2 = \frac{y(\Pi_s - 1)}{\gamma(y-1)} \qquad \text{and} \qquad \left(\frac{w_R}{c_R}\right)^2 = \frac{d\,y\,(\Pi_s - y)}{y^2 - 1}\,, \tag{5.29}$$

respectively. Combining these conditions and solving for y or Π_s gives

$$y = \frac{(d+1)\Pi_s + 1}{d + 1 + \Pi_s} \qquad \text{or} \qquad \Pi_s = \frac{(d+1)y - 1}{d + 1 - y}\,. \tag{5.30}$$

Substituting y back into (5.29), and choosing the branch of the square root that corresponds to a wave moving to the right, leads to the following expression for the shock speed,

$$u_s = v_R + c_R\sqrt{\frac{1 + (d+1)\Pi_s}{d+2}}\,. \tag{5.31}$$

Here v_R is the fluid speed in the heat bath on the right ($v_R = 0$ for a heat bath at rest). With this choice of sign, Lax's admissibility conditions (4.6) are satisfied for the shock wave. Indeed, with $\lambda_{3,R} = v_R + c_R = c_R$, the requirement is $u_s > c_R$, *i.e.* that the speed of the wave front exceeds the speed of sound in the medium that the shock wave expands into. This, in turn, amounts to the condition $P_s > P_R$.

Finally, we can use the relation $y = w_R/w_s$ from (5.28) to obtain the fluid speed v_{s2} in the region between the shock wave and the contact discontinuity in Figure 1,

$$v_{s2} = v_R + c_R \frac{d}{\sqrt{d+2}} \frac{(\Pi_s - 1)}{\sqrt{(d+1)\Pi_s + 1}} \,. \tag{5.32}$$

5.3 NESS variables and Galilean boost symmetry

Earlier we observed that pressure and fluid flow speed are the same on both sides of a contact discontinuity and the discontinuity itself propagates at the same speed. Demanding equality of the expressions for v_{s1} in (5.20) and v_{s2} in (5.32) gives us the following scale invariant condition on the pressure in the NESS region between the rarefaction and shock waves,

$$1 - \left(\frac{\Pi_s}{\Pi_L}\right)^{\frac{1}{d+2}} = \frac{1}{\sqrt{d+2}} \sqrt{\frac{\eta}{\Pi_L}} \frac{\Pi_s - 1}{\sqrt{(d+1)\Pi_s + 1}} \,. \tag{5.33}$$

The initial data of the two reservoirs enters through the ratios $\Pi_L = P_L/P_R$ and $\eta = n_L/n_R$. The above condition is non-linear but can be solved numerically and one finds a unique value of Π_s for given Π_L and η. The full solution to the Riemann problem can then be mapped out by evaluating the following expressions for the remaining NESS variables in

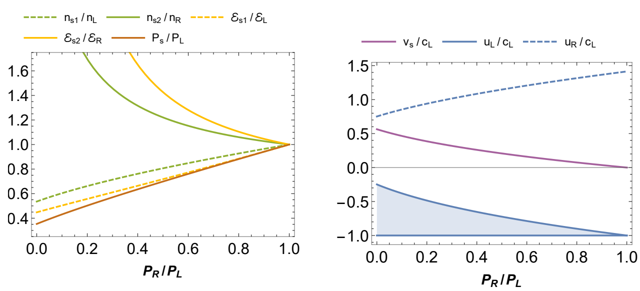

Figure 3: NESS variables for $z = 2$, $d = 3$ as a function of P_R/P_L for fixed $n_L/n_R = 2$. Left panel: Steady state pressure P_s, charge densities $n_{s1,s2}$, and energy densities $\mathcal{E}_{s1,s2}$. Right panel: Flow speed v_s, shock speed u_R, and wave speed u_L across rarefaction profile.

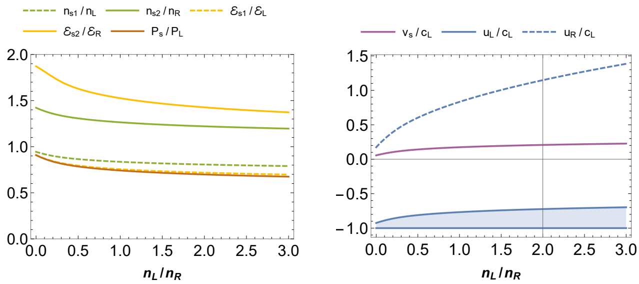

Figure 4: NESS variables for $z = 2$, $d = 3$ as a function of n_L/n_R for fixed $P_L/P_R = 2$. Left panel: Steady state pressure P_s, charge densities $n_{s1,s2}$, and energy densities $\mathcal{E}_{s1,s2}$. Right panel: Flow speed v_s, shock speed u_R, and wave speed u_L across rarefaction profile.

terms of the pressure,

$$\frac{n_{s1}}{n_L} = \left(\frac{\Pi_s}{\Pi_L}\right)^{\frac{d}{d+2}}, \tag{5.34}$$

$$\frac{n_{s2}}{n_R} = \frac{(d+1)\Pi_s + 1}{d+1+\Pi_s}, \tag{5.35}$$

$$\frac{\mathcal{E}_{s1}}{\mathcal{E}_L} = \frac{\Pi_s}{\Pi_L}\left(1 + (d+2)\left(\left(\frac{\Pi_L}{\Pi_s}\right)^{\frac{1}{d+2}} - 1\right)^2\right), \tag{5.36}$$

$$\frac{\mathcal{E}_{s2}}{\mathcal{E}_R} = \Pi_s + \frac{(\Pi_s - 1)^2}{d+1+\Pi_s}, \tag{5.37}$$

and evaluating (5.31) for the speed of the right-moving shock wave. The speed of the fluid flow in the NESS region can be obtained by evaluating either (5.20) or (5.32). Solutions for $d = 3$ spatial dimensions are presented in Figure 3 as a function of P_R/P_L for fixed n_L/n_R and in Figure 4 as a function of n_L/n_R for fixed P_R/P_L.

In the solution of the corresponding Riemann problem for a relativistic quantum critical fluid [8, 9] the NESS was described by a Lorentz boosted thermal state with a contact discontinuity in the charge density in the fluid rest frame. The behaviour of a $z = 2$ non-relativistic critical fluid is analogous, although in this case the boost symmetry is Galilean rather than Lorentzian. The fluid variables in the NESS region of the $z = 2$ flow have a stress-energy tensor and current of the form (2.14). The pressure and fluid speed are the same on both sides of the contact discontinuity but the energy density and the charge density take different values on the two sides. Nevertheless, if we perform a Galilean boost with velocity $-v_s$ to the NESS rest frame following the rule (2.13), we obtain a stress-energy tensor of the form (2.12) with $P = P_s$ and a *uniform* energy density,

$\mathcal{E}_0 = \mathcal{E}_{s1} - \frac{1}{2} n_{s1} v_s^2 = \mathcal{E}_{s2} - \frac{1}{2} n_{s2} v_s^2$. Furthermore, the fluid variables in the rest-frame satisfy the equation of state of $z = 2$ fluid at rest, $\mathcal{E}_0 = \frac{d}{2} P$. Since n does not transform under a Galilean boost, there is still a contact discontinuity in the charge density. Indeed, in the NESS rest frame the two fluids are at rest in hydrostatic equilibrium but the charge density is discontinuous across the contact surface. The charge density remains unchanged with time as there is no fluid flow across the boundary and therefore no charge transport. This kind of a sharp charge discontinuity is allowed when we restrict ourselves to leading-order hydrodynamics but is presumably smoothed out by higher-order corrections, which we do not consider here. We note that analogous behaviour was seen in the NESS rest frame of a relativistic fluid in [8, 9].

6 Rarefaction and shock waves at general z

In this section we turn our attention to a perfect Lifshitz fluid with a general dynamical critical exponent $z > 1$. This is motivated by the existence of quantum critical condensed matter systems with a general dynamical critical exponent $z \neq 2$, such as the heavy fermion metals discussed in [28] and [29]. For generic values of z such a system is without boost symmetry and it is interesting to see how this affects the solution to the fluid Riemann problem that we have been considering. The first thing to note is that the kinetic mass density ρ can no longer be proportional to the charge density n when $z \neq 2$. If we assume that ρ can still be expressed as a function of n alone, then the scaling relations (2.16) imply a relationship of the form

$$\rho = m\, n^{\alpha} \,, \tag{6.1}$$

with $\alpha = \frac{d+2-z}{d}$ and m a constant of proportionality. In principle, one could allow for more general behaviour, for instance by letting ρ depend explicitly on the velocity v as well as on the charge density, but we will not pursue this here. A scaling ansatz of the form (6.1) provides an example of a Lifshitz fluid without boost symmetry and this is sufficient for our present purposes. In what follows, we will take $m = 1$ for simplicity.

With the above ansatz the thermodynamic relation (2.9) takes the form

$$\mathrm{d}\mathcal{E} = T\,\mathrm{d}s + \frac{1}{2} n^{\alpha} \mathrm{d}v^2 + \left(\mu + \alpha\, n^{\alpha-1} v^2\right) \mathrm{d}n \,. \tag{6.2}$$

The $\mathrm{d}v^2$ terms can be absorbed by defining an internal energy and a shifted chemical potential,

$$\hat{\mathcal{E}} = \mathcal{E} - \frac{m}{2} n^{\alpha} v^2 \,, \quad \hat{\mu} = \mu + \alpha\, n^{\alpha-1} v^2 \,, \tag{6.3}$$

and then the familiar form of the first law of thermodynamics is recovered,

$$\mathrm{d}\hat{\mathcal{E}} = T\,\mathrm{d}s + \hat{\mu}\,\mathrm{d}n \,. \tag{6.4}$$

The equation of state (2.17) becomes

$$d\,P = z\mathcal{E} - n^{\alpha} v^2 \,, \tag{6.5}$$

and the conservation equations (3.4) can be expressed

$$\partial_t \begin{pmatrix} \mathcal{E} \\ q \\ n \end{pmatrix} = \partial_x \begin{pmatrix} \frac{d+z}{d}\, q\mathcal{E}n^{-\alpha} - \frac{1}{d}\, q^3 n^{-2\alpha} \\ \frac{z}{d}\,\mathcal{E} + \frac{d-1}{d}\, q^2 n^{-\alpha} \\ q\, n^{1-\alpha} \end{pmatrix}, \tag{6.6}$$

with $q = n^\alpha v$. The analysis of the Riemann problem proceeds along the same lines as before. The equations are more involved when $z \neq 2$, and we have to rely on numerical evaluation to a greater extent, but the NESS variables can still be solved for.

The Jacobian matrix, $df(\phi)$ for general z is

$$df(\phi) = \begin{pmatrix} \frac{d+z}{d}\, qn^{-\alpha} & \frac{d+z}{d}\,\mathcal{E}n^{-\alpha} - \frac{3}{d}\, q^2 n^{-2\alpha} & -\frac{\alpha(d+z)}{d}\, q\mathcal{E}n^{-1-\alpha} + \frac{2\alpha}{d}\, q^3 n^{-1-2\alpha} \\ \frac{z}{d} & \frac{2(d-1)}{d}\, qn^{-\alpha} & -\frac{\alpha(d-1)}{d}\, q^2 n^{-1-\alpha} \\ 0 & n^{1-\alpha} & (1-\alpha)\, q\, n^{-\alpha} \end{pmatrix}, \tag{6.7}$$

and its eigenvalues and eigenvectors can readily be evaluated. They correspond to a linearly degenerate wave,

$$\lambda_1 = q\, n^{-\alpha}, \quad r_1 = \begin{pmatrix} \frac{\alpha}{z}\, q^2 n^{-\alpha} \\ \alpha\, q \\ n \end{pmatrix}, \tag{6.8}$$

which is a contact discontinuity, together with two genuinely non-linear waves,

$$\lambda_2 = q\, n^{-\alpha}\left(1 + \frac{1}{d}(z-2-K)\right), \qquad r_2 = \begin{pmatrix} \frac{d+z}{d}\mathcal{E} - \frac{1}{d}\, q^2 n^{-\alpha}\,(1+K) \\ q(1-\frac{1}{d}\,K) \\ n \end{pmatrix}; \tag{6.9}$$

and

$$\lambda_3 = q\, n^{-\alpha}\left(1 + \frac{1}{d}(z-2+K)\right), \qquad r_3 = \begin{pmatrix} \frac{d+z}{d}\mathcal{E} - \frac{1}{d}\, q^2 n^{-\alpha}\,(1-K) \\ q(1+\frac{1}{d}\,K) \\ n \end{pmatrix}; \tag{6.10}$$

where we've introduced the shorthand notation,

$$K \equiv \sqrt{(d+z)\left(\frac{z\mathcal{E}n^\alpha}{q^2} - 1\right) - (z-2)}\,. \tag{6.11}$$

– 20 –

It is easily checked that the corresponding expressions in Section 5 are recovered when we insert $z = 2$ in (6.6) - (6.11). Furthermore, by using the equation of state (6.5) one obtains

$$K = d\sqrt{\frac{c^2}{v^2} - \frac{(z-2)}{d^2}}, \qquad \text{with} \qquad c = \sqrt{\frac{(d+z)}{d}\frac{P}{n^\alpha}}\,. \tag{6.12}$$

The eigenvalues corresponding to genuinely non-linear waves can then be written,

$$\begin{aligned}\lambda_2 &= v\left(1 + \frac{z-2}{d}\right) - \sqrt{c^2 - \frac{(z-2)}{d^2}v^2}\,,\\ \lambda_3 &= v\left(1 + \frac{z-2}{d}\right) + \sqrt{c^2 - \frac{(z-2)}{d^2}v^2}\,,\end{aligned} \tag{6.13}$$

As before, we find that λ_2 (λ_3) corresponds to a left-moving (right-moving) wave, and that the leading wavefront of a rarefaction wave will advance at the speed of sound in a heat bath at rest.

6.1 Rarefaction wave profile

Now consider initial data of form (3.1) for a Lifshitz fluid with general z and assume that $P_L > P_R$. In parallel with the $z = 2$ case considered in Section 5, this results in a left-moving rarefaction wave, a right-moving shock wave, and a central NESS region with constant flow velocity and a contact discontinuity moving with the fluid. The key difference compared to the $z = 2$ case is that now there is no boost symmetry and the steady state flow in the central region will no longer be a boosted thermal state.

We use Riemann invariants to analyse the $i = 1$ contact discontinuity and the $i = 2$ rarefaction wave. The Riemann invariants for the first family of wave solutions are again given by the pressure P and the velocity v, which coincides with the eigenvalue $\lambda_1 = \frac{q}{n^\alpha}$. Therefore, the contact discontinuity will still propagate at the same speed as the velocity of its surrounding fluid regions on the left and right.

For the genuinely non-linear families, we find generalisations of the pairs of Riemann invariants, which took the form (5.13) for $z = 2$, but are now given by

$$\begin{aligned}R_1^{(2)} &= n^{-\gamma}\left(P - \frac{(z-2)}{2d}v^2 n^\alpha\right), \qquad R_2^{(2)} = n^{-\xi}\, v\,(1+K)\left(\frac{K-\beta}{K+\beta}\right)^{\frac{\beta}{2}},\\ R_1^{(3)} &= n^{-\gamma}\left(P - \frac{(z-2)}{2d}v^2 n^\alpha\right), \qquad R_2^{(3)} = n^{-\xi}\, v\,(1-K)\left(\frac{K+\beta}{K-\beta}\right)^{\frac{\beta}{2}},\end{aligned} \tag{6.14}$$

where $\gamma = \frac{d+z}{d}$, $\xi = \frac{(z-2)(d+z)}{2d}$, $\beta = \sqrt{\frac{(z-2)(d+z-2)}{2}}$, and K may be read off from (6.12).

As before, we require that both Riemann invariants are constant along the characteristic curves of the left-moving rarefaction wave. From $R_1^{(2)}(P,v,n) = R_1^{(2)}(P_L,v_L,n_L)$ we obtain

$$\frac{P}{P_L} = \frac{\xi}{d}\frac{v^2}{c_L^2}\left(\frac{n}{n_L}\right)^\alpha + \left(\frac{n}{n_L}\right)^\gamma, \tag{6.15}$$

while $R_2^{(2)}(P,v,n) = R_2^{(2)}(P_L,v_L,n_L)$ gives

$$\left(\frac{n}{n_L}\right)^\xi = \frac{v}{d\,c_L}(1+K)\left(\frac{K-\beta}{K+\beta}\right)^{\frac{\beta}{2}}, \tag{6.16}$$

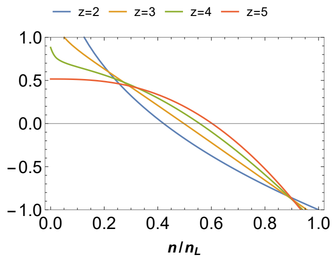

Figure 5: Variation of the characteristic speed λ_2 across a rarefaction wave profile parametrised by n for $d = 3$ and different values of z.

with K expressed as a function of P, v, and n through the relations in (6.12). These conditions are non-linear and do not allow for analytic solution for generic values of d and z. In order to facilitate their numerical solution, we find it convenient to first eliminate the pressure between them by inserting (6.15) into (6.16). This results, after some algebraic manipulations, in the following equation, relating the scale invariant variables n/n_L and v/c_L,

$$\left(\frac{n}{n_L}\right)^{\xi} = \left(\frac{v}{d\,c_L} + \widetilde{K}\right)\left(\frac{\widetilde{K} - \frac{\beta}{d}\frac{v}{c_L}}{\widetilde{K} + \frac{\beta}{d}\frac{v}{c_L}}\right)^{\frac{\beta}{2}}, \tag{6.17}$$

with $\widetilde{K} = \sqrt{\frac{\beta^2}{d^2}\frac{v^2}{c_L^2} + \left(\frac{n}{n_L}\right)^{\gamma-\alpha}}$. A numerical solution for v/c_L in terms of n/n_L can then be inserted into (6.15) to determine P/P_L. In order to check the validity of the rarefaction wave solution so obtained, we have evaluated the characteristic speed λ_2 along the integral curve for specific initial data. Numerical results for several different values of z are shown in Figure 5 and in each case the rarefaction condition (5.21) is indeed satisfied.

6.2 Shock wave

A shock wave solution for a Lifshitz fluid at general z satisfies the following Rankine-Hugoniot jump conditions,

$$\begin{aligned} u_s[n] &= [nv]\,, \\ u_s[n^{\alpha}v] &= [P + n^{\alpha}v^2]\,, \\ u_s[\mathcal{E}] &= [(\mathcal{E}+P)v]\,. \end{aligned} \tag{6.18}$$

Writing $w = v - u_s$ and $\nu = n^{\alpha}\,w$, these conditions can be expressed as

$$\begin{aligned} [n\,w] &= 0\,, \\ [P + \nu(w+u_s)] &= 0\,, \\ [(d+z)Pw + \nu(w+u_s)(w+u_s-zu_s)] &= 0\,, \end{aligned} \tag{6.19}$$

where we have used the equation of state (6.5). The contact discontinuity corresponds to the trivial solution $w = [P] = 0$.

To find a right-moving shock wave solution corresponding to the $i = 3$ eigenvalue family, we again introduce dimensionless variables,

$$\Pi_s \equiv \frac{P_s}{P_R}, \quad y \equiv \frac{n_{s2}}{n_R} = \frac{w_R}{w_s}, \tag{6.20}$$

where the right-most equality follows from the jump condition $[n\,w] = 0$. For a shock wave propagating into a fluid at rest, the other two jump conditions can be re-expressed as

$$\frac{u_s^2}{c_R^2} = \frac{y^{2-\alpha}(\Pi_s - 1)}{\gamma\,(y-1)} \qquad \text{and} \qquad \frac{u_s^2}{c_R^2} = \frac{d\,y^{2-\alpha}(\Pi_s - y)}{(y-1)(1+(z-1)y)}\,. \tag{6.21}$$

The two equations can now be combined and solved either for y or Π_s,

$$y = \frac{(d+z-1)\Pi_s + 1}{d+1+(z-1)\Pi_s}\,, \qquad \Pi_s = \frac{(d+1)y - 1}{d+z-1-(z-1)y}\,. \tag{6.22}$$

By substituting Π_s into (6.21), the speed of the shock wave can be written in terms of the dimensionless variable y as,

$$u_s = c_R\sqrt{\frac{d\,y^{2-\alpha}}{d+z-1-(z-1)y}}\,. \tag{6.23}$$

The shock wave admissibility conditions are satisfied when the shock front moves faster than the speed of sound in the medium the wave is expanding into, *i.e.* when $u_s > c_R$. It is easily checked that this holds for all values of y that correspond to $P_s > P_R$.

The fluid velocity in the region between the shock wave and the contact discontinuity can also be expressed in terms of y via the relation,

$$v_{s2} = \frac{(y-1)}{y}\,u_s\,. \tag{6.24}$$

6.3 NESS variables

We now have everything in place to construct the full solution to our Riemann problem for a Lifshitz fluid with general z in d spatial dimensions, with initial data given by P_L, P_R, n_L, and n_R (with $P_L \geq P_R$). Once again, there will be a growing NESS region between a left-moving rarefaction wave and a the right-moving shock wave, with a contact discontinuity in between, as depicted in Fig. 1. The solution can be constructed in a number of ways but the key observation is that pressure and fluid flow speed remain constant across the entire NESS region, while the charge density is piecewise constant and makes a jump at the contact discontinuity. We will proceed by first solving for the pressure and flow speed in terms of the charge density on either side of the contact discontinuity. We then require that the results are the same on both sides and this, in turn, fixes the charge densities in terms of the initial data.

On the one hand, the NESS pressure and flow speed are expressed in terms of the dimensionless variable $y = n_{s2}/n_R$ in (6.22) and (6.24), respectively. These relations follow directly from the Rankine-Hugoniot jump conditions across the shock wave front.

On the other hand, we can obtain the same quantities in terms of another dimensionless variable $x = n_{s1}/n_L$ by considering the trailing end of the rarefaction wave profile, where $n = n_{s1}$. In this case, (6.17) reduces to

$$x^{\xi} = \left(\frac{1}{d}\frac{v_s}{c_L} + \widetilde{K}_s\right)\left(\frac{\widetilde{K}_s - \frac{\beta}{d}\frac{v_s}{c_L}}{\widetilde{K}_s + \frac{\beta}{d}\frac{v_s}{c_L}}\right)^{\frac{\beta}{2}}, \tag{6.25}$$

with $\widetilde{K}_s = \sqrt{x^{\gamma-\alpha} + \frac{\beta^2}{d^2}\frac{v_s^2}{c_L^2}}$. This can be solved numerically for v_s as a function of x and the result is then inserted into (6.15) to obtain the NESS pressure,

$$\frac{\Pi_s}{\Pi_L} = x^{\gamma} + \frac{\xi}{d}\frac{v_s^2(x)}{c_L^2}x^{\alpha}\,. \tag{6.26}$$

The requirement that v_s and P_s take the same values on both sides of the contact discontinuity gives rise to two independent relations between the variables x and y, which is sufficient to determine their values for given initial data for the reservoirs.[5] The remaining NESS variables are easily obtained once the dimensionless charge densities x and y have been solved for numerically. For instance, the NESS pressure is obtained by inserting y into the equation on the right in (6.22), while the shock wave speed and the fluid speed in the NESS region are given by (6.23) and (6.24), respectively. Solutions for $d = 3$ spatial dimensions and $z = 3$ are presented in Figure 6 as a function of P_R/P_L. Figure 7 shows how the solution changes with z for a particular choice of P_L/P_R and n_L/n_R.

As stated above, the NESS for $z \neq 2$ cannot be recognized as a boosted thermal fluid. The equation of state (6.5) is incompatible with the Galilean boost transformations (2.14),

[5] As in the $z = 2$ case, the initial data only enters through the ratios P_L/P_R and n_L/n_R.

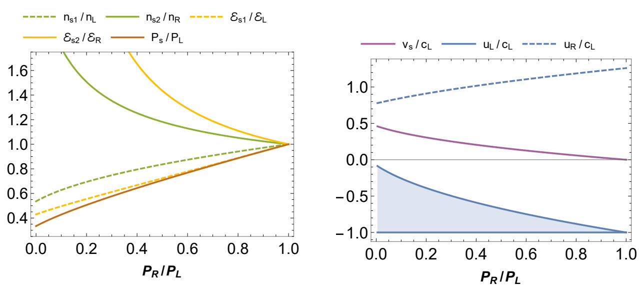

Figure 6: NESS variables for $z = 3$, $d = 3$ as a function of P_R/P_L for fixed $n_L/n_R = 2$.

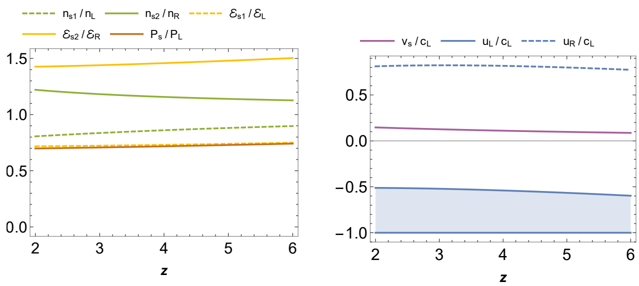

Figure 7: NESS variables as a function of z for $d = 3$ and fixed $P_L/P_R = n_L/n_R = 2$.

which leave invariant P and n while shifting $\mathcal{E} \to \mathcal{E} + \frac{1}{2} n\, v^2$. Furthermore, the momentum density $\mathcal{P} = \rho\, v$ does not match the one obtained from a Galilean boost. Therefore no temperature can be associated to the solution obtained here. It is genuinely a non-thermal out-of-equilibrium state in a theory without boost symmetry.

It is interesting to compare the NESS variables we find at $z = 1$ to the solution of the corresponding Riemann problem for a relativistic fluid presented in [8, 9] in the limit of low flow velocity. The steady state flow is slow when P_R/P_L is close to 1, *i.e.* when the pressure difference between the two reservoirs is small. Figure 8 shows the NESS variables n_{s1}, n_{s2}, Π_s, and v_s at different values of P_R/P_L for $d = 3$, $z = 1$, and $n_L = 2n_R$. The corresponding variables in a relativistic fluid (taken from [8]) are indicated by red dashed curves in the figure. We see a close match for all the NESS variables as $P_R/P_L \to 1$.

In the relativistic case, the charge density decouples from the equations that determine the steady state pressure and flow speed but in general this is not the case for our non-relativistic Lifshitz fluids. The decoupling of the charge density is, however, recovered in the limit of small pressure difference in the $z = 1$ Lifshitz case. To see this, one carries out an expansion in powers of small $\Delta = \Pi_L - 1$ in (6.25) and (6.26) that determine Π_s and v_s at $z = 1$ and observes that $\eta = n_L/n_R$ indeed decouples from the equations to leading order in Δ. For large values of Δ the steady state flow speed is no longer small and there is no reason to expect a match between a relativistic fluid and a $z = 1$ Lifshitz fluid.

7 Discussion

The above study of the Riemann problem for Lifshitz fluids had a twofold purpose. On the one hand, it extends to a non-relativistic setting some recent work on the out-of-equilibrium flow of relativistic quantum critical fluids [6–10], and, on the other hand, it provides an

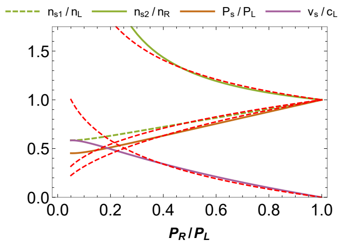

Figure 8: NESS variables for a Lifshitz fluid at $d = 3$, $z = 1$ and $n_L/n_R = 2$ as a function of P_R/P_L. For comparison, the corresponding variables for a relativistic fluid considered in [8, 9] are shown by the red dashed curves. The solutions are well matched as $P_R/P_L \to 1$.

application to a concrete physical setup of a recently developed general formalism for perfect fluids without boost symmetry [11].

We have established that a non-equilibrium steady state, of the type seen previously in a relativistic scale invariant fluid, will also develop in a non-relativistic critical fluid when two reservoirs are brought into contact across a hypersurface. Consistent with the Lax entropy conditions, the non-relativistic NESS is bounded on one side by an outgoing shock wave and on the other side by a rarefaction wave propagating in the opposite direction. Inside the NESS there is a contact discontinuity where the charge density jumps but the pressure stays unchanged.

In the special case of a $z = 2$ Lifshitz fluid the NESS is a Galilean boost of a thermal equilibrium state, in direct analogy with the Lorentz boosted thermal state seen in the corresponding relativistic problem. Using a simple scaling ansatz for the kinetic mass density of a Lifshitz fluid at generic z, we found that the fluid variables in the central region can be solved for and a NESS forms in this case as well, but the solution is genuinely non-thermal.

There are several future directions to be explored. In this study, we have concentrated on perfect fluids without impurities or lattice effects which break translational invariance. Proceeding along the lines of [8], where this has been done for a conformal fluid, one could allow for diffusion and momentum relaxation in the hydrodynamics equations, to obtain the time scale up to which the non-relativistic NESS persists.

Another interesting direction is to analyse a dual gravitational description of non-equilibrium steady states of Lifshitz fluids. In this context, it would especially be interesting to identify a gravitational dual of a $z \neq 2$ Lifshitz fluid flow without boost symmetry.

Acknowledgments

We thank Jelle Hartong, Niels Obers, Napat Poovuttikul, and Watse Sybesma for useful discussions. This work was supported in part by the Icelandic Research Fund grant 195970-051 and the University of Iceland Research Fund.

References

[1] L. D. Landau and E. M. Lifshitz, *"Fluid Mechanics" (vol. 6 of Course on Theoretical Physics)*, Pergamon Press (1959).

[2] Carlos Hoyos, Bom Soo Kim and Yaron Oz, *"Lifshitz Hydrodynamics"*, *JHEP* **11** (2013) 145 [arXiv:1304.7481].

[3] Carlos Hoyos, Bom Soo Kim and Yaron Oz, *"Lifshitz field theories at non-zero temperature, hydrodynamics and gravity"*, *JHEP* **11** (2013) 145 [arXiv:1309.6794].

[4] Elias Kiritsis and Yoshinori Matsuo, *"Charge-hyperscaling violating Lifshitz hydrodynamics from black-holes"*, *JHEP* **12** (2015) 076 [arXiv:1508.02494].

[5] Jelle Hartong, Niels A. Obers and Marco Sanchioni, *"Lifshitz Hydrodynamics from Lifshitz Black Branes with Linear Momentum"*, *JHEP* **10** (2016) 120 [arXiv:1606.09543].

[6] Denis Bernard and Benjamin Doyon, *"Energy flow in non-equilibrium conformal field theory"*, *J. Phys. A: Math. Theor.* **45** (2012) 362001 [arXiv:1202.0239].

[7] M. J. Bhaseen, Benjamin Doyon, Andrew Lucas and Koenraad Schalm, *"Far from equilibrium energy flow in quantum critical systems"*, *Nature Phys.* **11** (2015) 509 [arXiv:1311.3655].

[8] Andrew Lucas, Koenraad Schalm, Benjamin Doyon and M. J. Bhaseen, *"Shock waves, rarefaction waves, and nonequilibrium steady states in quantum critical systems"*, *Phys. Rev. D* **94** (2016) 025004 [arXiv:1512.09037].

[9] Michael Spillane and Christopher P Herzog, *"Relativistic hydrodynamics and non-equilibrium steady states"*, *J. Stat. Mech.* **1610** no. 10, (2016) 103208 [arXiv:1512.09071].

[10] Razieh Pourhasan, *"Non-equilibrium steady state in the hydro regime"*, *JHEP* **02** (2016) 103208 [arXiv:1509.01162].

[11] Jan de Boer, Jelle Hartong, Niels A. Obers, Watse Sybesma and Stefan Vandoren, *"Perfect fluids"*, *SciPost Phys.* **5** (2018) 003 [arXiv:1710.04708].

[12] V. Bargmann, *"The Formation and Decay of Shock Waves"*, *Ann. Math.* **59**, no. 1, 1-46 (1954).

[13] Roel Andringa, Eric Bergshoeff, Sudhakar Panda and Mees de Roo, *"Newtonian Gravity and the Bargmann Algebra"*, *Class. Quant. Grav.* **28** (2011) 105011 [arXiv:1011.1145].

[14] Marika Taylor, *"Lifshitz holography"*, *Class. Quant. Grav.* **33** no. 3, (2016) 033001 [arXiv:1512.03554].

[15] Géry de Saxcé and Claude Vallée, *"Bargmann group, momentum tensor and Galilean invariance of Clausius–Duhem inequality"*, *Int. J. Eng. Sci.* **50**, no. 1, 216-232 (2012).

[16] Géry de Saxcé and Claude Vallée, *"Galilean Mechanics and Thermodynamics of Continua"*, John Wiley & Sons, Inc. (2016).

[17] Kristan Jensen, *"Aspects of hot Galilean field theory"*, JHEP **04** (2015) 123 [arXiv:1411.7024].

[18] Guido Festuccia, Dennis Hansen, Jelle Hartong and Niels A. Obers, *"Torsional Newton-Cartan geometry from the Noether procedure"*, Phys. Rev. D **94** (2016) 105023 [arXiv:1607.01926].

[19] Bernhard Riemann, *"Über die Fortpflanzung ebener Luftwellen von endlicher Schwingungsweite"*, Abh. Konigl. Ges. Wiss. Gottingen **8**, 43-66 (1860).

[20] Han-Chih Chang, Andreas Karch and Amos Yarom, *"An ansatz for one dimensional steady state configurations"*, J. Stat. Mech. **1406** no. 6, (2014) P06018 [arXiv:1311.2590].

[21] Peter D. Lax, *"Weak solutions of nonlinear hyperbolic equations and their numerical computation"*, Comm. Pure Appl. Math. **7**, 159-163 (1954).

[22] Stefano Bianchini, *"On the Riemann Problem for Non-Conservative Hyperbolic Systems"*, Rational Mech. Anal. **166**, 1-26 (2003).

[23] P. D. Lax, *"Hyperbolic systems of conservation laws II"*, Comm. Pure Appl. Math. **10**, 537-566 (1957).

[24] Wissam Chemissany, David Geissbühler, Jelle Hartong and Blaise Rollier, *"Holographic renormalization for $z = 2$ Lifshitz Space-Times from AdS"*, Class. Quant. Grav. **29** (2012) 235017 [arXiv:1205.5777].

[25] Benjamín Grinstein and Sridip Pal, *"Existence and Construction of Galilean invariant $z \neq 2$ Theories"*, Phys. Rev. D **97** (2018) 125006 [arXiv:1803.03676].

[26] Matania Ben-Artzi, Jiequan Li and Gerald Warnecke, *"A direct Eulerian GRP scheme for compressible fluid flows"*, J. Comput. Phys. **218**, 19-43 (2006).

[27] Peter D. Lax, *"The Formation and Decay of Shock Waves"*, Am. Math. Mon. **79**, 227-241 (1972).

[28] Elihu Abrahams and Peter Wölfle, *"Critical quasiparticle theory applied to heavy fermion metals near an antiferromagnetic quantum phase transition"*, Proc. Natl. Acad. Sci. U.S.A. **109**, 3238-42 (2012).

[29] Elihu Abrahams, Jörg Schmalian and Peter Wölfle, *"Strong-coupling theory of heavy-fermion criticality"*, Phys. Rev. B **90** (2014) 045105 [arXiv:1303.3926].

Paper III

Lifshitz hydrodynamics at $z > 1$ from a moving black brane

Aruna Rajagopal, Lárus Thorlacius

Prepared for submission to JHEP, 2021, 21

Lifshitz hydrodynamics at generic z from a moving black brane

Aruna Rajagopal and Larus Thorlacius
University of Iceland, Science Institute, Dunhaga 3, IS-107, Reykjavik, Iceland

A Lifshitz black brane at generic dynamical critical exponent $z > 1$, with non-zero linear momentum along the boundary, provides a holographic dual description of a non-equilibrium steady state in a quantum critical fluid, with Lifshitz scale invariance but without boost symmetry. We consider moving Lifshitz branes in Einstein-Maxwell-Dilaton gravity and obtain the non-relativistic stress tensor complex of the dual field theory via a suitable holographic renormalisation procedure. The resulting black brane hydrodynamics and thermodynamics are a concrete holographic realization of a Lifshitz perfect fluid with a generic dynamical critical exponent.

CONTENTS

I. INTRODUCTION

Fluid dynamics [1] efficiently captures the long-wavelength, low frequency behavior of a large class of interacting physical systems at finite temperature. Based on general symmetry principles and the conservation of local currents, it is a universal theory, as even systems with varying microscopic dynamics, can have the same macroscopic, hydrodynamic description. An appropriate hydrodynamic model, incorporating the dissipative effects of the thermal medium that are essential for a fluid to equilibriate after being perturbed away from equilibrium, consists of a gradient expansion of the conserved currents. At a given order, the conservation equations determine the expansion up to a finite number of undetermined coefficients. These coefficients may then be obtained either from measurements or from microscopic computations. For strongly coupled quantum systems, explicit computations are difficult and a gauge/gravity formulation [2–4] can offer advantages. Einstein's equations with a negative cosmological constant, supplemented with appropriate regularity restrictions and boundary conditions, reduce to the nonlinear equations of fluid dynamics in an appropriate parameter range, and a systematic framework to construct this universal nonlinear fluid dynamics, order by order in a boundary derivative expansion has been developed [5, 6].

In standard anti-de Sitter (AdS) holography [7] the dual field theory is relativistic and much of the dual gravitational formulation of hydrodynamics has focused on relativistic systems. However, many strongly correlated systems in nature are inherently non-relativistic and this has motivated the application of holography to a wider setting involving gravitational bulk theories with asymptotic geometries that are not AdS [8–10]. Generic non-relativistic quantum critical fluids have an emergent scaling symmetry of the form

$$t \to \Lambda^z t, \qquad \vec{x} \to \Lambda \vec{x}, \tag{1.1}$$

commonly referred to as Lifshitz scaling and are characterised by a dynamical critical exponent $z \geq 1$. For $z > 1$, the scaling is asymmetric between the time and spatial directions and the system has scale invariance without conformal invariance. By now, there is a large body of work on holographic systems that realize Lifshitz scaling of the form (1.1) at the asymptotic boundary of the gravitational bulk space-time, including a number of papers with a specific focus on hydrodynamic aspects, see *e.g.* [11–19].

Quantum critical fluids with Lifshitz symmetry, or Lifshitz fluids for short, have interesting properties that set them aside from more conventional fluid systems. In particular, a Lifshitz fluid with generic dynamical critical exponent $z \neq 1, 2$ cannot have boost symmetry [20, 21]. A general formalism for perfect fluids without boost symmetry has been developed in [20, 22, 23] and a primary motivation for the present paper is to provide a concrete holographic setup for the study of such fluids.

In previous work [24], we have studied out-of-equilibrium energy transport in a quantum critical fluid with Lifshitz scaling symmetry following a local quench between two semi-infinite fluid reservoirs. The late time energy flow was found to be universal and was accommodated via a steady state occupying an expanding central region between outgoing shock and rarefaction waves, in accordance with earlier work on critical fluids with Lorentz boost symmetry [25–29]. In the relativistic case, a holographic version of the quench problem was considered in [25, 28] and it would be interesting to extend this to Lifshitz fluids without boost symmetry. As a first step in that direction, we consider a Lifshitz black brane at generic z, moving with uniform velocity v in one of the transverse directions, as a holographic dual description of a non-equilibrium steady state of the corresponding Lifshitz fluid.

The holographic model we choose to work with is a relatively simple variant of Einstein-Maxwell-Dilaton gravity with exact analytic solutions describing static Lifshitz black branes. The model can easily be generalised to include include charged matter in order to study holographic duality at finite temperature and chemical potential. The exact static black brane solution provides a convenient benchmark to test our formalism against, even if the moving brane solution is beyond exact analytic control. A drawback of this model, that has detracted from its usefulness for holography in the past, is the fact that the asymptotic Lifshitz symmetry is obscured by a running dilaton and non-standard asymptotic behaviour of the background vector field. It turns out, this can easily be remedied by taking advantage of a built-in symmetry of the model and a more or less standard holographic renormalisation is achieved by suitably adapting the formalism developed for a holographic model involving a massive vector field in [12]. We find the following results:

- A physically distinct class of moving Lifshitz black brane solutions in four spacetime dimensions, dual to a uniformly moving 2+1 dimensional Lifshitz fluid. The fluid velocity plays the role of chemical potential, dual to a kinetic mass density, in line with the perfect fluid formalism developed in [20, 22].

- A renormalised boundary stress tensor complex whose components express the energy density $\mathcal{E}$, energy flux $\mathcal{E}^i$, momentum density $\mathcal{P}_i$, and spatial stress tensor Π_{ij} of the dual Lifshitz fluid.
- The Ward identity associated to Lifshitz scaling leads to the equation of state $z\mathcal{E}-\rho v^2 = d_s P$, where $d_s = 2$ is the number of transverse dimensions. This is precisely the equation of state hypothesised for a perfect Lifshitz fluid with an arbitrary dynamic exponent z in [19, 20].

II. THE GRAVITATIONAL THEORY

We restrict our attention to a holographic theory with Lifshitz scaling defined in 4 bulk space-time dimensions but our results can easily be generalised to an arbitrary number of dimensions. The model we work with is a simple variant of Einstein-Maxwell-Dilaton (EMD) theory, which consists of Einstein gravity along with a massless $U(1)$ gauge field, A_μ and a dilaton field, ϕ. Using a normalisation where $16\pi G_4 = 1$, the action is given by,

$$S_0 = \int d^4x\sqrt{-g}\left[R - 2\Lambda - \frac{1}{2}(\partial\phi)^2 - \frac{1}{4}e^{\lambda\phi}F^2\right] + 2\int d^3x\sqrt{-\gamma}K, \tag{2.1}$$

where the last term is the usual Gibbons-Hawking-York boundary term, which is needed in order to have a well-defined variational problem for the metric. The equations of motion for (2.1) are,

$$R_{\mu\nu} - \frac{1}{2}Rg_{\mu\nu} + \Lambda g_{\mu\nu} = T^{\phi}_{\mu\nu} + T^{(1)}_{\mu\nu} \tag{2.2}$$

$$\nabla^2\phi - \frac{\lambda}{4}e^{\lambda\phi}F_{\mu\nu}F^{\mu\nu} = 0 \tag{2.3}$$

$$\nabla_\mu e^{\lambda\phi}F^{\mu\nu} = 0, \tag{2.4}$$

with,

$$T^{\phi}_{\mu\nu} = \frac{1}{2}\partial_\mu\phi\partial_\nu\phi - \frac{1}{4}g_{\mu\nu}(\partial\phi)^2, \tag{2.5}$$

$$T^{F}_{\mu\nu} = \frac{1}{2}e^{\lambda\phi}\left(F_{\mu\sigma}F^{\sigma}_{\nu} - \frac{1}{4}g_{\mu\nu}F_{\sigma\rho}F^{\sigma\rho}\right). \tag{2.6}$$

Models of this kind were introduced in the context of non-relativistic holography in [11]. This is by no means the only possible model for Lifshitz holography but it has an important advantage in that there exists a full analytic solution to the field equations that describes a static black brane in asymptotically Lifshitz space-time. The model can easily be generalized to include charged black brane solutions that are Lifshitz analogs of AdS-Reissner-Nordström black branes [30], which are key to a holographic dual description of non-relativistic quantum critical matter at finite temperature and chemical potential, see *e.g.* [31]. The bulk theory can also include matter fields of various types, but this is not needed for the main purpose of this paper, which is to carry out holographic renormalisation for moving Lifshitz branes and establish thermodynamic relations that hold for the resulting Lifshitz hydrodynamics.

The model (2.1) admits the so-called Lifshitz space-time as a solution,

$$ds^2 = \ell^2 \left(-r^{2z} dt^2 + \frac{dr^2}{r^2} + r^2 d\vec{x}^2 \right), \tag{2.7}$$

where ℓ is a characteristic length scale of the geometry which we set to unity for notational simplicity. The metric exhibits the required Lifshitz scaling,

$$t \to \Lambda^z t \ , \qquad x \to \Lambda x \ , \qquad r \to \Lambda^{-1} r, \tag{2.8}$$

with $z \geq 1$. Space-time geometries that are asymptotic to this metric provide a holographic dual description of a scale-invariant non-relativistic field theory formulated on a $\mathbb{R}^t \times \mathbb{R}^2$ boundary.

The metric (2.7) is a solution to the equations of motion provided the parameters of the model satisfy $\lambda = -\frac{2}{\sqrt{z-1}}$ and $\Lambda = -\frac{1}{2}(z+1)(z+2)$, and it is accompanied by a gauge field and dilaton background of the form,

$$A_t = \sqrt{\frac{2(z-1)}{z+2}} \left(\frac{r}{r_0} \right)^2 r^z, \qquad e^{\phi} = \left(\frac{r}{r_0} \right)^{2\sqrt{z-1}}, \tag{2.9}$$

where r_0 is an arbitrary constant. While this model has the advantage of analytic control, it has the disadvantage of a logarithmically running dilaton and diverging vector field at the boundary. However, this is not a very serious disadvantage because the vector field only serves to provide the background to support a Lifshitz geometry at the boundary and does not couple to any non-gravitational fields.

Charged matter fields can be added to the model, but they should then be charged under some additional gauge field and not couple directly to the A_μ field considered here. The need for a further gauge field to accommodate charged matter can also be seen from the fact that the background field profile (2.9) is not of the standard form that corresponds to having a chemical potential for an unbroken $U(1)$ symmetry in the dual field theory. In fact, A_μ should not be viewed as a gauge field but simply as a massless vector field that only interacts gravitationally (with a coupling that depends on the dilaton). With this in mind, we do not have to respect the $U(1)$ gauge symmetry of the bulk action in (2.1) when we construct boundary counterterms for holographic renormalisation of the model.

The counterterms instead respect another symmetry. The action (2.1) is invariant under a constant shift of the dilaton field while simultaneously absorbing a constant normalisation factor into the gauge field,

$$\phi \to \phi - \frac{2}{\lambda} \log \alpha, \qquad A_\mu \to \alpha A_\mu, \tag{2.10}$$

and this will be a symmetry of our boundary action as well. The shift symmetry is also helpful in analysing the asymptotic behaviour of bulk fields.

A. Black branes with linear momentum

We would like to construct the gravitational dual of a perfect Lifshitz fluid moving at non-vanishing velocity. We are particularly interested in fluids at generic z, which do not have boost symmetry. In this case, it is not enough to perform a boost of the black brane along one of the transverse directions and study the associated thermodynamics as this does not give us a genuine dual of a moving Lifshitz fluid, but instead corresponds to studying a fluid at rest from a moving coordinate frame. The way around this is to construct from scratch a bulk solution that describes a moving Lifshitz black brane at generic $z \neq 1$, with metric and gauge fields that encode the fluid momentum. For this we adopt an ansatz employed in [19] for a $z = 2$ moving brane and adapt it to the more general case. With the linear momentum taken to be in one of the transverse directions, say the y direction, the metric becomes

$$ds^2 = -F_1(r)r^{2z}dt^2 + \frac{dr^2}{r^2F_2(r)} + r^2F_3(r)dx^2 + F_4(r)(rdy + N(r)r^z dt)^2, \tag{2.11}$$

and the gauge field is

$$A = r^z G_1(r)dt + G_2(r)(rdy + N(r)r^z dt). \tag{2.12}$$

Note that this ansatz includes as a special case an exact solution for a static black brane by simply setting $G_2 = N = 0$, $F_3 = F_4 = 1$, and letting $F_1 = F_2 = 1 - (r_h/r)^{z+2}$. The dilaton field of the static black brane solution is unchanged from (2.9) provided we use the shift symmetry (2.10) to set r_0 equal to r_h, the radial location of the event horizon.

There is no known analytic solution for a brane with non-vanishing linear momentum. The field equations can be solved numerically, by imposing appropriate boundary conditions at the black brane horizon, but we will not pursue a numerical solution here. The results we are after can instead be obtained by employing a combination of asymptotic analysis and radially conserved charges along the lines of [19]. In the following subsections we first derive a set of Noether charges that are constant along the radial coordinate. We then introduce boundary counterterms and implement them in the holographic renormalisation of the boundary stress tensor. Finally, we solve the linearised field equations around the Lifshitz fixed point in (2.7) and (2.9). The different elements are then brought together in Section III where we analyse the thermodynamics of the moving black brane.

B. Noether charges

The fields that enter in the moving brane ansatz (2.11) - (2.12) are functions of the radial coordinate and in this case the action (2.1) can be reduced to an integral over a one-dimensional Lagrangian by factoring off the integrals over the time and transverse coordinates. The Gibbons-Hawking-York term cancels against boundary terms resulting from integration by parts of terms in the radial bulk action, leading to the result,

$$\begin{aligned} L_{1D} =& r^{z+1}\sqrt{F_1F_2F_3F_4}\Bigg(-2(z^2+2z+3) + \frac{1}{2}\frac{F_4N^2}{F_1}\Big(z-1+\frac{rN'}{N}\Big)^2 - z\frac{rF_1'}{F_1} \\ & - (z+2)\frac{rF_2'}{F_2} - \frac{rF_3'}{F_3} - \frac{rF_4'}{F_4} + \frac{r^2}{2}\Big(\frac{F_1'}{F_1}\frac{F_3'}{F_3} + \frac{F_1'}{F_1}\frac{F_4'}{F_4} + \frac{F_3'}{F_3}\frac{F_4'}{F_4}\Big) - \frac{2\Lambda}{F_2} - \frac{1}{2}(r\phi')^2 \\ & + \frac{1}{2}e^{\lambda\phi}\Big(\frac{1}{F_1}(zG_1 + rG_1' + G_2((z-1)N + rN'))^2 - \frac{1}{F_4}(G_2 + rG_2')^2\Big)\Bigg), \end{aligned} \tag{2.13}$$

where $' \equiv \frac{d}{dr}$. The terms in the 1D Lagrangian are arranged so as to make apparent the following two scaling symmetries,

$$F_1 \to \alpha^2 F_1, \quad F_3 \to \alpha^{-1} F_3, \quad F_4 \to \alpha^{-1} F_4, \tag{2.14}$$

$$N \to \alpha^{\frac{3}{2}} N, \quad G_1 \to \alpha G_1, \quad G_2 \to \alpha^{-\frac{1}{2}} G_2, \tag{2.15}$$

and

$$F_3 \to \beta^2 F_3, \quad F_4 \to \beta^{-2} F_4, \tag{2.16}$$

$$N \to \beta N, \quad G_2 \to \beta^{-1} G_2. \tag{2.17}$$

They represent a diffeomorphism which preserves the volume element $dtdxdy$, and can thus be thought of as a Noether symmetry inherited by L_{1D}. They are also symmetries of the boosted metric ansatz (2.11), as long as the coordinates transform as $t \to \alpha^{-1} t$, $x \to \alpha^{\frac{1}{2}} x$, $y \to \alpha^{\frac{1}{2}} y$ and $x \to \beta^{-1} x$, $y \to \beta y$ respectively.

The two Noether charges associated with these symmetries are found to be,

$$\begin{aligned} Q_\alpha = r^{z+2}\sqrt{F_1F_2F_3F_4}\Big(2(z-1) + \frac{r}{2}\Big(\frac{2F_1'}{F_1} - \frac{F_3'}{F_3} - \frac{F_4'}{F_4}\Big) - \frac{3}{2}\frac{F_4 N^2}{F_1}\Big(z-1+\frac{rN'}{N}\Big) \\ - \frac{1}{2}e^{\lambda\phi}\frac{G_2}{F_4}(G_2 + rG_2') - e^{\lambda\phi}\Big(\frac{G_1}{F_1} + \frac{3}{2}\frac{G_2 N}{F_1}\Big)\Big(zG_1 + rG_1' + G_2 N\Big(z-1+\frac{rN'}{N}\Big)\Big)\Big), \end{aligned} \tag{2.18}$$

$$\begin{aligned} Q_\beta = r^{z+2}\sqrt{F_1F_2F_3F_4}\Big(r\Big(\frac{F_3'}{F_3} - \frac{F_4'}{F_4}\Big) - \frac{F_4 N^2}{F_1}\Big(z-1+\frac{rN'}{N}\Big) \\ - e^{\lambda\phi}\frac{G_2}{F_1}\Big(\frac{F_1}{F_4}(G_2 + rG_2') + (zG_1 + rG_1')N + G_2 N^2\Big(z-1+\frac{rN'}{N}\Big)\Big) \end{aligned} \tag{2.19}$$

These charges are combinations of bulk fields that do not depend on the radial bulk coordinate. This is particularly useful in relating horizon data to boundary data, and plays an important role in determining the thermodynamic equation of state when the exact bulk interpolating solution is not known, as we will see later on.

There is another conserved charge in our system associated with the shift symmetry of the dilaton (2.10). While it does not play a direct role in the thermodynamics, it will be useful later on when we consider solutions of the linearized field equations. It is given by,

$$Q_\phi = r^{z+2}\sqrt{F_1F_2F_3F_4}\Big(e^{\lambda\phi}\frac{G_2}{F_4}(G_2 + rG_2') - e^{\lambda\phi}\frac{G_1}{F_1}\Big(zG_1 + rG_1' + G_2 N\Big(z-1+\frac{rN'}{N}\Big) - \frac{2r\phi'}{\lambda}\Big). \tag{2.20}$$

In addition to the above symmetries, there is also a local gauge symmetry involving r diffeomorphisms, which we fix by setting $F_3(r) = 1$ in (2.11).

C. Holographic renormalisation

In this section, we work out the renormalised stress-energy tensor at the boundary for the EMD model. The conservation of the stress tensor gives us the standard energy and momentum conservation equations, while its scaling behaviour under a Lifshitz transformation will give us the equation of state of a Lifshitz fluid. For holographic renormalization of gravity models in asymptotically Lifshitz spacetime see *e.g.* [12–14, 32–35].

The variation of the action (2.1) around a solution to the field equations reduces to a boundary term,

$$\delta S_0 = \int d^3x\sqrt{-\gamma}\big((K_{\alpha\beta} - K\gamma_{\alpha\beta})\delta\gamma^{\alpha\beta} - e^{\lambda\phi}n^\alpha F_{\alpha\beta}\,\delta A^\beta - n^\alpha\nabla_\alpha\phi\,\delta\phi\big), \tag{2.21}$$

where n^α refers to the outward directed unit normal at the boundary. As usual, regularisation and renormalisation are needed in order to make sense of this expression. For regularisation, we place the boundary at a large but finite value of the radial coordinate r and introduce boundary counterterms to cancel divergences that would otherwise appear as the boundary regulator is taken to infinity. A number of possible counterterms present themselves, but, as we will see, there is a simple construction that removes all divergences associated with the field variations in (2.21). Furthermore, the resulting finite stress tensor complex has precisely the form expected for a general z Lifshitz fluid. The remainder of this subsection draws heavily on reference [12], where holographic renormalisation was carried out for gravity coupled to a massive vector field in asymptotically Lifshitz spacetime.

The model at hand instead has a massless vector field that diverges at the boundary and a logarithmically running dilaton field but the shift symmetry (2.10) suggests a way around that. We can construct a shift-invariant scalar combination of the fields, which takes a constant value, independent of r, when evaluated on the pure Lifshitz solution,

$$e^{\lambda\phi}A_\mu A^\mu\Big|_{(2.9)} = -\frac{2(z-1)}{(z+2)}. \tag{2.22}$$

In asymptotically Lifshitz spacetime any function of this scalar will contribute at the same order in r to the boundary action and we are led to consider a counterterm action of the form,

$$S_{c.t.} = \int d^3x\sqrt{-\gamma}\big(-4 + f(e^{\lambda\phi}A^2)\big). \tag{2.23}$$

where f is some, as yet, undetermined function. The counterterm involving the vector field explicitly breaks the gauge symmetry of the bulk theory. As discussed in Section II, this is allowed because the only role of A_μ is to provide the background source that supports the asymptotically Lifshitz geometry and it does not couple directly to matter fields. It can in fact be viewed as an advantage that the gauge symmetry is broken as there is then no question of a conserved $U(1)$ charge in the dual field theory. Such a charge can easily be introduced via an additional bulk gauge field as in [30].

The first term in the counterterm action (involving $-4\sqrt{-\gamma}$) is a standard counterterm in AdS gravity. With it in place, the variation in (2.21) involving $\delta\gamma^{tt}$ vanishes for the Lifshitz background (2.7). This restricts the function in the matter counterterm to be of the form $f(-e^{\lambda\phi}A^2) = \xi\sqrt{-e^{\lambda\phi}A^2}$, with some constant ξ. The argument is the same as in [12] for the massive vector theory, *i.e.* the matter counterterm should not contribute at all to the $\delta\gamma^{tt}$ variation and this is ensured if the factor of $\sqrt{-\gamma_{tt}}$ that comes from the $\sqrt{-\gamma}$ prefactor is cancelled by a factor $\sqrt{-\gamma^{tt}}$

from $\sqrt{-e^{\lambda\phi}A_\mu A_\nu \gamma^{\mu\nu}}$. By this simple argument the counterterm action has been determined up to a single constant,

$$S_{c.t.} = \int d^3x \sqrt{-\gamma}\big(-4 + \xi \sqrt{-e^{\lambda\phi}A^2}\big), \tag{2.24}$$

and the variation of the full action $S = S_0 + S_{c.t.}$ can be written,

$$\delta S = \int d^3x \Big(s_{\alpha\beta}\, \delta\gamma^{\alpha\beta} + s_\alpha\, \delta A^\alpha + s\, \delta\phi \Big), \tag{2.25}$$

with,

$$s_{\alpha\beta} = \sqrt{-\gamma}\Big(K_{\alpha\beta} - K\gamma_{\alpha\beta} + 2\gamma_{\alpha\beta} - \frac{\xi e^{\lambda\phi}}{2\sqrt{-e^{\lambda\phi}A^2}}\big(A_\alpha A_\beta - A^2\gamma_{\alpha\beta}\big)\Big), \tag{2.26}$$

$$s_\alpha = \sqrt{-\gamma}\Big(- e^{\lambda\phi} n^\beta F_{\beta\alpha} - \frac{2\xi e^{\lambda\phi}A_\alpha}{2\sqrt{-e^{\lambda\phi}A^2}}\Big), \tag{2.27}$$

$$s = \sqrt{-\gamma}\Big(- n^\alpha \nabla_\alpha \phi - \frac{\xi\, \lambda e^{\lambda\phi}A^2}{2\sqrt{-e^{\lambda\phi}A^2}}\Big). \tag{2.28}$$

Remarkably, all the variations vanish for the Lifshitz background (2.7) for a single value of the free parameter in the boundary counterterm,

$$\xi = -\sqrt{2(z-1)(z+2)}, \tag{2.29}$$

and no further counterterms are needed for the problem at hand. For more general backgrounds, including Lifshitz black branes that are asymptotic to the Lifshitz solution, these variations will cancel at leading order and interesting physics resides in subleading terms that do not cancel. For instance, requiring the action to be invariant under the Lifshitz scaling (1.1) leads to a Ward identity,

$$z\, s^t_t + s^x_x + s^y_y + \frac{z-2}{2} s^t\, A_t - \sqrt{z-1}\, s = 0, \tag{2.30}$$

which encodes information about the fluid equation of state, as we will see in Section III below.

The Ward identity brings out the different scaling behaviour of temporal and spatial components and this difference should also be manifest in the renormalised stress tensor complex. Indeed, in a non-relatistic system the energy flux $\mathcal{E}^i$ and the momentum density $\mathcal{P}_i$ are independent variables and this appears to be at odds with the symmetry of $s_{\alpha\beta}$ under interchange of α and β. The resolution involves a subtle issue in holographic renormalisation which arises when a system has background vector fields [12, 36]. In this case, we are instructed to introduce orthonormal frame fields $e^{(A)}_\alpha$, with tangent space index A, and re-express the metric and vector variations in (2.25) in terms of variations involving frame variables,

$$\delta S = \int d^3x \Big((-2s^\alpha{}_\beta + s^\alpha A_\beta)\, e^\beta_{(B)} \delta e^{(B)}_\alpha + s_B\, \delta A^B + s\, \delta\phi \Big). \tag{2.31}$$

The elements of the boundary stress tensor complex are obtained by considering frame field variations while keeping fixed the dilaton and tangent space components of the vector field [12],

$$\mathcal{E} = 2s^t{}_t - s^t A_t, \qquad \mathcal{E}^i = 2s^i{}_t - s^i A_t, \tag{2.32}$$

$$\mathcal{P}_i = -2s^t{}_i + s^t A_i, \qquad \Pi^i{}_j = -2s^i{}_j + s^i A_j. \tag{2.33}$$

In a relativistic theory this prescription ensures a conserved stress tensor. An alternative prescription involving metric variations, keeping fixed spacetime components of a background vector field, would still produce a finite stess tensor but one that does not satisfy the usual conservation law [36]. In a non-relativistic theory, however, the tangent space prescription is indispensable. Without the extra terms in (2.33) that come from the vector field the elements of the stress tensor complex are not guaranteed to be finite, let alone conserved [12]. We will see this explicitly in the following subsection. When we consider the asymptotic fields of a moving Lifshitz black brane, the metric variation yields a divergence in the energy flux which is exactly cancelled by the contribution from the vector sector.

It is worth noting that for generic z the thermodynamic quantities in the stress tensor complex have different scaling dimensions. Straightforward dimensional analysis (see *e.g.* [13]) gives the following scaling behavior in d spatial dimensions,

$$\mathcal{E}' = \Lambda^{-d-z}\,\mathcal{E}\,, \quad \mathcal{E}'^{i} = \Lambda^{1-d-2z}\,\mathcal{E}^{i}\,, \quad \mathcal{P}'_i = \Lambda^{-1-d}\,\mathcal{P}_i\,, \quad P' = \Lambda^{-d-z}\,P\,. \tag{2.34}$$

D. The asymptotic solution

We now wish to consider general backgrounds that approach the Lifshitz solution as $r \to \infty$. While the metric and gauge field ansatz (2.11) and (2.12) is particularly well suited for deriving conserved Noether charges as in Section II B, it is less convenient for evaluating the stress tensor complex. For the asymptotic analysis we instead adopt a set of orthonormal frame fields,

$$e^{(0)} = r^z\,H_1(r)\,dt + r\,v_1(r)\,dy, \tag{2.35}$$

$$e^{(R)} = \frac{dr}{r\,H_2(r)}, \tag{2.36}$$

$$e^{(1)} = r\,H_3(r)\,dx, \tag{2.37}$$

$$e^{(2)} = r^z\,v_2(r)\,dt + r\,H_4(r)\,dy, \tag{2.38}$$

and orient the frame field $e^{(0)}$ parallel to the gauge field, $A_\mu = A_0(r)\,e^{(0)}_\mu$, with

$$A_0(r) = \sqrt{\frac{2(z-1)}{(z+2)}\,\frac{r^2}{r_h^2}}\,a_0(r). \tag{2.39}$$

Fixing the radial gauge $F_3(r) = 1$ amounts to setting $H_3(r) = 1$.

In order for the space-time to be asymptotically Lifshitz, we require that $H_1(r), H_2(r), H_4(r)$, and $a_0(r)$ tend to unity as $r \to \infty$ while $v_1(r)$ and $r^{1-z}\,v_2(r)$ tend to zero. With these assumptions, the field equations for a Lifshitz black brane with linear momentum reduce to a set of coupled linear ordinary differential equations for small deviations from the Lifshitz background in the asymptotic region.

The linearised field equations corresponding to the ty component of Einstein's tensor and the y component of Maxwell's equations decouple from the rest of the equations and can be solved separately for v_1 and v_2. The general solution of the resulting 2×2 eigenvalue problem consists of four eigenmodes,

$$v_1 = c_{1y}\, r^{z-1} + \frac{c_{2y}}{r^3} + \frac{z+2}{3z}\frac{c_{3y}}{r^{2z+1}} \tag{2.40}$$

$$v_2 = \frac{c_{4y}}{r^{z-1}} + \frac{c_{2y}}{r^3} + \frac{c_{3y}}{r^{2z+1}}, \tag{2.41}$$

The c_{1y} and c_{4y} modes are non-renormalisable source modes while c_{2y} and c_{3y} will appear in the momentum density and energy flux, respectively, in the renormalised stress energy complex [13].

The remaining linearised Einstein, Maxwell and dilaton equations can be solved in a straightforward manner along the lines of [31]. The full linearised solution has eigenmodes that go as r^{-z-2}, $r^{\frac{1}{2}(-z-2\pm\sqrt{(z+2)(9z+10)})}$ as well as r^0. A general holographic analysis of asymptotically Lifshitz space-times ([12, 14, 32, 33]) shows that a r^{-z-2} mode carries finite energy and is accordingly of primary interest for the analysis that follows. The remaining eigenmodes include a growing mode that would disrupt the asymptotic Lifshitz geometry and must therefore be absent in a physical solution and a mode that falls off at a faster rate than r^{-z-2} and can thus be ignored in our asymptotic analysis. Finally, we also leave out the constant mode which can be interpreted as a non-normalisable source mode.

We find that the finite energy mode takes the following form,

$$H_1 = 1 + \frac{c_1}{2}\, r^{-z-2}, \tag{2.42}$$

$$H_2 = 1 + \frac{c_2}{2}\, r^{-z-2}, \tag{2.43}$$

$$H_3 = 1 \tag{2.44}$$

$$H_4 = 1 + \frac{c_3}{2}\, r^{-z-2}, \tag{2.45}$$

$$a_0 = 1 + c_4\, r^{-z-2}, \tag{2.46}$$

$$\phi = 2\sqrt{z-1}\Big(\log\big(\frac{r}{r_h}\big) + \frac{c_5}{2}\, r^{-z-2}\Big), \tag{2.47}$$

with the following relations between the various constants,

$$c_2 = c_1 + c_3, \qquad c_5 = \frac{c_3}{2}. \tag{2.48}$$

Radial conservation of the charge (2.20), associated with the shift symmetry of the dilaton field, gives an additional relation,

$$c_4 = \frac{c_1}{2} - \frac{z-2}{4}c_3, \tag{2.49}$$

leaving us with two independent constants, c_1 and c_3.

Plugging in the asymptotic solution (2.42)-(2.47) into the renormalised stress tensor complex

(2.33) and eliminating constants using (2.48) and (2.49) gives the following expression

$$\mathcal{E} = -2c_1 + zc_3, \tag{2.50}$$

$$\mathcal{E}^x = 0, \tag{2.51}$$

$$\mathcal{E}^y = -2(z-1)c_{3y}, \tag{2.52}$$

$$\Pi^x{}_x = zc_1 - \frac{1}{2}(z^2 - z - 2)c_3, \tag{2.53}$$

$$\Pi^y{}_y = zc_1 - \frac{1}{2}(z^2 + z + 2)c_3, \tag{2.54}$$

$$\mathcal{P}_y = -2(z-1)c_{2y}. \tag{2.55}$$

The modes c_{2y} and c_{3y} appear only in the off-diagonal terms of the stress tensor complex and can be interpreted as the momentum density ρv and energy flux $(\mathcal{E} + P)v$ respectively. While they cannot be related with the other modes in the absence of the full bulk solution, it appears safe to make this statement, as they show the exact scaling dimensions as required by (2.34).

In this calculation it was essential to include the vector field contribution to the stress tensor complex in (2.32)-(2.33). The energy flux, given by $\mathcal{E}^i = 2s^i{}_t - s^i A_t$, is divergent if only the contribution from the $s^i{}_t$ term is included but when both terms are present the divergence is cancelled, leaving behind a finite result for $\mathcal{E}^i$. Moreover, the resulting finite energy flux (2.52) and the momentum density (2.54) are independent in that they involve different eigenmodes of the linearised solution.

III. THERMODYNAMICS

Having constructed a finite renormalised stress energy complex, we can proceed to study the thermodynamics of the fluid described by the above holographic dual. We expect to find a perfect Lifshitz fluid, whose description is invariant under time and space translations as well as rotations, but without boost symmetry.

The thermodynamic relations that we wish to establish require us to supplement the linearised solution in the asymptotic region with near-horizon data. This can be done via the Noether charges that we obtained earlier, even in the absence of an exact (or numerical) solution that interpolates between the near-horizon and asymptotic regions.

A. The near-horizon solution

Using similar arguments to those made in [19], we find that an appropriate near-horizon Taylor series expansion of the various metric and gauge fields in (2.11) and (2.12) is given by,

$$F_1 = f_1 \frac{r - r_h}{r_h} + \dots \tag{3.1}$$

$$F_2 = h_1 \frac{r - r_h}{r_h} + \dots \tag{3.2}$$

$$F_3 = 1 \tag{3.3}$$

$$F_4 = p_0 + p_1 \frac{r - r_h}{r_h} + \dots \tag{3.4}$$

$$N = n_0 + n_1 \frac{r - r_h}{r_h} + \dots \tag{3.5}$$

$$G_1 = g_1 \frac{r - r_h}{r_h} + \dots \tag{3.6}$$

$$G_2 = m_0 + m_1 \frac{r - r_h}{r_h} + \dots \tag{3.7}$$

$$\phi = l_0 + l_1 \frac{r - r_h}{r_h} + \dots, \tag{3.8}$$

where, as before, we are working in the $F_3 = 1$ gauge. The location of the horizon r_h is where g^{rr} vanishes. This means that F_2 will have a first order zero at r_h. Also, regularity of the metric in Eddington-Finklestein coordinates requires F_1 to have a first order zero at r_h as well. Finally, G_1 should also have a first order zero at r_h, but the remaining fields are regular there.

The near horizon metric is then given by,

$$ds^2 = -f_1 \rho r_h^{2z-1} dt^2 + \frac{d\rho^2}{r_h h_1 \rho} + r_h^2 dx^2 + p_0 r_h^2 (dy + N(r_h) r_h^{z-1} dt)^2, \tag{3.9}$$

where $\rho = r - r_h$. Making a change of coordinates,

$$\tilde{\rho}^2 = \frac{4\rho}{r_h h_1}, \ \tilde{t} = (f_1 h_1)^{\frac{1}{2}} \frac{r_h^z t}{2}, \tag{3.10}$$

the metric takes the following form,

$$ds^2 = -\tilde{\rho}^2 d\tilde{t}^2 + d\tilde{\rho}^2 + r_h^2 dx^2 + p_0 r_h^2 (dy + N(r_h) r_h^{z-1} dt)^2. \tag{3.11}$$

After going to Euclidean coordinates, the Hawking temperature is found to be $T = \frac{r_h^z}{4\pi}(f_1 h_1)^{\frac{1}{2}}$. Meanwhile (using units where $16\pi G_N = 1$), the entropy is given by $s = \frac{A}{4G_N} = 4\pi p_0^{\frac{1}{2}} r_h^2$, and we have

$$Ts = (p_0 f_1 h_1)^{\frac{1}{2}} r_h^{z+2}. \tag{3.12}$$

In the following subsections we consider in turn the static and the moving black branes and compare this expression to the Noether charge(s) obtained in the near-horizon region. Via the conservation of the Noether charges, this can then be related to the asymptotic solution and the stress tensor complex evaluated at the boundary.

The radial gauge conditions $F_3(r) = 1$ and $H_3(r) = 1$ ensure that we can identify the radial variable r in our near-horizon solution with that in our asymptotic solutions and then there is a straightforward mapping between the frame fields defined in (2.35)-(2.38) and coordinate fields (2.11), which we can use to evaluate the Noether charges at the boundary.

B. Static Lifshitz black brane

As a warm-up exercise, let us first study thermodynamics of a static Lifshitz brane with general z given by the static limit of (2.11) by evaluating the renormalised stress tensor at the boundary and using the method of Noether charges.

For a static black brane we have $c_3 = 0$ and the stress tensor complex in (2.50)-(2.55) reduces to

$$\mathcal{E} = -2c_1, \tag{3.13}$$

$$\mathcal{E}^x = 0, \tag{3.14}$$

$$\mathcal{E}^y = 0, \tag{3.15}$$

$$\Pi_x^x = zc_1, \tag{3.16}$$

$$\Pi_y^y = zc_1, \tag{3.17}$$

$$\mathcal{P}_y = 0. \tag{3.18}$$

One can easily verify that the scaling Lifshitz Ward identity (2.30) is satisfied. In fact, s_α and s vanish trivially for the static brane. Identifying $-2c_1$ and $-z\,c_1$ as the energy and pressure P, respectively, we obtain

$$z\mathcal{E} = 2P, \tag{3.19}$$

which is the well-known equation of state for a static perfect Lifshitz fluid.

Plugging in the near horizon metric anstaz defined in (III A) into our Noether charges obtained in (II B), we find that Q_β vanishes and Q_α reduces to

$$Q_\alpha = Ts, \tag{3.20}$$

with T the Hawking temperature and s the entropy density of the static brane. Plugging in the asymptotic metric ansatz (2.42)-(2.47) into the non-vanishing Noether charge gives

$$Q_\alpha = -(z+2)c_1. \tag{3.21}$$

Equating the right hand sides of (3.20) and (3.21) and identifying $\mathcal{E} = -2c_1$ from (3.13), we get precisely the Gibbs-Duhem relation expected for a Lifshitz fluid,

$$\mathcal{E} = \frac{2}{z+2}Ts, \tag{3.22}$$

or, equivalently,

$$\mathcal{E} + P = Ts. \tag{3.23}$$

C. Moving Lifshitz black brane

Let us now proceed to repeat the above exercise for the case of interest, that is, a Lifshitz black brane with linear momentum along one of the transverse directions (which we chose to be the y-direction without loss of generality).

For a perfect fluid moving in the y-direction the pressure is identified via $\Pi^x{}_x = -P$ while $\Pi^y{}_y = -P - \rho\, v^2$ is the combined stress due to pressure and momentum flow along the y direction. The stress tensor complex for the moving Lifshitz black brane was obtained in (2.50)-(2.55) and we can read off the energy density, pressure, and momentum flux,

$$\mathcal{E} = -2c_1 + z\, c_3, \quad P = -z\, c_1 + \frac{1}{2}(z^2 - z - 2)c_3, \quad \rho\, v^2 = (z+2)c_3. \tag{3.24}$$

Using the linearised solution we can easily verify that the Lifshitz Ward identity (2.30) is indeed satisfied and gives us the equation of state for a perfect Lifshitz fluid in motion,

$$z\mathcal{E} - \rho v^2 = 2P, \tag{3.25}$$

as hypothesised in [20, 22]. As discussed above, the modes c_{2y} and c_{3y} appear only in the off-diagonal terms of the stress tensor complex. Although they cannot be related to the other modes in the absence of an interpolating solution, they do have the right scaling to be interpreted as the momentum density ρv and energy flux $(\mathcal{E} + P)v$, respectively.

Plugging in the near horizon metric anstaz defined in (III A) into our Noether charges Q_α and Q_β obtained in (II B), we find that a simple linear combination of the two in fact gives us (3.12). Specifically,

$$Q_\alpha - \frac{3}{2} Q_\beta = Ts. \tag{3.26}$$

Plugging in the asymptotic metric ansatz (2.42)-(2.47) into the same Noether charges gives

$$Q_\alpha = \frac{(z+2)}{2}\,(-2c_1 + z\, c_3), \tag{3.27}$$

$$Q_\beta = (z+2)c_3 = \rho\, v^2. \tag{3.28}$$

Now use (3.24) and the equation of state (3.25) to express the Noether charges in terms of fluid variables,

$$Q_\alpha = \mathcal{E} + P + \frac{1}{2}\rho\, v^2, \tag{3.29}$$

$$Q_\beta = \rho\, v^2, \tag{3.30}$$

and it immediately follows that the combination of Noether charges in (3.26) gives the Gibbs-Duhem relation for a moving Lifshitz perfect fluid,

$$\mathcal{E} + P = Ts + \rho v^2. \tag{3.31}$$

Interpreting the various boundary data as field theory sources in this manner, we find that the velocity of the fluid v appears as the chemical potential conjugate to the kinetic mass density ρ in accordance with [19, 20].

Finally, it is interesting to consider the special value of $z = 2$, for which the Lifshitz scaling symmetry is consistent with Galilean boost symmetry. In this case, the energy density, pressure, and momentum flux in (3.24) reduce to

$$\mathcal{E} = -2c_1 + 2c_3, \quad P = -2c_1, \quad \rho v^2 = 4c_3, \tag{3.32}$$

The energy density can be written as the sum of an internal energy density and a kinetic energy density, $\mathcal{E} = \mathcal{E}_0 + \frac{1}{2}\rho v^2$. In a Galilean boost invariant system $\mathcal{E}_0$ is simply the energy density in the rest frame of the fluid and the pressure, $P = \mathcal{E}_0$, is frame independent. For general $z \neq 2$, these last two statements do not hold.

IV. CONCLUSION AND FUTURE OUTLOOK

In this paper, we have investigated the holographic dual of a perfect Lifshitz fluid with an arbitrary dynamical exponent, z, moving with a velocity, v. The moving black brane we have considered is a solution of the Einstein-Maxwell-Dilaton theory, and is obtained by constructing a new class of metrics that correspond to a black brane having a linear momentum, rather than boosting a static black brane.

By evaluating the Noether charges associated with various scaling symmetries of our metric, and equating their values at the horizon and boundary (as they are radially conserved quantities), we were able to obtain the expected equation of state for the perfect Lifshitz fluid with an arbitrary dynamical exponent, z ([20]). Moreover we note that the velocity indeed appears as a chemical potential, conjugate to the dual kinetic mass density ([20], [19]).

By solving the linearised perturbations of the Einstein, Maxwell and dilaton equations, we found the asymptotic solutions of the metric and gauge fields, and used these to construct the boundary stress tensor of the fluid. By working in an orthonormal frame and using counterterms similar to those proposed in [12], we were able to construct the renormalised stress tensor complex and read off the various thermodynamic variables. The result has the expected form for a non-relativistic fluid, and satisfies the Ward identity associated with Lifshitz scaling.

There are several interesting questions to be investigated. A straightforward extension of the present work would be to study the gravitational dual of charged perfect Lifshitz fluids via the addition of other $U(1)$ fields to the theory, for which the boundary theory that one might need to study would be that of non-relativisitc electrodynamics coupled to torsionless Newton-Cartan theory, as explored in [37]. Another extension would be to carry out the analysis performed in this paper on theories with a non-trivial coupling between the dilaton and cosmological constant, that is, moving hyperscale-violating Lifshitz geometries, and study the resulting thermodynamics.

Lifshitz holography is still a relatively unexplored area as compared to it's relativistic counterpart. Following the work done in [22] where the complete first-order energy-momentum tensor in curved space-time for a fluid without boost symmetry was computed, one can now consider trying to find the hydrodynamic modes of Lifshitz fluids from quasinormal modes and compare the results. In this study, we have concentrated on perfect fluids without impurities or lattice effects which break translational invariance. Physical systems that break boost invariance, however, often also exhibit other spontaneous symmetry breaking patterns. While the main objective of the work carried out in [38] was to provide a general hydrodynamic framework for fluids that break boost symmetry, it also offers a controlled framework for studying other patterns of symmetry breaking. It would be of interest to study Lifshitz gravity duals that could model this behaviour, in order to better understand their microscopics. With the current holographic model for a moving Lifshitz fluid established, one can also proceed to calculate two point correlation functions related to transport and other quantities of interest from a gauge-gravity perspective.

Acknowledgements: We would like to thank Valentina Giangreco M. Puletti, Jelle Hartong, Niels Obers, Nick Poovuttikul, and Watse Sybesma for useful discussions and input. This research was supported in part by the Icelandic Research Fund under grant 195970-052 and by the University of Iceland Research Fund.

---

[1] L. D. Landau and E. M. Lifshitz, *Fluid Mechanics*. Butterworth-Heinemann, 2nd ed., 1987.

[2] G. Policastro, D. T. Son, and A. O. Starinets, "The Shear viscosity of strongly coupled N=4 supersymmetric Yang-Mills plasma," *Phys. Rev. Lett.* **87** (2001) 081601, arXiv:hep-th/0104066.

[3] G. Policastro, D. T. Son, and A. O. Starinets, "From AdS / CFT correspondence to hydrodynamics," *JHEP* **09** (2002) 043, arXiv:hep-th/0205052.

[4] G. Policastro, D. T. Son, and A. O. Starinets, "From AdS / CFT correspondence to hydrodynamics. 2. Sound waves," *JHEP* **12** (2002) 054, arXiv:hep-th/0210220.

[5] S. Bhattacharyya, V. E. Hubeny, S. Minwalla, and M. Rangamani, "Nonlinear Fluid Dynamics from Gravity," *JHEP* **02** (2008) 045, arXiv:0712.2456 [hep-th].

[6] R. Baier, P. Romatschke, D. T. Son, A. O. Starinets, and M. A. Stephanov, "Relativistic viscous hydrodynamics, conformal invariance, and holography," *JHEP* **04** (2008) 100, arXiv:0712.2451 [hep-th].

[7] J. M. Maldacena, "The Large N limit of superconformal field theories and supergravity," *Int. J. Theor. Phys.* **38** (1999) 1113–1133, arXiv:hep-th/9711200.

[8] D. Son, "Toward an AdS/cold atoms correspondence: A Geometric realization of the Schrodinger symmetry," *Phys. Rev. D* **78** (2008) 046003, arXiv:0804.3972 [hep-th].

[9] K. Balasubramanian and J. McGreevy, "Gravity duals for non-relativistic CFTs," *Phys. Rev. Lett.* **101** (2008) 061601, arXiv:0804.4053 [hep-th].

[10] S. Kachru, X. Liu, and M. Mulligan, "Gravity duals of Lifshitz-like fixed points," *Phys. Rev. D* **78** (2008) 106005, arXiv:0808.1725 [hep-th].

[11] M. Taylor, "Non-relativistic holography," arXiv:0812.0530 [hep-th].

[12] S. F. Ross and O. Saremi, "Holographic stress tensor for non-relativistic theories," *JHEP* **09** (2009) 009, arXiv:0907.1846 [hep-th].

[13] S. F. Ross, "Holography for asymptotically locally Lifshitz spacetimes," *Class. Quant. Grav.* **28** (2011) 215019, arXiv:1107.4451 [hep-th].

[14] R. B. Mann and R. McNees, "Holographic Renormalization for Asymptotically Lifshitz Spacetimes," *JHEP* **10** (2011) 129, arXiv:1107.5792 [hep-th].

[15] G. Bertoldi, B. A. Burrington, and A. W. Peet, "Thermodynamics of black branes in asymptotically Lifshitz spacetimes," *Phys. Rev. D* **80** (2009) 126004, arXiv:0907.4755 [hep-th].

[16] C. Hoyos, B. S. Kim, and Y. Oz, "Lifshitz Hydrodynamics," *JHEP* **11** (2013) 145, arXiv:1304.7481 [hep-th].

[17] C. Hoyos, B. S. Kim, and Y. Oz, "Lifshitz Field Theories at Non-Zero Temperature, Hydrodynamics and Gravity," *JHEP* **03** (2014) 029, arXiv:1309.6794 [hep-th].

[18] E. Kiritsis and Y. Matsuo, "Charge-hyperscaling violating Lifshitz hydrodynamics from black-holes," *JHEP* **12** (2015) 076, arXiv:1508.02494 [hep-th].

[19] J. Hartong, N. A. Obers, and M. Sanchioni, "Lifshitz Hydrodynamics from Lifshitz Black Branes with Linear Momentum," *JHEP* **10** (2016) 120, arXiv:1606.09543 [hep-th].

[20] J. de Boer, J. Hartong, N. A. Obers, W. Sybesma, and S. Vandoren, "Perfect Fluids," *SciPost Phys.* **5** no. 1, (2018) 003, arXiv:1710.04708 [hep-th].

[21] B. Grinstein and S. Pal, "Existence and construction of galilean invariant z $\neq$ 2 theories," *Physical Review D* **97** no. 12, (Jun, 2018) . http://dx.doi.org/10.1103/PhysRevD.97.125006.

[22] J. de Boer, J. Hartong, E. Have, N. A. Obers, and W. Sybesma, "Non-Boost Invariant Fluid Dynamics," *SciPost Phys.* **9** no. 2, (2020) 018, arXiv:2004.10759 [hep-th].

[23] I. Novak, J. Sonner, and B. Withers, "Hydrodynamics without boosts," *JHEP* **07** (2020) 165, arXiv:1911.02578 [hep-th].

[24] D. Fernández, A. Rajagopal, and L. Thorlacius, "Non-equilibrium steady states in quantum critical systems with Lifshitz scaling," *JHEP* **12** (2019) 115, arXiv:1909.06377 [hep-th].

[25] M. J. Bhaseen, B. Doyon, A. Lucas, and K. Schalm, "Far from equilibrium energy flow in quantum critical systems," *Nature Phys.* **11** (2015) 5, arXiv:1311.3655 [hep-th].

[26] A. Lucas, K. Schalm, B. Doyon, and M. Bhaseen, "Shock waves, rarefaction waves, and nonequilibrium steady states in quantum critical systems," *Phys. Rev. D* **94** no. 2, (2016) 025004, arXiv:1512.09037 [hep-th].

[27] M. Spillane and C. P. Herzog, "Relativistic hydrodynamics and non-equilibrium steady states," *Journal of Statistical Mechanics: Theory and Experiment* **2016** no. 10, (Oct, 2016) 103208. http://dx.doi.org/10.1088/1742-5468/2016/10/103208.

[28] I. Amado and A. Yarom, "Black brane steady states," *JHEP* **10** (2015) 015, arXiv:1501.01627 [hep-th].

[29] R. Pourhasan, "Non-equilibrium steady state in the hydro regime," *Journal of High Energy Physics* **2016** no. 2, (Feb, 2016) . http://dx.doi.org/10.1007/JHEP02(2016)005.

[30] J. Tarrio and S. Vandoren, "Black holes and black branes in Lifshitz spacetimes," *JHEP* **09** (2011) 017, arXiv:1105.6335 [hep-th].

[31] V. Keranen and L. Thorlacius, "Thermal Correlators in Holographic Models with Lifshitz scaling," *Class. Quant. Grav.* **29** (2012) 194009, arXiv:1204.0360 [hep-th].

[32] T. Zingg, "Thermodynamics of Dyonic Lifshitz Black Holes," *JHEP* **09** (2011) 067, arXiv:1107.3117 [hep-th].

[33] M. Baggio, J. de Boer, and K. Holsheimer, "Hamilton-Jacobi Renormalization for Lifshitz Spacetime," *JHEP* **01** (2012) 058, arXiv:1107.5562 [hep-th].

[34] J. Tarrio, "Asymptotically Lifshitz Black Holes in Einstein-Maxwell-Dilaton Theories," *Fortsch. Phys.* **60** (2012) 1098–1104, arXiv:1201.5480 [hep-th].

[35] B. W. Langley and P. W. Phillips, "Quantum Critical Diffusion and Thermodynamics in Lifshitz Holography," arXiv:1812.08164 [hep-th].

[36] S. Hollands, A. Ishibashi, and D. Marolf, "Counter-term charges generate bulk symmetries," *Phys. Rev. D* **72** (2005) 104025, arXiv:hep-th/0503105.

[37] G. Festuccia, D. Hansen, J. Hartong, and N. A. Obers, "Symmetries and Couplings of Non-Relativistic Electrodynamics," *JHEP* **11** (2016) 037, arXiv:1607.01753 [hep-th].

[38] J. Armas and A. Jain, "Effective field theory for hydrodynamics without boosts," arXiv:2010.15782 [hep-th].

References

Abrahams, E. and Wölfle, P. (2012). Critical quasiparticle theory applied to heavy fermion metals near an antiferromagnetic quantum phase transition. *Proceedings of the National Academy of Sciences*, 109(9):3238–3242.

Anile, A. M. (2005). *Relativistic fluids and magneto-fluids: With applications in astrophysics and plasma physics*. Cambridge University Press.

Armas, J. and Jain, A. (2019). Magnetohydrodynamics as superfluidity. *Phys. Rev. Lett.*, 122(14):141603.

Armas, J. and Jain, A. (2020). One-form superfluids & magnetohydrodynamics. *JHEP*, 01:041.

Arnold, P. B., Moore, G. D., and Yaffe, L. G. (2000). Transport coefficients in high temperature gauge theories. 1. Leading log results. *JHEP*, 11:001.

Baggio, M., de Boer, J., and Holsheimer, K. (2012). Hamilton-Jacobi Renormalization for Lifshitz Spacetime. *JHEP*, 01:058.

Baier, R., Romatschke, P., Son, D. T., Starinets, A. O., and Stephanov, M. A. (2008). Relativistic viscous hydrodynamics, conformal invariance, and holography. *JHEP*, 04:100.

Balasubramanian, K. and McGreevy, J. (2008). Gravity duals for non-relativistic CFTs. *Phys. Rev. Lett.*, 101:061601.

Banerjee, N., Bhattacharya, J., Bhattacharyya, S., Dutta, S., Loganayagam, R., and Surowka, P. (2011). Hydrodynamics from charged black branes. *JHEP*, 01:094.

Beekman, A. J., Nissinen, J., Wu, K., and Zaanen, J. (2017). Dual gauge field theory of quantum liquid crystals in three dimensions. *Physical Review B*, 96(16).

Berkooz, M., Sever, A., and Shomer, A. (2002). 'Double trace' deformations, boundary conditions and space-time singularities. *JHEP*, 05:034.

Bernard, D. and Doyon, B. (2012). Energy flow in non-equilibrium conformal field theory. *Journal of Physics A: Mathematical and Theoretical*, 45(36):362001.

Bhaseen, M. J., Doyon, B., Lucas, A., and Schalm, K. (2015). Far from equilibrium energy flow in quantum critical systems. *Nature Phys.*, 11:5.

Bhattacharyya, S., Hubeny, V. E., Minwalla, S., and Rangamani, M. (2008). Nonlinear Fluid Dynamics from Gravity. *JHEP*, 02:045.

Bianchini, S. (2003). On the riemann problem for non-conservative hyperbolic systems. *Archive for Rational Mechanics and Analysis*, 166:1–26.

Blake, M. (2015). Momentum relaxation from the fluid/gravity correspondence. *Journal of High Energy Physics*, 2015(9).

Blandford, R. and Znajek, R. (1977). Electromagnetic extractions of energy from Kerr black holes. *Mon. Not. Roy. Astron. Soc.*, 179:433–456.

Buchel, A. (2005). On universality of stress-energy tensor correlation functions in supergravity. *Phys. Lett. B*, 609:392–401.

Callan-Jones, A. C. and Jülicher, F. (2011). Hydrodynamics of active permeating gels. *New Journal of Physics*, 13(9):093027.

Chang, H.-C., Karch, A., and Yarom, A. (2014). An ansatz for one dimensional steady state configurations. *Journal of Statistical Mechanics: Theory and Experiment*, 2014(6):P06018.

Chemissany, W. and Papadimitriou, I. (2015). Lifshitz holography: The whole shebang. *JHEP*, 01:052.

Christensen, M. H., Hartong, J., Obers, N. A., and Rollier, B. (2014a). Boundary Stress-Energy Tensor and Newton-Cartan Geometry in Lifshitz Holography. *JHEP*, 01:057.

Christensen, M. H., Hartong, J., Obers, N. A., and Rollier, B. (2014b). Torsional Newton-Cartan Geometry and Lifshitz Holography. *Phys. Rev. D*, 89:061901.

Crossley, M., Glorioso, P., and Liu, H. (2017). Effective field theory of dissipative fluids. *JHEP*, 09:095.

Davison, R. A. and Goutéraux, B. (2015). Dissecting holographic conductivities. *JHEP*, 09:090.

de Boer, J., Hartong, J., Have, E., Obers, N. A., and Sybesma, W. (2020). Non-Boost Invariant Fluid Dynamics. *SciPost Phys.*, 9(2):018.

de Boer, J., Hartong, J., Obers, N. A., Sybesma, W., and Vandoren, S. (2018). Perfect Fluids. *SciPost Phys.*, 5(1):003.

de Boer, J., Heller, M. P., and Pinzani-Fokeeva, N. (2019). Holographic Schwinger-Keldysh effective field theories. *JHEP*, 05:188.

de Haro, S., Skenderis, K., and Solodukhin, S. N. (2001). Holographic reconstruction of spacetime and renormalization in the ads/cft correspondence. *Communications in Mathematical Physics*, 217(3):595–622.

de Saxcé, G. (2016). *Galilean mechanics and thermodynamics of continua / Géry de Saxcé, Claude Vallée*. Mechanical engineering and solid mechanics series. ISTE Ltd John Wiley and Sons, Inc, London Hoboken (N.J.).

de Saxcé, G. and Vallée, C. (2012). Bargmann group, momentum tensor and galilean invariance of clausius–duhem inequality. *International Journal of Engineering Science*, 50(1):216 – 232.

D'Hoker, E. and Kraus, P. (2009). Magnetic Brane Solutions in AdS. *JHEP*, 10:088.

Dixon, W. G. (1982). *Special relativity: the foundation of macroscopic physics*. CUP Archive.

Erdmenger, J., Haack, M., Kaminski, M., and Yarom, A. (2009). Fluid dynamics of R-charged black holes. *JHEP*, 01:055.

Esposito, A., Krichevsky, R., and Nicolis, A. (2017). Vortex precession in trapped superfluids from effective field theory. *Physical Review A*, 96(3).

Faulkner, T. and Iqbal, N. (2013). Friedel oscillations and horizon charge in 1D holographic liquids. *JHEP*, 07:060.

Fernández, D., Rajagopal, A., and Thorlacius, L. (2019). Non-equilibrium steady states in quantum critical systems with Lifshitz scaling. *JHEP*, 12:115.

Festuccia, G., Hansen, D., Hartong, J., and Obers, N. A. (2016a). Symmetries and Couplings of Non-Relativistic Electrodynamics. *JHEP*, 11:037.

Festuccia, G., Hansen, D., Hartong, J., and Obers, N. A. (2016b). Torsional newton-cartan geometry from the noether procedure. *Physical Review D*, 94(10).

Forster, D. (1995). *Hydrodynamic Fluctuations, Broken Symmetry, and Correlation Functions*. Perseus Books.

Gaiotto, D., Kapustin, A., Seiberg, N., and Willett, B. (2015). Generalized Global Symmetries. *JHEP*, 02:172.

Glorioso, P., Crossley, M., and Liu, H. (2018). A prescription for holographic Schwinger-Keldysh contour in non-equilibrium systems.

Glorioso, P. and Son, D. T. (2018). Effective field theory of magnetohydrodynamics from generalized global symmetries.

Goedbloed, J. P. H. and Poedts, S. (2004). *Principles of Magnetohydrodynamics: With Applications to Laboratory and Astrophysical Plasmas*. Cambridge University Press.

Goldreich, P. and Julian, W. H. (1969). Pulsar Electrodynamics. 157:869.

Gralla, S. E. and Iqbal, N. (2019). Effective Field Theory of Force-Free Electrodynamics. *Phys. Rev. D*, 99(10):105004.

Gralla, S. E. and Jacobson, T. (2014). Spacetime approach to force-free magnetospheres.

Mon. Not. Roy. Astron. Soc., 445(3):2500–2534.

Grozdanov, S., Hofman, D. M., and Iqbal, N. (2017). Generalized global symmetries and dissipative magnetohydrodynamics. *Phys. Rev. D*, 95(9):096003.

Grozdanov, S., Lucas, A., and Poovuttikul, N. (2019). Holography and hydrodynamics with weakly broken symmetries. *Phys. Rev. D*, 99(8):086012.

Grozdanov, S. and Poovuttikul, N. (2019). Generalised global symmetries in holography: magnetohydrodynamic waves in a strongly interacting plasma. *JHEP*, 04:141.

Haehl, F. M., Loganayagam, R., and Rangamani, M. (2016). Topological sigma models \& dissipative hydrodynamics. *JHEP*, 04:039.

Hartnoll, S. A. (2009). Lectures on holographic methods for condensed matter physics. *Class. Quant. Grav.*, 26:224002.

Hartnoll, S. A. and Hofman, D. M. (2012). Locally Critical Resistivities from Umklapp Scattering. *Phys. Rev. Lett.*, 108:241601.

Hartnoll, S. A., Lucas, A., and Sachdev, S. (2016). Holographic quantum matter.

Hartong, J., Kiritsis, E., and Obers, N. A. (2015a). Field Theory on Newton-Cartan Backgrounds and Symmetries of the Lifshitz Vacuum. *JHEP*, 08:006.

Hartong, J., Kiritsis, E., and Obers, N. A. (2015b). Lifshitz space–times for Schrödinger holography. *Phys. Lett. B*, 746:318–324.

Hartong, J., Obers, N. A., and Sanchioni, M. (2016). Lifshitz Hydrodynamics from Lifshitz Black Branes with Linear Momentum. *JHEP*, 10:120.

Hatwalne, Y., Ramaswamy, S., Rao, M., and Simha, R. A. (2004). Rheology of active-particle suspensions. *Phys. Rev. Lett.*, 92:118101.

Hernandez, J. and Kovtun, P. (2017). Relativistic magnetohydrodynamics. *JHEP*, 05:001.

Herzog, C. and Son, D. (2003). Schwinger-Keldysh propagators from AdS/CFT correspondence. *JHEP*, 03:046.

Hofman, D. M. and Iqbal, N. (2018). Generalized global symmetries and holography. *SciPost Phys.*, 4(1):005.

Hollands, S., Ishibashi, A., and Marolf, D. (2005). Counter-term charges generate bulk symmetries. *Phys. Rev. D*, 72:104025.

Horn, B., Nicolis, A., and Penco, R. (2015). Effective string theory for vortex lines in fluids and superfluids.

Hoyos, C., Kim, B. S., and Oz, Y. (2013). Lifshitz Hydrodynamics. *JHEP*, 11:145.

Hoyos, C., Kim, B. S., and Oz, Y. (2014). Lifshitz Field Theories at Non-Zero Temperature, Hydrodynamics and Gravity. *JHEP*, 03:029.

Huang, C., Fuchs, D., Wissinger, M., Schneider, R., Ling, M., Scheurer, M., Schmalian, J., and Löhneysen, H. (2015). Anomalous quantum criticality in an itinerant ferromagnet. *Nature communications*, 6:8188.

Hubeny, V. E., Minwalla, S., and Rangamani, M. (2011). The fluid/gravity correspondence. In *Theoretical Advanced Study Institute in Elementary Particle Physics: String theory and its Applications: From meV to the Planck Scale*.

Jensen, K. (2015). Aspects of hot galilean field theory. *Journal of High Energy Physics*, 2015(4).

Jensen, K., Pinzani-Fokeeva, N., and Yarom, A. (2018). Dissipative hydrodynamics in superspace. *JHEP*, 09:127.

Kachru, S., Liu, X., and Mulligan, M. (2008). Gravity duals of Lifshitz-like fixed points. *Phys. Rev. D*, 78:106005.

Keranen, V. and Thorlacius, L. (2012). Thermal Correlators in Holographic Models with Lifshitz scaling. *Class. Quant. Grav.*, 29:194009.

Kiritsis, E. and Matsuo, Y. (2015). Charge-hyperscaling violating lifshitz hydrodynamics from black-holes. *Journal of High Energy Physics*, 2015(12):1–51.

Komissarov, S. (2002). On the properties of time dependent, force-free, degenerate electrodynamics. *Mon. Not. Roy. Astron. Soc.*, 336:759.

Komissarov, S. (2004). Electrodynamics of black hole magnetospheres. *Mon. Not. Roy. Astron. Soc.*, 350:407.

Komissarov, S. S. (1999). A Godunov-type scheme for relativistic magnetohydrodynamics. *Monthly Notices of the Royal Astronomical Society*, 303(2):343–366.

Kovtun, P., Son, D. T., and Starinets, A. O. (2003). Holography and hydrodynamics: Diffusion on stretched horizons. *JHEP*, 10:064.

Kovtun, P., Son, D. T., and Starinets, A. O. (2005). Viscosity in strongly interacting quantum field theories from black hole physics. *Phys. Rev. Lett.*, 94:111601.

Landau, L. D. and Lifshitz, E. M. (1987). *Fluid Mechanics*. Butterworth-Heinemann, 2nd edition.

Lax, P. D. (1954). Weak solutions of nonlinear hyperbolic equations and their numerical computation. *Communications on Pure and Applied Mathematics*, 7(1):159–193.

Lax, P. D. (1957). Hyperbolic systems of conservation laws ii. *Communications on Pure and Applied Mathematics*, 10(4):537–566.

Lax, P. D. (1972). The formation and decay of shock waves. *The American Mathematical Monthly*, 79(3):227–241.

Lucas, A., Crossno, J., Fong, K. C., Kim, P., and Sachdev, S. (2016a). Transport in inhomogeneous quantum critical fluids and in the dirac fluid in graphene. *Physical Review B*, 93(7).

Lucas, A. and Fong, K. C. (2018). Hydrodynamics of electrons in graphene. *Journal of Physics: Condensed Matter*, 30(5):053001.

Lucas, A., Schalm, K., Doyon, B., and Bhaseen, M. (2016b). Shock waves, rarefaction waves, and nonequilibrium steady states in quantum critical systems. *Phys. Rev. D*, 94(2):025004.

Maldacena, J. M. (1999). The Large N limit of superconformal field theories and supergravity. *Int. J. Theor. Phys.*, 38:1113–1133.

Mann, R. B. and McNees, R. (2011). Holographic Renormalization for Asymptotically Lifshitz Spacetimes. *JHEP*, 10:129.

Nickel, D. and Son, D. T. (2011). Deconstructing holographic liquids. *New J. Phys.*, 13:075010.

Nicolis, A. and Penco, R. (2018). Mutual interactions of phonons, rotons, and gravity. *Physical Review B*, 97(13).

Policastro, G., Son, D. T., and Starinets, A. O. (2001). The Shear viscosity of strongly coupled N=4 supersymmetric Yang-Mills plasma. *Phys. Rev. Lett.*, 87:081601.

Policastro, G., Son, D. T., and Starinets, A. O. (2002a). From AdS / CFT correspondence to hydrodynamics. *JHEP*, 09:043.

Policastro, G., Son, D. T., and Starinets, A. O. (2002b). From AdS / CFT correspondence to hydrodynamics. 2. Sound waves. *JHEP*, 12:054.

Poovuttikul, N. and Rajagopal, A. (2021). Operator lifetime and the force-free electrodynamic limit of magnetised holographic plasma.

Pourhasan, R. (2016). Non-equilibrium steady state in the hydro regime. *Journal of High Energy Physics*, 2016(2).

Rajagopal, A. and Thorlacius, L. (2021). Lifshitz hydrodynamics at generic z from a moving black brane.

Riemann, B. (1860). *"Über die Fortpflanzung ebener Luftwellen von endlicher Schwingungsweite"*. Abh. Konigl. Ges. Wiss. Gottingen, 8:43–66.

Ross, S. F. (2011). Holography for asymptotically locally Lifshitz spacetimes. *Class. Quant. Grav.*, 28:215019.

Ross, S. F. and Saremi, O. (2009). Holographic stress tensor for non-relativistic theories. *JHEP*, 09:009.

Schubring, D. (2015). Dissipative String Fluids. *Phys. Rev. D*, 91(4):043518.

Son, D. (2008). Toward an AdS/cold atoms correspondence: A Geometric realization of the Schrodinger symmetry. *Phys. Rev. D*, 78:046003.

Son, D. T. and Surówka, P. (2009). Hydrodynamics with triangle anomalies. *Physical Review Letters*, 103(19).

Spillane, M. and Herzog, C. P. (2016). Relativistic hydrodynamics and non-equilibrium steady states. *Journal of Statistical Mechanics: Theory and Experiment*, 2016(10):103208.

Susskind, L. (1995). The World as a hologram. *J. Math. Phys.*, 36:6377–6396.

't Hooft, G. (1993). Dimensional reduction in quantum gravity. *Conf. Proc. C*, 930308:284–296.

Taroni, A. (2014). Protection mechanism. *Nature Physics*, 11(1):5–5.

Tarrio, J. and Vandoren, S. (2011). Black holes and black branes in Lifshitz spacetimes. *JHEP*, 09:017.

Taylor, M. (2008). Non-relativistic holography.

Taylor, M. (2016). Lifshitz holography. *Classical and Quantum Gravity*, 33(3):033001.

Toner, J., Tu, Y., and Ramaswamy, S. (2005). Hydrodynamics and phases of flocks. *Annals of Physics*, 318(1):170 – 244. Special Issue.

Wiegelmann, T. and Sakurai, T. (2012). Solar Force-free Magnetic Fields. *Living Rev. Sol. Phys.*, 9:5.

Witten, E. (2001). Multitrace operators, boundary conditions, and AdS / CFT correspondence.

Wölfle, P., Schmalian, J., and Abrahams, E. (2017). Strong coupling theory of heavy fermion criticality II. *Rept. Prog. Phys.*, 80(4):044501.

Zingg, T. (2011). Thermodynamics of Dyonic Lifshitz Black Holes. *JHEP*, 09:067.

Zwanzig, R. W. (1961). *Statistical mechanics of irreversibility*. Lectures on Theoretical Physics Volume 3, 139 (Interscience, 1961).